Manuscript Details

Manuscript number	EARTH_2018_56_R2
Title	Morphometry and elevation of the Last Interglacial tidal notches in tectonically stable coasts of the Mediterranean Sea.
Article type	Review Article

Abstract

We report detailed morphometric observations on several MIS 5.5 and a few older (MIS 11, 21, 25) fossil tidal notches shaped along carbonate coasts at 80 sites in the central Mediterranean Sea and at an additional six sites in the eastern and western Mediterranean. At each site, we performed precise measurements of the fossil tidal notch (FTN) width and depth, and of the elevation of its base relative to the base of the present tidal notch (PTN). The age of the fossil notches is obtained by correlation with biologic material associated with the notches at or very close to the site. This material was previously dated either through radiometric analysis or by its fossiliferous content. The width (i.e. the difference in elevation between base and top) of the notches ranges from 1.20 to 0.38 m, with a mean of 0.74 m. Although the FTN is always a few centimetres wider than the PTN, probably because of the lack of the biological reef coupled with a small erosional enlargement in the FTN, the broadly comparable width suggests that tide amplitude has not changed since MIS 5.5 times. This result can be extended to the MIS 11 times because of a comparable notch width, but not to the MIS 21 and 25 epochs. Although observational control of these older notches is limited, we regard this result as suggesting that changes in tide amplitude broadly occurred at the Early-Middle Pleistocene transition. The investigated MIS 5.5 notches are located in tectonically stable coasts, compared to other sectors of the central Mediterranean Sea where they are uplifted or subsided to ~100 m and over. In these stable areas, the elevation of the base of the MIS 5.5 notch ranges from 2.09 to 12.48 m, with a mean of 5.7 m. Such variability, although limited, indicates that small land movements, deriving from slow crustal processes, may have occurred in stable areas. We defined a few sectors characterized by different geologic histories, where a careful evaluation of local vertical land motion allowed the selection of the best representative elevation of the MIS 5.5 peak highstand for each sector. This elevation has been compared against glacial isostatic adjustment (GIA) predictions drawn from a suite of ice-sheet models (ICE-G5, ICE-G6 and ANICE-SELEN) that are used in combination with the same solid Earth model and mantle viscosity parameters. Results indicate that the GIA signal is not the main cause of the observed highstand variability and that other mechanisms are needed. The GIA simulations show that, even within the Mediterranean Basin, the maximum highstand is reached at different times according to the geographical location. Our work shows that, besides GIA, even in areas considered tectonically stable, additional vertical tectonic movements may occur with a magnitude that is significantly larger than the GIA.

Keywords	Fossil and Present Tidal Notches, glacial isostatic adjustment (GIA), Vertical tectonic movements

Corresponding Author	fabrizio antonioli
Corresponding Author's Institution	enea
Order of Authors	fabrizio antonioli, Luigi Ferranti, Paolo Stocchi, GIACOMO DEIANA, Valeria Lo Presti, Stefano Furlani, Camilla Marino, paolo E. Orru, Gianfranco scicchitano, EGIDIO TRAINITO, Marco Anzidei, Marco Bonamini, Paolo Sansò, Giuseppe Mastronuzzi

Suggested reviewers	CARMELO MONACO, Cherith Moses, W. Roland Gehrels, Marco Meschis
Opposed reviewers	Alessio Rovere

Submission Files Included in this PDF

File Name [File Type]

lettera editor 2.docx [Cover Letter]

letter to editor 01.05.docx [Response to Reviewers]

annotated manuscript Antonioli et al. 19.06.docx [Revised Manuscript with Changes Marked]

ABSTRACT.docx [Abstract]

Antonioli et al. 19.06.docx [Manuscript File]

Figure 1.jpg [Figure]

Figure 2.jpg [Figure]

Figure 3.JPG [Figure]

Figure 4.jpg [Figure]

Figure 5.jpg [Figure]

Figure 6.jpg [Figure]

Figure 7.jpg [Figure]

Figure 8.jpg [Figure]

Figure 9.jpg [Figure]

FigurE 10.jpg [Figure]

Figure 11.jpg [Figure]

Figure 12.jpg [Figure]

Figure 13.jpg [Figure]

Table 1.docx [Table]

table 2.docx [Table]

Table 3.docx [Table]

table 4.docx [Table]

Table 5.docx [Table]

Table 6.doc [Table]

S1.docx [Supporting File]

S3.jpg [Supporting File]

S4.jpg [Supporting File]

S5.jpg [Supporting File]

S6.jpg [Supporting File]

S7.docx [Supporting File]

Submission Files Not Included in this PDF

File Name [File Type]

S2.kmz [Interactive Map Data (.kml, .kmz)]

Research Data Related to this Submission

There are no linked research data sets for this submission. The following reason is given:
Data will be made available on request

ENTE PER LE NUOVE TECNOLOGIE,
L'ENERGIA E L'AMBIENTE

ENEA, Casaccia, Via Anguillarese 301, 00123 Roma, Italy

Dear Editor in chief,

the present paper we submit to Earth Science Review deals with the fossil tidal notches, carved on the carbonatic cliff of the Mediterranean Sea and attributed to the Marine Isotope Stage 5.5 (125 ka BP, Last Interglacial). When well-preserved, these notches are the most precise markers of past sea levels because they are closely linked to the local tidal range.
We provide a database for more than 80 sites, mostly located in Italy, but also including locations in the eastern and western Mediterranean Sea. All these sites are considered tectonically stable and were already studied. We gathered high-resolution morphometric observations and reviewed the geometric and elevation parameters on a regional perspective.
The elevation of the fossil tidal notch base (measured relative to the base of the present tidal notch) varies from 2 to 12 meters above the current sea level. To understand the reasons for this large variability even in areas considered tectonically stable, these numbers were compared with three different models of Glacial and hydro-isostatic adjustment (GIA), namely ICE-5G, ICE-6G and Anice-Selen.
The results show that in the Mediterranean Sea the variability of the maximum GIA elevation is of the order of 1–2.5 m. Even at sites commonly inferred to be on stable crustal sectors, the current MIS 5.5 FTN elevation is affected by low-rate, albeit significant, local or regional tectonic motions, whose mechanisms and effects are described on a case-by-case basis.
In addition, the morphometric dimension of the fossil notch (width), when compared with the present notch, allows us to speculate that tides during MIS 5.5 were the same as today. For the fossil tidal notches older than 760 ka Bp, the tide amplitudes of the Mediterranean Sea were three time higher than today (up to about 1.8 meters).
All co-authors have approved the manuscript, and agree to its submission. The manuscript has not been previously published and is not under consideration for publication elsewhere.

Sincerely yours,

Fabrizio Antonioli

Reasearch Director - Laboratory Climate Modelling and Impacts, Roma, Italy.
00393315331121 - fabrizio.antonioli@enea.it

Dear Prof Kandy,

We have accepted and reported corrections requested by Reviewers 1 and 2 in text, figures and tables. We have also answered to all the questions, as highlighted in this letter and shown (in red) in the annotated manuscript.

Concerning the section on older notches that show a width that is three times that of the of PTN and MIS 5.5 FTN, we agree with Rev. 2 hat they are a secondary part of the research, however we believe that they add an important piece of information about the tide amplitude through time. Because this is a morphometric result, and the paper morphometric observations have strong implications on ancient tides, we would prefer to leave this section. Because of the strong correlation between the width notch, the MIS 5.5 and the current tide amplitude, this result implies that the tide amplitude in the Mediterranean sea has significantly changed since the middle\lower Pleistocene.

Reviewer 1

The paper focuses on global warming and sea level change, which are topics of global concern and significance. It specifically considers evidence for the MIS 5.5 sea level high-stand derived from fossil tidal notches in the Mediterranean. The paper is very well illustrated and is data-rich, including primary field data and secondary data. The title suggests that the paper uses field-measured tidal notch data, from tectonically stable coasts, as indicators of past sea levels in order to evaluate GIA model predictions but I am not sure it is what it delivers (or, indeed if that is what the title really means). There is a lack of clarity around the specific aim of the paper – although a number of objectives/goals are specified early on there is no clear specification of the research question. It would be helpful for the authors to provide a specific research question that the objectives/goals address because, as it currently stands it is a little difficult to follow and to know how the conclusions address the overall aim.

Introduction par 2 – the reader is told that there is an uncertainty of +/- 5 m in estimates of MIS 5.5 highstand above psl using coral reefs but is not given the estimates – how do they compare with those derived from FTN? Is it reasonable to compare them if coral reefs are not common in the Mediterranean?

We think that it is reasonable to assign an error bar on the use of corals as sea level markers, whose accuracy is not so clear, but was reported by Muhs et al., 2017 (cited in the reference list) in a recent paper. We wanted to underline in the introduction the high precision of a tidal notch as sea level marker (few centimeters) in comparison with a coral (Acrocora Palmata, Cervicornis, ecc.) that lives few meters under sea level.

There is a lack of clarity around the specific aim of the paper – although a number of objectives/goals are specified early on there is no clear specification of the research question. It would be helpful for the authors to provide a specific research question that the objectives/goals address because, as it currently stands it is a little difficult to follow and to know how the conclusions address the overall aim.

The overall aim of the work could be made clearer – there are a list of objectives at the end of the introduction but no clear over-arching research question. It is to assess the validity of GIA models using evidence from FTN of known age or something else?

The goals of our work are the following:

to carry precise morphometric measurements of FTNs found along coasts in Italy and few other locations in the Mediterranean Sea that are considered tectonically stable, and attributed to the MIS 5.5;

to link the FTNs to the closest outcrops with deposits aged to the MIS 5.5;

to reference the elevation and morphometry of the FTNs with respect to the modern tidal notch;

to make, at some of these localities, morphometric measurements of more elevated and older notches, whose age is known or can be estimated, and compare them with the MIS 5.5 FTNs;

to map the regional variability in the elevation of the MIS 5.5 notches, and compare this variability with predictions of specifically built GIA models including different ice-sheets scenarios;

to evaluate the residual difference between GIA-corrected elevation of notches in light of slow, mostly tectonically-induced land motions.

we changed and inserted this phrase in the manuscript.

Section 2.1 par 1 – page number for quotations.

We added the page number (pag 81)

2.3 what is MIS 5e (others are all numbers) and according to whom are there over 1000 sites recorded with MIS 5e evidence? (reference).

We changed in the ms MIS 5e in MIS 5.5

Are Tyrrhenian sites the same as MIS 5? Final par – what does it mean to calibrate the whole Mediterranean? Not clear what this par means.

We explained in the text the calibration of Hearty (1986) on the amino acid ratios measured on mollusk shells based on U/Th or paleontologically dated MIS 5.5 deposits.

3. this is a little unclear. Did you measure notches at 80 sites and only in areas that are considered to be tectonically stable?

Yes from MIS 5.5.

Are the additional sites also only on tectonically stable coastlines?

Yes, uplifted notches at 6 sites are older (Middle\Lower Pleistocene) than MIS 5.5 and they are all on tectonically stable coasts since MIS 5.5 times but before are uplifting.

It is not clear what ‘presented good morphological continuity with a certain origin’ means in respect of the FTN at the additional sites.

we modified and clarified in the ms as follows:

We established that a tidal notch it is defined as continuous when it can be followed laterally for at least 50 meters.

Page 8 'we solved the gravitationally self-consistent sea level equation (SLE)' – add some explanation as to what this is and why it needs to be solved

We have modified the Section according to the comment from the reviewer. We have added in the ms further details and information about the numerical modeling and expanded the text to provide the reader with a broad and comprehensive explanation of the theory of the GIA models.

Page 8 – models of GIA – if the purpose of this section is to identify potential elevations of stillstands in order to see which model the FTN fit best - which is what appears to be stated at the end of the section – then it would be helpful to make this clear at the start of the section.

First we want to investigate the GIA contribution to the elevation of the highstand and how it works. We do this for three ice-sheet models just to appreciate the variability of the signal. It is what we call "sensitivity test". How does the RSL change respond throughout the Mediterranean Sea? Are there regional patterns? Are they consistent among the employed ice-sheet models How are they modulated by the solid Earth response? What is the contribution of the earth mantle viscosity profile?

We then attempt to find a "best" model for explaining the observations.

Page 9, section 4.1 – explain why you would exclude notched lower than 2.5 m and higher that 10 m elevation as this is not clear.

It is only a statistic choice: take off maximum and minimum values. As we have specified in the manuscript the result remains the same: general mean **5,75,** cutting maximum and minimum values: **5,95** m.

It is also not clear what the measure correction is that has not been applied by the other authors when their notch elevations are included. It that the elevation correction for the presence of vermitid rim? Or something else?

We personally measured 80 sites, but we haven't personally measured 6 published sites at non-Italian locations (Table 3). All this is clearly illustrated in Table 3 caption. Anyway we clarified with a sentence in the text.

Page 11 section 5.1 par 1 – 'This difference supports, based on a larger data set, the conclusions of Antonioli et al. (2015)' – what were their conclusions? Did they find the same differences in width – if so it would be better to state that.

In the paper Antonioli et al., 2015 in addition to the Present day tidal notch, measurements on the FTN morphometry at 8 sites were published. They found that the width of FTN was larger of 8 -15 cm than PTN (Table 1 of Antonioli et al., 2015). In the present paper we extend the comparison to the 80 sites and found the same result based on a more robust dataset.

Section 5.1 par 4 – solution rates are extrapolated over long time periods – it would be helpful to discuss some of the limitations of doing this. The implication is that the notches simply retreat but this assumes parallel retreat of the rock surface. Studies have shown that notches may reach a certain depth, due to differential weathering and erosion on the base, back, roof and surrounding rock surfaces, and then collapse. So, the process of notch retreat is episodic rather than linear and means that it may not be possible to apply microerosion rates over such long time scales as is the case here.

We added a discussion about the extrapolations regarding long-term rates of erosion. In particular, we discussed the lack of instrumental data older than 50 years, the lack of information related to past climate changes and the probable covering by younger deposits now completely lacking.

Anyway, these notches do not collapse because they are cut in hard Mesozoic limestones. In general, karst landforms are formed, not collapses, that are common in soft rocks, such as siltstones, claystones, etc.

Micro erosion rates are commonly used to study notch development, such as many cases in the Mediterranean and in the tropics (Torunski, 1979; Moses, 2013, Furlani et al., 2011, Furlani and Cucchi, 2013, etc)

Regarding the comment included in the pdf copy, FTNs are wider because the rim is now absent. It does not mean more erosion, but it means that our measures of the FTN base refers to a different point than the old rim, whose exact position we do not know. The result is that FTN is larger than PTN. Hopefully, our measures refer to the unknown base of the rim so the two are fully comparable, although the base of the present rim is not measured.

This is also the contribution of the “rim question” to the discussion, claimed in a comment by the reviewer. Anyway, we better explained in the ms these questions reported by the reviewer.

Section 5.3 this section is not entirely clear – were the field-measured FTN elevations corrected according to their geological setting? It would be helpful to clarify what has been done – perhaps in a simple table that shows exactly how the elevation data for each site are adjusted and why?

We made clearer in the manuscript how we selected the 13 observations considered less affected by local slow tectonic or volcanic processes. We also pointed that the processes still operating in individual sectors and the resulting selection criteria were already illustrated in Table 6.

Perhaps this is the uncertainty value in Table 1?

We explain the uncertain variation (in column 3 of Table 1) in the section 3.1 of ms, and we have added some further clarifications in this chapter.

We underlined in the manuscript the uncertain for each kind of measurement, also, we added in the manuscript the quotation of Table S7 were we provide a complete data set containing (in column 9) the kind of measurement technique used. As requested also by Rewiever 2 we changed error bar in Table 1, 2 and S7.

Section 5.6 par 2 – remove the tentatively that comes after same as

We removed the expression

Conclusion 8 – is a 1.5 m discrepancy significant? In the introduction the reader is told that the uncertainty associated with coral reefs is +/- 5 m – a 1.5 m discrepancy in that context is relatively small – how and why is it significant in the context of FTN?

In the present study we use tidal notches that are much better sea-level markers than corals. The uncertainty stipulated by us for the FTNs is maximum 0.25 m, typically 0.1 m or less. Therefore, we retain that the observed discrepancy is significant.

Fig 1 – key has both m and km – should it just be km? [metres and km (not Km)].

Fig. 1: we corrected metres and changed km, also cleared the caption on sections B, C, D, E, F, G .

Fig 2 – coverage *of the notch* by fans or aeolianites? What does the downward arrow in the land block indicate?

We added in section C of Fig. 2 the phrase "sea level going down" above the arrow. In the caption of Fig. 2 we wrote " the final coverage by detrital fans or aeolianites deposits preserves the notches from the dissolution."

Fig 3 mentions aeolian erosion of the FTN – but these are not aeolian features – should the word be marine? (subaerial and marine rather than chemical and aeolian?; unclear). Decimal places not needed on the scale bar.

We corrected in the ms the caption changing the word aeolian with subaerial :

Fig. 3. Sections of fossil and present tidal notch morphology. The letters refer to the width (w), depth (d) and the base of the notch (c). On the right an overlap between the present and the fossil tidal notch (for the sites 52, 71 and 2 of Table 1) morphology highlights the marine and ~~aeolian~~ subaerial erosion that slightly modified the original morphology, but preserves a similar width.

Fig 10 – there is no green on this figure

We changed the caption:

Fig. 10. In blue, the Lisiecki and Raymo (2005) curve corrected by Stocchi et al. (2017) for GIA calculated for Custonaci, Sicily. In red, the same corrected curve for a rate of vertical tectonic movement of 0.81 mm/a. In yellow, the calculated age of the uplifted tidal notches of Table 3.

Fig 12 it is not clear how these maps are predicted.

Description of how maps in Fig. 2 are predicted is given now in the caption of Fig. 2.

Fig 4 is referred to on p 10 ‘Overall, the maximum peaks predicted according to ICE-5G and ICE-6G could explain the observed lower limits (Fig. 12).’ but it is not clear how this statement related to Fig 12.

We have rephrased the sentence in the ms

Similarly on p 16 ‘Based on the curve corrected with tectonics in Fig. 12’ – there is no curve in Fig 12. Unclear.

We corrected in the quotation on ms of Fig. 12 in Fig. 10

Fig 13 – what does ‘projected from north’ and ‘projected from south’ mean? The latter is a black dot but there are no black dots anywhere on the Fig.

The two sites in Tuscany and Sicily have the highest projection compared to all the others, so we preferred to show these two sites in a different way. We added a sentence in the text about the projection. We changed Fig. 13 now the “white” dots are clearly visible.

Table 4 Most of the references in this table do not appear in the reference list.

Thanks, we added the lacking references:

Cucchi, F., Forti, F., Furlani, S. 2006. Erosion/Dissolution Rates Of Limestone Along The Western Istrian Shoreline And The Gulf Of Trieste. Geografia Fisica e Dinamica Quaternaria 29, 61-69.

De Waele, J., Furlani, S. 2013. Seawater and biokarst effects on coastal karst. In: Shroeder, J.F., Frumkin A. (Eds), Treatise on Geomorphology, Vol. 6, Elsevier, Amsterdam, 341-350.

Gomez-Pujol, L., Fornos, J.J., Swantesson, J.O.H. 2006. Rock surface millimeter-scale roughnessand weathering of supratidal Mallrcan carbonate coasts (Balearic Islands).Earth Surface Processes and Landforms 31(14), 1792-1801.

Moses, C.A. 2013. Tropical rock coasts: Cliff, notch and platform erosion dynamics. Progress in Physical Geography 37(2), 206-226.

Moses, C.A., Robinson, D., Kazmer, M., Williams, R. 2015. Earth Surface Processes and Landforms 40(6), 771-782.

Swantesson, J.O.H., Moses, C.A., Berg, G.E., Jansson, K.M., 2006. Methods for measuring shore platform micro erosion: A comparison of the micro-erosion meter and laser scanner. Zeitschrift fur Geomorphologie N.F. Suppl. 144, 137-151.

-Reviewer 2

- My detailed comments are both on the PDF and the letter to the editor, attach.

The paper contains a large amount of data: re-assessed previous observations and newly measure notches' parameters (elevations, width, etc.) compared to GIA evaluations for the MIS5e in various places mainly in central Mediterranean but with a comparison both to Spain in the west and to Israel in the east. The figures are of high quality (see some remarks below regarding them) and present the data clearly. The paper is important to the relative sea level (RSL) community of the Mediterranean and beyond. Therefore, I recommend the paper for publication, following the corrections suggested below and in the text.

In general:

The paper presents comparison of modern morphological features of notches to fossil ones, mainly to those dated to the MIS5.5, from stable coasts, that are now exist in various elevations. The field data is compared to GIA calculations but the final conclusion is that the GIA cannot be the only explanation and other crustal movements are assumed. Therefore, to my opinion the title does not fit the final conclusion that "Our work shows that, besides GIA, even in areas considered tectonically stable, additional vertical tectonic movements may occur with a magnitude that is significantly larger than the GIA". To my understanding this challenging and interesting conclusion claims that there are other crustal processes, not only the GIA as a suggested mechanism for various elevations of notches (or other sea level indicators). In cases, these other factors are even more effective than the GIA and the part of the title: "implications for Glacial Isostatic Adjustment model predictions" is not representing this conclusion. It even contradicts it. Therefore, I can suggest a better title: "Last Interglacial tidal notches in tectonically stable coasts in the Mediterranean Sea: various factors involved in their elevations".

As suggested by reviewer 2 we changed the title in:

Morphometry and elevation of the Last Interglacial tidal notches in tectonically stable coasts of the Mediterranean Sea.

The paper actually deals with the MIS5.5 notches. Like other indications from this period, they add important and significant data to the records that already exist. To my opinion, the MIS 11, 21 and 25 notches do not contribute to the discussion and I suggest deleting them from the paper.

It is true that most of the data concerns the FTN aged to MIS 5.5. However, we have discovered and measured 6 higher and older tidal notches that show a threefold larger width than the FTN or PTN. This observation allows us to reach the important result that the tide amplitude in the Mediterranean Sea was threefold larger in pre-MIS 5.5 times. This result stems from a morphometric observation that is the main goal/method of the paper. Therefore we propose to maintain in the paper the section on the older FTNs. In addition as for the uplifted notches studied in the Custonaci area (sites 75, 76, 77, 78 of Table 2) we provided a precise age (Stocchi et al., 2017) we cancelled the FTN ages (sites 79, 80 of Table 2) because far from Custonaci, in column 11 of Table 2 we decided to write more simply "Middle Pleistocene".

The **Introduction** need corrections/additions: please follow my remarks in the text. 2.4; the GIA factor, is well written .

arrow 42 Using various methods

We modified and added this phrase and many comment on corals uncertain as requested also by Rev. 1:

the elevation above the present sea level (p.s.l.) of the highstand, measured in globally stable areas (Rovere et al., 2016), has been estimated based on coral reefs using various methods (Bard et al., 1990; Chen et al., 1991; Chappel et al., 1996; Schellmann and Radtke, 2004; Blanchon et al., 2009; Dutton et al., 2015). These estimates show a significant uncertainty (some meters) in the assessment of the palaeo sea level (Muhs et al., 2017) because corals do not live at sea level.

I think that an addition of summary of other methods used for assessing the elevations of the MIS5.5, each with it's uncertainties, is needed.

We added in the manuscript a reference to a paper that discusses on the measurement for assessing elevation of the MIS 5.5 (Rovere et al., 2016). In our paper we only present measurements of tidal notches; in the section Method we described with details the different measurement systems and their error bar.

Observation on Section 2.1

Delete "the oceans" if you do not mention exactly where.

We deleted “in the Oceans” as requested by the reviewer, because the paper regards only the Mediterranean area.

what is the meaning of this limit of 4.o m? Not clear.

4.0 m is the maximum width of a tidal notch, according to the local tide, as suggested by Trenhaile (2015).

The sentence has to be corrected: it has to be: "half of the notches are in carbonate rocks" right? otherwise there is no sense in the sentence.

We removed the sentence:

~~Nearly half of the Mediterranean’s rocky coasts are generated on carbonate rocks (Furlani et al., 2014b) as roof notches.~~

Also, while the timing of the onset of the MIS 5.5 acme is relatively simultaneous, mostly taking place from 129 ka to 126 ka, the timing of the demise of the LIG acme is more variable and ranges from 122 ka to 113 ka (Rovere et al., 2016). **I suggest to add also a short paragraph explaining that different GIA models yield different contributions. It's important. No model is "the Bible"....**

We have expanded the original Section 3.2 Glacial- and hydro-isostatic adjustment by including further details on the GIA models in general and on the contribution of the ice-sheet models, which are indeed forcing functions within the formalism of the Sea Level Equation, i.e. the equation that relates RSL changes to GIA through the imposition of mass conservation.

Yes the three ice sheet models have different ice thickness variations in space and time and are characterized by different lengths of the MIS 5 interval. Actually ICE-5G and ICE-6G share the same length, while ANICE-SELEN is characterized by a longer interglacial.

Methods: in chapter 3.1 please see my remarks, mainly regarding the uncertainties: the various error ranges need be explained

.Arrow 114 there is a repetition. Refer to Antonioli 2015 in the first sentence and delete the second.

we deleted arrows 114 and 113:

~~When well-preserved, this landform is the most precise marker of past sea levels because its width is closely linked to the local tidal range.~~

arrow 135 Well dated deposits. The dating of the notches is not trivial and it has to be presented in a paragraph in the Introduction.

We changed it between arrows 123 and 127 :

~~In the Mediterranean, fossil coral reefs are quite rare, while cemented fossil deposits containing Senegalese fauna (*Persististrombus latus* and others molluscs) are often found near and at the same elevation of the measured fossil notches. This correspondence in elevation made possible the chronological attribution of the measured notches.~~

In the Mediterranean Sea, the prevailing tide is microtidal, and several late Holocene tidal notches, mainly on carbonates, occur (e.g. Benac et al., 2004, 2008; Antonioli et al., 2007; Furlani et al., 2011, 2014a). These considerations allow us to discuss data on the sea level elevation reached during the MIS 5.5 highstand. The obtained values have been corrected on the basis of GIA and other vertical tectonic movements that we located on the basis of a large amount of observed data.

arrow 207 But we have to bear in mind that these are totally different time scales....

We are aware of this, but we point that there is a strong correlation between the vertical tectonic movements detected at geological and at instrumental time scales. We have however simplified the section

arrow 229 Either explain that 5e was the previous terminology or use the same terminology of 5.5

A requested also by Rev. 1 we cancelled 5e and used always MIS 5.5.

arrow 241 Add: all attributed to the MIS 5.5

We added this phrase in the ms

243-248 But what information about the 5.5 sea levels this section obtain?

See also the reply to Rev 1, anyway we removed the sentence:

~~A recent integrated study (Amorosi et al., 2014; Negri et al., 2015) of Fronte Section nearTaranto, Italy detailed one of the more representative and thick sections of the MIS 5.5 along the coasts of the Mediterranean Sea. Facies analysis, detailed macro- and microfaunal characterization and sequence stratigraphy (using Senegalese fauna and ten U-series dates on Cladocora caespitosa samples) permitted an unequivocal MIS 5.5 age (132–116ka) identification. These results show the composite section to be a very promising candidate (named Tarentiano) in the search for the Upper Pleistocene global boundary stratotype section and point (GSSP).~~

arrow 263 what do you mean by "historical". I suggest to delete and just to refer to this paper.

we removed the word historical

arrow 340 why corrected by 3 cm? Explain

It is explained in the manuscript : “The measure was corrected by 3 cm; this value corresponds to the estimated average width of the biological rim (Vermetids, Corallinaes Algae and others living at Present sea level) once formed and currently eroded at the base of a FTN”.

Arrow 350 Please explain why 5 cm uncertainty.

We performed a new clearer calculation of the uncertainty (described in the text) which derives from the summed contribution of: 1) marker identification error; 2) instrumental error; 3) lack of vermetid rim.

MARKER IDENTIFICATION ERROR: ± 2.5 cm

INSTRUMENTAL ERROR

a) ± 5.0 cm instrumental error for levelling, total station, GPS

b) ± 1.0 cm instrumental error for invar telecopic rod (assumed vertically positioned)

c) ± 15.0 cm instrumental error for the tape

d) ± 50.0 cm instrumental error for digital altimeter used for the older more uploifted notches

in case of lack of the vermetid reem: ± 10 cm in the section Method we better explained how assigned the uncertain depending on the kind of measurement technique. Here the modification (in red) in the ms:

The measurements of the 80 studied sites (**Tables 1 and 2 and table S7**) were performed using different tools and with an estimated error ranging from ±1 up to ± 5 cm along the vertical error depending on both the tool and the adopted reference level (MSL, vermetid reef etc., see **Fig. 5 and S5**). All measurements were referred to the base of the PTN or zones where the vermetid reef was present and considered as representative of the MSL (H = 0). Vertical profiles along the notch sections were realized through several measurements. An uncertainty of ± 2.5 cm was assumed to account for the identification of the marker.

The tools we used and related instrumental uncertainty are the following:

a) Global Positioning System/Real Time Kinematic (GPS/RTK) technique. In eight sites (50, 51, 52, 54, 74, 75, 79 and 80, respectively, in **Figs. 4 and 5; Tables 1 and 2, table S7**), we used the GPS/RTK technique which has an accuracy better than ± 3 cm along the vertical. This depends on both the tool and the adopted measurement base (MSL, vermetid reef etc., see **S5**), but it often depends on the setting of MSL. An accuracy of ± 5 cm was estimated.

b) Levelling surveys. Sites 50, 51, 52 and 54 were surveyed by a levelling technique, using a Leica Runner4 instrument. Elevation data were referred to the local sea level at the time of the surveys and corrected for tides by the nearest tide station (**Fig. 5)**. An accuracy of ± 5 cm was estimated

c) Total station. Sites 79 and 80 were surveyed with a Total Station Leica TCRP 1203, equipped with an infrared laser beam, capable of capturing targets at a distance up to one km. For the measurements in the range of about 700 m, we used the laser beam without a prism, keeping a precision of a few mm along the distance. (**Fig. 5**). An accuracy of ± 5 cm along the vertical was estimated

d) Telescopic rod. In 19 sites (**Figs. 4 and 5; Tables 1 and 2, table S7**), a 10 m long telescopic measuring gauge was used (Telefix). This device provides direct readings on a graduated tape and is built with non-extensible material which ensures an accuracy of about 3 mm when fully extended to 10 m. We estimated an error comprised from 1 to 5 cm depending on the morphological conditions of the PTN and on the position of the MIS 5.5 FTN (**Figure in S5**). This is always used when the FTN is orthogonal above the PTN. Otherwise, when a few degrees of inclination occurred (1–6°) between the platforms of the PTN and the FTN, the top of the instrument was placed a few cm from the FTN base. The level was defined by an operator located on a nearby boat and were taken photos to roughly verify the positioning of the rod with respect to the significant morphologies. An accuracy of ± 1 cm along the vertical was estimated.

d) Tape. In 46 sites (**Figs. 4 and 5; Tables 1 and 2, Table S7**), we used a 20 m long measuring tape, positioned on morphological markers by two operators. This measurement tool was used in sites where the cliff was not back drawn and the tape could therefore be positioned vertically or with an acceptable slant (**Figure S5**) . The use of the tape was done with an operator on the FTN and one on the PTN that is in the sea. Because of the presence of some vertical offset in the position of the two markers, and resulting tilt of the tape from the vertical, these measurements have been assigned an error bar of ± 15 cm.

e) Digital altimeter: In three sites (**Figs. 4 and 5; Tables 1, 2 and Figure S5, Table S7**) where uplifted notches were far from the present day coast, position and elevation measurements were performed by a digital altimeter (Garmin Oregon 650) with a vertical accuracy of 50 cm and were calibrated with respect to the sea level along the nearby coast. Measurements were taken at the base of the FTN and at the vermetid platform. An accuracy of ± 50 cm along the vertical was estimated.

When the Vermetid rim was lacking, an uncertain ty of ± 10 cm was summed to the marker identification and instrumental error.

arrow 358 The top, living part of the reef?

Yes

Arrow 397 Again, explain why this is the uncertainty

See below, we added the phrase:

The use of the tape was done with an operator on the FTN and one on the PTN that is in the sea. Because of the presence of some vertical offset in the position of the two markers, and resulting tilt of the tape from the vertical, these measurements have been assigned an error bar of ± 15 cm.

Arrow 486 What is the meaning of the mean?

the arithmetic mean of all measurements

Arrow 518 between what? between the notch and the dated fossil? not clear.

We modified in the text adding between the notch

Arrow 520 This is crucial and needs better explanation since dating of notches is the main challenge.

We explained it in the Method section

Arrow 597 Add **notches**; "on MIS 5 notches morphology"

Done

Arrows 603 and what is the explanation for it?

The mix fresh water\salt water greatly increases the chemical dissolution of limestone and the so deeply carved PTN tend to collapse. We added this remark in the ms

Arrow 615 What is the contribution of the elevated rim to the discussion?

The existence of vermetid rim also during MIS 5.5

Arrow 617 The argument is not well presented: do you claim that the fossil notches are wider because the rim is now absent which means more erosion? What about the time factor? The MIS6.5 lasted 15ka years. The notches were not created during the whole period but still, maybe during longer periods?

No, today we haven't the fossil rim, and therefore the fossil notch is wider.

Results. See my remarks in the text and please pay specific intention to chapter 4.4 remarks: dating the notches is the main challenge and it's not trivial. It needs better explanation. Chapter 4.5: as mentioned above, to my opinion, the older notches are out of context in the current study: there is no s how they were dated, what is the GIA contribution for these old periods, etc. I suggest deleting 4.5.

See response to Editor Prof. Kandy at the onset of the Rebuttal letter

Discussion: lines 603-616 has to be reviewed. Please see my comments there. The fact that the mean width of fossil notches is higher than the mean of the present ones has to be better explained. Chapter 5.1 is too long and actually not contributing to the Discussion which is mainly about the combination of the notches indicating RSL and the GIA. The discussion regarding the rates is not in place and to my opinion not relevant

arrow 603 - 616 See before regarding long-term erosion rates.

arrow 667 levering o levelling

We changed in the manuscript in levering

Chapter 5.4 deals with the dating issue that is essential for the subject. The most challenging part of dating the notches is not the discussion about the dating methods or the Senegalese fauna (mainly the *Strombus bubonius*, now known as *Persististrombus latus*) but the correlation between the dated units and the notches (sometimes with a long distances between them). Therefore, the chapter has to be revised: to better explain the correlations made and to shorten the discussion about the fossil fauna.

As I mentioned above already twice: to my opinion 5.5 is out of the scope of the paper (see the title), but it's up to the authors to decide whether to leave or to remove it. 5.6: please see my comment there: either combine to 5.1 or delete since it is a repetition.

See response to Editor Prof. Kandy at the onset of the Rebuttal letter

Arrow 808 Delete the RSL. The GIA signal show elevations.....

We deleted RSL

Arrow **837** delicate is not the right word

We removed the sentence:

~~Age of the FTN This is a very delicate aspect of our paper: we define the age of FTN in areas of the Mediterranean~~

And changed in:

In this section of the study, we define the age of FTN in areas of the Mediterranean...

Arrow 843 the correlation has to be better explained. It's not trivial

As previously written if the FTN is continuous and at same places it is associated with a dated deposit, we take the dating for the whole notch, we added thgis phrase in the ms:

Figure 9 shows that in the sites 41-44 the distance of the dated deposit is more than 20 km. We are in the gulf of Orosei (Sardinia, Italy) one of the wildest and least anthropized coasts of the central Mediterranean sea, the distance between the measure of the FTN and the dated deposit is in this case linked only to the inaccessibility for study the deposits of the MIS 5.5, but on the contrary we are in one of the sites where the FTN is longer and continuous of the entire Mediterranean, between the sites 38 and the 44, the FTN is always constantly exposed and visible, there is no doubt that it is always the same notch and present the same age.

Arrow 927 This issue has been discussed on chapter 5.1 (lines 603-616). therefore, either copmbine or delete 5.6.

In Section 5.1 Notch morphometry between arrow 603 – 616 we exposed the **morphometry** data

In Section 5.6 Tide, In this section we discuss of **TIDE**, I remind that the tidal notch width is stricly connected with the local tide. We added a phrase in Section 5.6 and cancelled some repetitive phrases:

Antonioli et al. (2015) demostrated that the tidal notches are strictly connected with the local tide. But the width of the present tidal notch shows higher values when compared with the local tide (on average the notch has a width slightly less than twice in respect to the mean tidal range). Comparing the FTN width with the PTN width, our results show that the FTN width (mean 0.73 m) is wider by about 0.14 m than that of the PTN (mean 0.59 m); we interpret this greater amplitude as being due to the lack of the biological reef and to the chemical and mechanical erosion of the notch.

Therefore, we believe that the tides of the Mediterranean Sea during the MIS 5.5 highstand were the same as ~~. Temptatively~~ today. Tentatively, considering the mean width of PTNs as 0.59 m and 0.38 m as the current mean Mediterranean tide (Antonioli et al., 2015), we can extrapolate the palaeo-tide of MIS 25–21 (when the mean width of the uplifted tidal notches is 1.82 meters), resulting in a possible tide of 1.21 m, before 780 ka BP, more than three times that of today.

Conclusions: 1-5 are not conclusions but summary of the results. I suggest deleting them and starting the conclusions from 6 (there is no no. 7 and after 6 is no. 8….).

We accept the observations of the reviewer and have improved the conclusions as follows:

points 1, 2 and 3 have been refurbished and merged, eliminating results and illustrating conclusions;

point 4 has been similarly reorganized;

point 5 has been delated as requested;

points 6 to 10 (now points 3 to 6) have been rearranged and rewritten.

New conclusions of ms:

6. Conclusions

At 80 sites in Italy and subordinately in the eastern and western Mediterranean Sea (Tables 1 and 2), the MIS 5.5 and few older notches have been accurately measured. The main conclusions of this study are:

1. The morphometric parameters of the PTN and FTN are broadly similar, with only a slightly larger FTN width due to the lack of the biological reef and to the chemical/mechanical erosion of the cliff during later exposure. This result implies that tide amplitude has not changed in the last 125 ka.

2. Differently, during the MIS 25–21 highstands (1.2–0.6 Ma BP), the Mediterranean tides had amplitude three times larger than today.

3. The GIA-driven RSL changes within the Mediterranean Basin are regionally varying and significantly different from the eustatic signal. Two main typologies of RSL curves can be expected: monotonous rise followed by a late highstand in the central areas and initial (early) highstand followed by an RSL drop in the marginal regions at the western and eastern borders. Overall, the variability of the maximum GIA elevation is between 1 and 2.5 m, i.e. comparable to the expected eustatic contribution of the GrIS. 10.

4. Provided that the notches represent the maximum peak of local RSL rise, which may occur at different times and with different elevations from place to place (as explained by GIA), the observed spatial variability of MIS 5.5 notches is 1–12. m. This implies that GIA plays a secondary role in driving the regional variability of the maximum MIS 5.5 RSL elevation, and other regionally varying signals, either geologic or oceanographic, are operating.

5. Geologic processes are represented by volcanic intrusions (e.g. at the Orosei Gulf in Sardinia and at Minturno in Latium), or by tectonic displacement (e.g. continental margin down-faulting in western Sardinia and on the eastern Tyrrhenian coast, or contractional uplift in northern Sicily). These low-rate processes cause a spread of up to 10 m in the FTN elevation, five times larger than the GIA variability, even at sites commonly regarded to be on stable crustal sectors.

6. The elevation of the MIS 5.5 notch at selected sites which are less affected by these low tectonic or volcanic movements has a trend that, along a regional E-W transect, mimics but is 1–2 m lower than the predicted values from the GIA ANICE-SELEN model. The 6.5 m elevated MIS 5.5 notch on the Tyrrhenian

margin, which is assumed as a reference elevation, has a 1.5 m discrepancy with the model, thus casting doubt on the currently accepted amount of glacio-eustatic contribution to the RSL during the MIS 5.5.

Figures: The figure number is not mentioned on the figures. Please add (Figure 1, Figure 2, etc. on each one).

Figures are all regularly numbered in the Elsevier files, in the creation of the pdf they are however put in increasing order

Figure 1 B to G, please enlarge the font sizes. In Israel (No. F and in the caption) the notches are in Rosh Hanikra, not in Akko

We made all requested variations in the new Figure 1

Fig. 2 is a very good figure!! Only the caption has to be improved (mainly the English). If possible, enlarge the font's sizes of 2a.

We enlarged the font of all sections of new Fig. 2 and improved the caption

Fig. 6: Are the curves (model predictions) the same for all sites? This is how it looks…or maybe I'm wrong?

The predicted RSL curves are very similar for sites very close to each other. In fact, the GIA signal is smooth and generally characterized by a very long wavelength, especially for ice-distal regions such as the Mediterranean Sea.

Fig. 8 Why the data in the figure is up to 80 and in the paper you have up to 86 sites?

In Fig. 8 there are the 80 sites we personally measured (Table 1 and 2). The 6 additional sites (Table 3) were published by different Authors with different measurement methods and without providing the morphometric parameters.

Fig. 9: For sites 39 to 44 the distances are huge. It has to be mentioned in the Discussion, relating to the degree of the age accuracy of these sites.

We have done it on the Discussion adding this phrase:

Figure 9 shows that in the sites 41-44 the distance of the dated deposit is more than 20 km. We are in the gulf of Orosei (Sardinia, Italy) one of the wildest and least anthropized coasts of the central Mediterranean sea, the distance between the measure of the FTN and the dated deposit is in this case linked only to the inaccessibility for study the deposits of the MIS 5.5, but on the contrary we are in one of the sites where the FTN is longer and continuous of the entire Mediterranean, between the sites 38 and the 44, the FTN is always constantly exposed and visible, there is no doubt that it is always the same notch and has the same age.

Fig. 10. Following my comments regarding these ancient notches, I suggest to delete.

As previously discussed we want to leave this result regarding an important tide variation during middle-lower Pleistocene in the Mediterranean sea.

Arrow1097 What time period is it "after 120ka? 117ka is also after 120ka.... Not clear

We changed: at 120 ka

Tables: table 2 is missing

NO, Table 2 is on the pdf!!!

Tables 1 and 3 are very well presented (Again, correct in Israel: the notches are in the vicinity of Rosh Hanikra and not Akko)

Yes we corrected the name site. And we added on the caption some explanation about uncertain

Table 4: write the title above as in tables 1 and 3.

The title is already written under the letters A .... H in Table 4

Pages 52-53: not clear to what they belong.

Not clear the question, the ms contains 30 pages in the pdf,

Why same pictures are presented again?

Not clear the question. If the reviewer 2 refers to the Supplementary Tables S3, S4, S5 (A complete collection of images of all the studied notches (numbers refer to Table 1) in these tables **all** the studied sites are shown, on the contrary in Fig 4 (not supplementary material), are described some representative morphology of the studied tidal notches.

The paper needs English review. In places, I commented on it, but an overall review will improve the paper.

We made a review from a native English.

Morphometry and elevation of the Last Interglacial tidal notches in tectonically stable coasts of the Mediterranean Sea.

Antonioli F.[1], Ferranti L. [2], Stocchi P.[3], Deiana G. [4], Lo Presti V. [1], Furlani S. [5], Marino C. [2], Orru P. [4], Scicchitano G. [6], Trainito E. [7], Anzidei M. [8], Bonamini M. [9], Sansò P. [10], Mastronuzzi G. [11]

1 ENEA, Laboratory Climate Modelling and Impacts, Roma, Italy.

2 Dipartimento di Scienze della Terra, delle Risorse e dell'Ambiente, Università Federico II, Napoli, Italy.

3 NIOZ Royal Netherlands Institute for Sea Research, Department of Coastal Systems (TX), and Utrecht University, P.O. Box 59, 1790 AB, Den Burg, Texel, The Netherlands.

4 Dipartimento di Scienze Chimiche e Geologiche - Università degli Studi di Cagliari, Italy.

5 Department of Mathematics and Geosciences, University of Trieste, Italy.

6 Studio Geologi Associati T.S.T. Misterbianco, Catania Italy.

7 Villaggio i Fari, Loiri Porto San Paolo, Italy.

8 Istituto Nazionale di Geofisica e Vulcanologia, Rome, Italy.

9 Marco Bonamini Palermo via Trinacria 4, Palermo, Italy

10 Dipartimento di Scienze e Tecnologie Biologiche e Ambientali, Università del Salento Ecotekne, Lecce, Italy.

11 Dipartimento di Scienze della Terra e Geoambientali, Università degli Studi di Bari "Aldo Moro", Bari, Italy.

Keywords

Fossil and Present Tidal Notches, glacial isostatic adjustment (GIA), Vertical tectonic movement

ABSTRACT

We report detailed morphometric observations on several MIS 5.5 and a few older (MIS 11, 21, 25) fossil tidal notches shaped along carbonate coasts at 80 sites in the central Mediterranean Sea and at an additional six sites in the eastern and western Mediterranean. At each site, we performed precise measurements of the fossil tidal notch (FTN) width and depth, and of the elevation of its base relative to the base of the present tidal notch (PTN). The age of the fossil notches is obtained by correlation with biologic material associated with the notches at or very close to the site. This material was previously dated either through radiometric analysis or by its fossiliferous content.

The width (i.e. the difference in elevation between base and top) of the notches ranges from 1.20 to 0.38 m, with a mean of 0.74 m. Although the FTN is always a few centimetres wider than the PTN, probably because of the lack of the biological reef coupled with a small erosional enlargement in the FTN, the broadly comparable width suggests that tide amplitude has not changed since MIS 5.5 times. This result can be extended to the MIS 11 features because of a comparable notch width, but not to the MIS 21 and 25 epochs. Although observational control of these older notches is limited, we regard this result as suggesting that changes in tide amplitude broadly occurred at the Early-Middle Pleistocene transition.

The investigated MIS 5.5 notches are located in tectonically stable coasts, compared to other sectors of the central Mediterranean Sea where they are uplifted or subsided to ~100 m and over. In these stable areas, the elevation of the base of the MIS 5.5 notch ranges from 2.09 to 12.48 m, with a mean of 5.7 m. Such variability, although limited, indicates that small land movements, deriving from slow crustal processes, may have occurred in stable areas. We defined a number of sectors characterized by different geologic histories, where a careful evaluation of local vertical land motion allowed the selection of the best representative elevation of the MIS 5.5 peak highstand for each sector. This elevation has been compared against glacial isostatic adjustment (GIA) predictions drawn from a suite of ice-sheet models (ICE-G5, ICE-G6 and ANICE-SELEN) that are used in combination with the same solid Earth model and mantle viscosity parameters. Results indicate that the GIA signal is not the main cause of the observed highstand variability and that other mechanisms are needed. The GIA simulations show that, even within the Mediterranean Basin, the maximum highstand is reached at different times according to the geographical location. Our work shows that, besides GIA, even in areas considered tectonically stable, additional vertical tectonic movements may occur with a magnitude that is significantly larger than the GIA.

Keywords

Fossil and Present Tidal Notches, glacial isostatic adjustment (GIA), Vertical tectonic movements

1. Introduction

1. Introduction

Quantifying the elevation and duration of the high-stand that occurred during the Last interglacial, Marine Isotope Stage (MIS) 5.5, is of key importance as it allows the sensitivity of the Greenland and Antarctic Ice Sheets (GrIS and AIS, respectively) to climate conditions that are warmer than the present day to be assessed (all acronyms are defined in table S1). The MIS 5.5 highstand can, therefore, be used as an analogue for future scenarios of global warming, which is of key importance to 2100 sea-level projections. The elevation above the present sea level (p.s.l.) of the highstand, measured in globally stable areas (Rovere et al., 2016), has previously been estimated based on coral reefs using various methods (Bard et al., 1990; Chen et al., 1991; Chappel et al., 1996; Schellmann and Radtke, 2004; Blanchon et al., 2009; Dutton et al., 2015). These estimates show a significant uncertainty (some meters) in the assessment of the palaeo sea level (Muhs et al., 2017) because corals do not accurately mark the sea level but live in the photic zone. Furthermore, in many regions of the world coral reefs are absent and cannot be relied on to constrain the ~~heioght~~height of MIS 5.5 sea levels.

In tectonically stable areas of the Mediterranean Sea (Fig. 1A), fossil tidal notches (FTNs) of MIS 5.5 age are found at 6–8 m above present sea level (Ferranti et al., 2006; Lambeck et al., 2011, Present tidal notches or PTNs). The base of a tidal notch is considered the best and most precise marker of average palaeo sea level because its width is closely linked to the local tidal range (Antonioli et al., 2015; Rovere et al., 2016; Lorscheid et al., 2017a). The age of FTNs is constrained through correlation with adjacent marine deposits that are either; 1) ~~radiomnetrically~~radiometrically dated using the Th/U method or 2) contain the “Senegalese” fauna (a biostratigraphically distinct ~~assmeblage~~assemblage of marine mollusca the appearance of which, in the Mediterranean, is robustly constrained to MIS 5.5). The Mediterranean Sea is microtidal in character and many examples of late Holocene tidal notches formed in carbonate bedrock occur (e.g. Benac et al., 2004, 2008; Antonioli et al., 2007; Furlani et al., 2011, 2014a). These features allow the relationship between tidal notches and sea level ~~elevatiuon~~elevation to be discussed and estimates of MIS 5.5 sea level to be assessed and corrected.

The aim of this study is to investigate the role of crustal movements in the height ~~distirbution~~ distribution of MIS 5.5 FTNs in the Mediterranean, ~~primarilly~~primarily Italy but also from other locations across the basin. ~~The stidy is based upon precise~~ In this study we present a database of the ~~morphometeric~~morphometric measurements and height elevation of MIS 5.5 FTNs from across the Mediterranean as well as a summary of the chronological information that has been used to correlate these features to the Last Interglacial. The elevation and morphometric relationship between these MIS 5.5 FTNs and modern tidal notches is discussed and ~~presnted~~ presented in order to make observations about crustal movements (furthermore a number of older TFNs are identified and discussed). The paper then maps the regional variability of the elevation of MIS 5.5 notches and compares this variability with predictions of specifically built GIA models that include different ice-sheet scenarios. The paper concludes by evaluating the residual difference between the measured heights of MIS 5.5 FTNs and the GIA-corrected ~~elevetaion of nothcs~~elevation of notches in the light of tectonic movement.

2. Background setting

2.1. The tidal notch

Nearly half of the Mediterranean’s rocky coasts are generated on carbonate rocks (Furlani et al., 2014b). Such coasts are characterized by a typical set of landforms (Taborosi and Kazmer, 2013), which are related to a combination of mechanical (Trenhaile, 2002), chemical (Higgins, 1980; Furlani et al., 2014a) and biological processes (Torunski, 1979), although recently Trenhaile (2014) has argued that notches form also as a consequence of wetting and drying cycles. While bioerosion plays a role in the lowering of rocks in the intertidal zone, some hard bottom biological communities can protect the bedrock from erosion (Laborel, 1987; Naylor and Viles, 2002). ~~A common landforms in these settings are Tidal notches, these~~ Tidal notches are indentations or undercuttings that are mainly cut in steep carbonate cliffs at sea level; they are amongst the most common landforms along the Mediterranean's coasts and range from a few centimetres to several meters in width. Antonioli et al. (2015) defined a tidal notch as the undercutting found at, or near, the tidal level on carbonate sea cliffs shaped with characteristic morphology. Tidal notches have been widely used as sea level indicators for more than 150 years, and many authors have suggested that they are cut by complex and polygenetic processes (Spratt et al., 1895; Carobene, 1972; Higgins, 1980; Pirazzoli, 1986; Antonioli et al., 2004, 2006; Kelletat, 2005; Furlani et al., 2011, 2014a; Trenhaile, 2014, 2015; Moses, 2013; Moses et al., 2015). Antonioli et al. (2015) measured the morphometric parameters of notches at 73 sites in the central Mediterranean Sea, together with the occurrence and features of the biological rims at their bases, and they correlated these parameters with wave energy, tidal range and rock lithology. Their conclusions were that *'tidal notches in the Mediterranean are, rather than the effect of a single process, the result of several processes that co-occur with different rates'*(pag. 81).

When the floor is lacking, a tidal notch is defined as a marine notch (Pirazzoli, 1986; Kelletat, 2005; Boulton and Stewart, 2015; Trenhaile, 2015), ~~which~~ although some authors still ~~is sometimes~~ calll it~~led~~ a tidal notch ~~by some authors~~ (e.g. Antonioli et al., 2015; Furlani et al., 2017) in order to distinguish it from an inland notch (Shtober-Zisu et al., 2017). Its shape is, in fact, affected by the local tidal range, with a maximum width, *sensu* Antonioli et al. (2015), up to 400 cm (Trenhaile, 2015). In the Mediterranean Sea, present day notch width ranges from 13 to 95 cm. When the floor is lacking, we define the notch as a roof notch. A notch which develops near the sea floor, with sand and pebbles that ~~which~~ mechanically erode the rock, is defined as an abrasional notch. It has no correlation with sea level, as it shows a depth and width which are different from the local tidal regime (Antonioli et al., 2015).

2.2. Geotectonic setting of the central Mediterranean Sea

The indented coasts of the Mediterranean Basin and the present configuration of the coastal landscape are the result of the interaction between tectonic and morphoclimatic processes that acted during the long-lasting convergence, active since the Late Cretaceous, between the African and European plates along an east-west boundary (Rosenbaum et al., 2002). The region is characterized by n~~N~~arrow as well as broader zones of seismicity and geodetic deformation, which highlight the position of the major plate boundary and of the boundaries of minor plates whose interiors appear to be largely aseismic (Anzidei et al., 2014; De Mets et al., 2015).~~, characterize the region.~~

The basins of the central Mediterranean Sea are the result of different tectonic processes (Oldow et al., 2002; Rosenbaum et al., 2002; Anzidei et al., 2014). The Adriatic Sea and the surrounding promontories are the remaining parts of the Adriatic continental lithospheric block, caught between Europe and Africa, which served as the foreland domain for the southern Alpine, Dinarid-Hellenid and Apennine thrust belts. The Tyrrhenian Sea is a back-arc basin that opened behind the Apennines in the wake of the retreating Adriatic-Ionian slab and is partially floored by oceanic crust. The Ionian Sea is a remnant of the old Ionian oceanic lithosphere, closed between the Calabria and Hellenic subductions. The result of this tectonic evolution is a complex mosaic in which, during the Late Pleistocene and the Holocene, areas of recognized tectonic stability (Sardinia, western and southeastern Sicily, Campania, southern Apulia, Ligury and Tuscany) alternated with areas marked by often large vertical movements (eastern Sicily, Calabria, Basilicata, Veneto and Friuli, ~~i) (~~Ferranti et al., 2006, 2010; Antonioli et al., 2009). This pattern of vertical stability or deformation is supported by the analysis of seismicity and of global positioning system (GPS) data (Oldow et al., 2002; Devoti et al., 2017; Serpelloni et al., 2014).

In addition to tectonic processes, glacio-eustatic sea level changes ~~driven by astronomical causes~~ induced the extensive reshaping of the coastal areas during the Quaternary. Terraced marine deposits and landforms, such as notches, sea caves, inner margins and paleocliffs, mark the past sea-~~-~~level stands, which~~and~~ are found ~~today recognizable~~ below and above present-~~-~~day sea level. The study of these geomorphological features ~~and the constraining of them chronologically~~ has ~~permitted~~ allowed the recognition of the regional tectonic ~~behaviour~~behavior and the long-term ~~to rent~~ sea-~~-~~level trend, which have been summarized in recent papers by Ferranti et al. (2006; 2010), Antonioli et al. (2009) and Furlani et al. (2014a).

2.3. The MIS 5.5 highstand

The marine isotope substage (MIS) 5.5 corresponds to the last interglacial period.~~, and i~~Its geochronology is based on orbital tuning of high-resolution deep-sea oxygen isotope stratigraphy. The geochronological subunit MIS 5.5 occurred between Termination II (end of MIS 6) and the onset of MIS 5.4 and lasted from 132 to 116 ka (Stirling et al., 1998; Shackleton et al., 2003; Kopp et al., 2009; Murray-Wallace and Woodroffe, 2014). The study of Last Interglacial shorelines dates back at least a century (Gignoux, 1913), and sea level indicators that formed during MIS 5.5 have been reported from over one thousand sites worldwide (Pedoja et al., 2011).

With respect to the Mediterranean Sea, since the identification and definition of the *Tirreniano* interglacial stage (effectively MIS 5.5) by Blanc in Sardinia at Cala Mosca in 1908, numerous studies ~~have been published that~~ have identified and dated hundreds of Last Interglacial, or 'Tyrrhenian', sites throughout the Mediterranean (Blanc, 1936; Malatesta, 1985; Hearty 1986, 1987; Zazo et al., 1999; Lambeck and Bard, 2000; Nisi et al., 2003). Using a compilation of 246 sites, all attributed to the MIS 5.5, Ferranti et al. (2006) found a significant alongshore difference in site elevation from +175 to −125 m in respect to the present sea level, which they attributed to the interplay of regional and local tectonic processes, including faulting and volcanic deformation.

A recent integrated study (Amorosi et al., 2014; Negri et al., 2015) of *Fronte Section* near Taranto, Italy detailed one of the most representative and extensive MIS 5.5 sequences to be found in the

Mediterranean. Facies analysis, detailed macro- and microfaunal characterization and sequence stratigraphy (using Senegalese fauna and ten U-series dates on *Cladocora caespitosa* samples) permitted an unequivocal MIS 5.5 age (132–116 ka) to be attributed to these deposits. These results portray~~show~~ the composite section ~~to be~~as a very promising candidate (named Tarentiano) in the search for the Upper Pleistocene global boundary stratotype section and point (GSSP).

In the Mediterranean Sea, *Cladocora caespitosa* is one of the few scleractinian corals~~s~~ that build extended bioherms and the only one that does so at the present time. Its presence is recorded at depths of a ~~few metres (4–10 m)~~4-10 m as well as down~~up~~ to 30–40 m ~~of water depth~~ (Peirano et al., 2004; Silenzi et al., 2005; Peirano et al., 2009). Existing banks of *Cladocora* are reported in Croatia (Kružić and Benković, 2008), ~~the largest of which~~where ~~-~~the most extensive one that is known in the Mediterranean covers an area of more than 650 m^2~~, and is the most extensive known from the Mediterranean~~. The depth of the Croatians banks ranges between ~~is~~ 6 and ~~–~~21 m. Hence, the presence of this coral as fossil allows for the age determination~~the age~~ of the past sea-level ~~high~~ stands~~, to be dated~~ but it is definitely not a reliable indicator of ~~the~~ paleo water depth ~~depth to be established~~. The presence in fossil deposits of *Persististrombus latus* (= *Strombus bubonius*) and other Senegalese fauna have allowed the dating of thousands of deposits, giving a precise chronological attribution.

Finally, Hearty (1986) used available U\th dates and the presence of Senegalese fauna on some MIS 5.5 fossil deposits to calibrate the amino acid ratio of shells from these sediments and landforms across the whole Mediterranean area (in particular, *Arca*, *Glicymeris* and *Cerastoderma*). Using this approach, he was able to use the amino acid ratios to infer a MIS 5.5 age of undated or barren deposits from elsewher ~~e~~in the region.

2.4 "Senegalese fauna".

In the Mediterranean geological context, the term Senegalese fauna indicates a fossil faunistic assemblage consisting of warm species, from the Atlantic (Gignoux, 1911a, b) where ‘‘the most famous and common is *Strombus bubonius* Lamarck 1791’’ (Gignoux, 1913). Other warm water species are represented by *Patella ferruginea*, *Conus ermineus*, *Gemophos viverratus*, *Cardita calyculata senegalensis* and *Hyotissa hyotis*. The gastropod *Persististrombus latus* (Gmelin, 1791) (named until 2010 *S. bubonius*) entered in the Mediterranean sea only during the Tyrrhenian time corresponding to the Last Interglacial Time ; this last term - in the form "Tirreno" - has been proposed for the first time by Issel (1914) and then by Dépéret (1918) for indicating the age of raised marine terraced deposits characterised by the presence of Senegalese fauna with or without *P. latus*.

It is generally correlated to the last interglacial (MIS 5.5), which occurred between 132 and 116 ka roughly, but generally extended up to 80k a; this lap of time has been defined thanks to different age determinations performed by means of U/Th analysis on the coral *Cladocora caespitosa* and amino acid racemization analyses on mollusc shells as *Glycymeris sp*, *Arca sp* and *Cerastoderma sp.* associated to the before mentioned taxa (e.g.: Amorosi et al., 2014; Negri et al., 2015 and references therein).

Bonifay and Mars (1963) affirmed that the *S. bubonius* (today *P. latus*) is not the characteristic element of the Tyrrhenian and Senegalese deposits. In fact, it is very important to underline that the presence of this tropical gastropod defines only a fossil facies and not all Tyrrhenian deposits ("Tirreno" in Issel, 1914) with warm fauna of Atlantic origin (sensu Gignoux, 1911a,b; 1913) or Senegalese (sensu Bonifay and Mars, 1963).

2.54. Glacial- and hydro-isostatic adjustment

Quantifying the melting of the GrIS and AIS during the MIS 5.5 on the basis of paleo RSL indicators from tectonically stable areas requires that the GIA process ~~to be~~is accounted for (Dutton and Lambeck, 2012). This is usually accomplished by means of numerical modelling. The latter demands that an ice-sheet model, which describes the forcing function (i.e. the surface loading variation), is combined with a solid Earth model, which describes the response function (i.e. solid Earth and geoid deformations). The outcome yields the space- and time-dependant RSL changes that accompany and follow the ice-sheet fluctuations. The GIA-driven RSL changes incorporate all the solid Earth and geoid deformations that stem from the pre-MIS 5.5 glacial-interglacial cycles (in particular the melting of MIS 6 ice sheets) as well as from the retreat of the GrIS and AIS during the actual MIS 5.5 interglacial period. ~~The departure of the GIA-induced RSL changes from the eustatic signal is a function of the distance with respect to the ice sheets and of the shape and size of the ocean basins. In the proximity of the ice sheets, the RSL changes are at odds with respect to the eustatic signal, while, in the far-field sites, the RSL changes are in tune with the eustatic signal, but are different because of the solid Earth and gravitational and rotational changes that affect the meltwater redistribution. Overall, these studies show that the local~~ The predicted local RSL change can be very different from the eustatic signal, the difference being~~,~~ a function of the distance with respect to the ice sheets and of the shape and size of the ocean basins. ~~and, in particular,~~It is expected that, even within an enclosed basin such as the Mediterranean Sea, the MIS 5.5 highstand reached~~s~~ different elevations at different times as a function of the geographical location (Lorscheid et al., 2017a; Stocchi et al., 2018). ~~In other words, each site experiences a different elevation that occurs at different times, i.e. the transgressions are not coeval.~~

Neglecting the GIA might significantly hamper the quantification of the eustatic sea-level peak, which ~~is~~ mostly stems from ~~composed of~~ GrIS and AIS ~~glacio-eustatic contributions~~melting. In fact, as discussed by Rovere et al. (2016), early global-scale studies did not (properly) take GIA into account and resulted in estimates of 3–6 m above mean sea level (MSL) (Stearns, 1976; Harmon et al., 1981; Neumann and Hearty, 1996; Stirling et al., 1998). However, more recent studies have incorporated state-of-the-art GIA modelling and independently estimated values from 5 to 9.5 m above MSL (Kopp et al., 2009; Dutton and Lambeck, 2012). These recent results suggest that not only did the GrIS and W~~w~~est~~tern~~ AIS collapse, but also the E~~e~~ast~~tern~~ AIS might have contributed to global sea level at this time.

In the Mediterranean, few studies up to this point have explicitly included the GIA contribution to the MIS 5.5 RSL fluctuations. As highlighted by Sivan et al. (2016), the local GIA-driven RSL highstand in Israel could contribute from 2–2.5 m to the highstand. Creveling et al. 2015 also show that the GIA contribution is significant and cannot be neglected when investigating the tectonic rates of deformation. Rovere et al. (2016), Lorscheid et al. (2017b) and Stocchi et al. (2018) show that the GIA signal is not uniform within the Mediterranean Basin and can contribute from 1–2.5 m of RSL highstand without accounting for extra melting from Greenland and Antarctica. For the latter ice sheets, several chronologies of melting have been proposed so far, but it is still uncertain whether there was a single peak, a two-stand peak or actual fluctuations (see Kopp et al., 2009). Furthermore, Austermann et al. (2017) show that dynamic topography could contribute quite significant subsidence in the Mediterranean that could explain 1–2 m of RSL change at the MIS 5.5. However, these results are not accurate enough for the Mediterranean Basin given the low-resolution model used by the authors. Finally, while the timing of the onset of the MIS 5.5 acme is relatively simultaneous, mostly taking place from 129 ka to 126 ka, the timing of the demise of the LIG acme is more variable and ranges from 122 ka to 113 ka (Rovere et al., 2016).

3. Materials and Methods

We selected and re-measured the features of a set of FTNs from areas that are ~~already known from~~located in the central Mediterranean Sea (S2, ~~-~~Fig. 1) and ~~, but only in areas~~ that ~~have been~~are considered stable since the MIS 5.5 (Ferranti et al., 2006, 2010; Antonioli et al., 2015). ~~In Fig. 1A, the~~The ~~considered~~ stable areas ~~are indicated~~ as well as the 80 surveyed sites are portrayed, respectively, in Fig. 1 A and Fig.1 B-E ~~(Fig. 1B–E)~~. ~~We have also found s~~Six additional sites from~~in~~ other regions~~,~~ such as Morocco, Gibraltar and France (Fig. 1 F–G) (Rodriguez Vidal et al., 2007, 2010; Abad et al., 2012, 2013) were considered because they~~, which~~ show carved FTNs along~~in~~ coasts that are considered stable since the MIS 5.5. All of these were then included in a database (Tables 1, 2, 3 and S7)~~,~~ that included only well-carved FTNs on limestone rocks which presented morphological continuity. We established that a tidal notch ~~it~~ can be~~is~~ defined ~~as~~ continuous when it can be followed laterally for at least 50 meters.

3.1 Measures

The measurements of the FTNs were performed from the base of the FTN to the base of the PTN (**Figs. 2, 3, 4 and 5**). The measure was corrected by 3 cm because it corresponds to the average width of the biological rim once formed and currently eroded at the base of an FTN (Vermetids, Corallinaes Algae and others living at Present sea level). This is the reason why no correction has been introduced about sea level, unless in rare cases where a roof notch and an FTN are present (Circeo and Capri, sites 50 and 55), and therefore a PTN base is lacking (Ferranti and Antonioli, 2007). Even though we recorded the date and time for all measurements, these are the only cases where the measurements of the base of the FTN were referred to the local sea level, corrected for tides.

The measurements of the 80 studied sites (Tables 1 and 2 and table S7) were performed using different tools and with an estimated error ranging from ±1 up to ± 5 cm along the vertical error depending on both the tool and the adopted reference level (MSL, vermetid reef etc., see Fig. 5 and S5). All measurements were referred to the base of the PTN or zones where the vermetid reef was present and considered as representative of the MSL (H = 0). Vertical profiles along the notch sections were realized through several measurements. An uncertainty of ± 2.5 cm was assumed to account for the identification of the marker.

The tools we used and related instrumental uncertainty are the following:

a) Global Positioning System/Real Time Kinematic (GPS/RTK) technique. In eight sites (50, 51, 52, 54, 74, 75, 79 and 80, respectively, in Figs. 4 and 5; Tables 1 and 2, **table S7**), we used the GPS/RTK technique which has an accuracy better than ± 3 cm along the vertical. This depends on both the tool and the adopted measurement base (MSL, vermetid reef etc., see S5), but it often depends on the setting of MSL. An accuracy of ± 5 cm was estimated.

b) Levelling surveys. Sites 50, 51, 52 and 54 were surveyed by a levelling technique, using a Leica Runner4 instrument. Elevation data were referred to the local sea level at the time of the surveys and corrected for tides by the nearest tide station (Fig. 5). An accuracy of ± 5 cm -was estimated

c) Total station. Sites 79 and 80 were surveyed with a Total Station Leica TCRP 1203, equipped with an infrared laser beam, capable of capturing targets at a distance up to one km. For the measurements in the range of about 700 m, we used the laser beam without a prism, keeping a precision of a few mm along the distance. (Fig. 5). An accuracy of ± 5 cm along the vertical was estimated

d) Telescopic rod. In 19 sites (**Figs. 4 and 5; Tables 1 and 2, table** S7), a 10 m long telescopic measuring gauge was used (Telefix). This device provides direct readings on a graduated tape and is built with non-extensible material which ensures an accuracy of about 3 mm when fully extended to 10 m. We estimated an error comprised from 1 to 5 cm depending on the morphological conditions of the PTN and on the position of the MIS 5.5 FTN (**Figure in S5**). This is always used when the FTN is orthogonal above the PTN. Otherwise, when a few degrees of inclination occurred (1–6°) between the platforms of the PTN and the FTN, the top of the instrument was placed a few cm from the FTN base. The level was defined by an operator located on a nearby boat and were taken photos to roughly verify the positioning of the rod with respect to the significant morphologies. An accuracy of ± 1 cm along the vertical was estimated.

d) Tape. In 46 sites (**Figs. 4 and 5; Tables 1 and 2, Table S7**), we used a 20 m long measuring tape, positioned on morphological markers by two operators. This measurement tool was used in sites where the cliff was not back drawn and the tape could therefore be positioned vertically or with an acceptable slant (**Figure S5**) . The use of the tape was done with an operator on the FTN and one on the PTN that is in the sea. Because of the presence of some vertical offset in the position of the two markers, and resulting tilt of the tape from the vertical, these measurements have been assigned an error bar of ± 15 cm.

e) Digital altimeter: In three sites (**Figs. 4 and 5; Tables 1, 2 and Figure S5, Table S7**) where uplifted notches were far from the present day coast, position and elevation measurements were performed by a digital altimeter (Garmin Oregon 650) with a vertical accuracy of 50 cm and were calibrated with respect to the sea level along the nearby coast. Measurements were taken at the base of the FTN and at the vermetid platform. An accuracy of ± 50 cm along the vertical was estimated. When the Vermetid rim was lacking, an uncertain ty of ± 10 cm was summed to the marker identification and instrumental error. Any other specifications about the formation, morphology and spatial variations of the morphological measurements of the PTN can be found in Antonioli et al. (2015).

3.2 Glacial- and hydro-isostatic adjustment

In this paper we investigated the role of GIA in modulating the elevation of the MIS 5 sea-level highstand across the Mediterranean Sea ~~.~~ by means of process-based numerical modelling. We employed three different ice-sheet models to *(i)* quantify the sensitivity of the Mediterranean RSL sites to the GIA process and (ii) evaluate, albeit without recurring specific statistics, which glacio-eustatic scenario better represents the observations.

~~The contribution of GIA to regional RSL changes can only be evaluated by means of forward process-based modelling. The numerical models that account for all the relevant GIA feedbacks usually combine a pre-defined ice-sheet model, which is the forcing function consisting in ice-sheets thickness variations, and a solid Earth model that operates as response function by returning solid Earth deformations and mean sea surface (i.e. the geoid) variations. The difference between the coupled geoid variations and solid Earth deformations results in RSL changes.~~

~~We employ the three ice-sheet models to *(i)* investigate the sensitivity of the Mediterranean RSL sites to the GIA process and (i) evaluate, albeit without recurring specific statistics, which glacio-eustatic scenario better represents the observations.~~

To evaluate the contribution of GIA to the observed RSL changes from the MIS 5.5, we solved the gravitationally self-consistent sea level equation (SLE) (Farrell and Clark, 1976). The SLE incorporates all the GIA feedbacks and yields RSL changes that accompany and follow continental (i.e. land-based) ice-sheet thickness variations ~~(Spada and Stocchi, 2007)~~. We make use of of the SELEN Fortran 90 program (Spada and Stocchi, 2007), which solves the SLE by means of the pseudo-spectral approach (Mitrovica and Peltier, 1991). Accordingly, the SLE solution consists of spatio-temporal convolutions where ice-sheets thickness variations are coupled to solid Earth responses and propagated through time in order to account for the time-dependent viscous relaxation of the mantle. At the core of the SLE formalism is the concept that, at any time *t* since the beginning of the ice-sheet model chronology, the RSL changes of each point of the Earth's surface stem from the solid Earth and geoid deformations induced by all the ice- and water-loading variations that have occurred since the initial time t^0. Accordingly, the solid Earth is assumed to be spherically symmetric, radially stratified, self-gravitating, rotating and deformable, but not compressible (Spada et al., 2003). We assume an elastic lithosphere and a Maxwell viscoelastic mantle. We devide the latter into three layers: upper mantle, transition zone and lower mantle. The core of the Earth is considered inviscid.

We consider three global ice-sheet models that describe the last 240 kyrs of fluctuations (i.e. two glacial-interglacial cycles). This is necessary in order to accurately account for the GIA which accompanies and follows the melting of the MIS 6 ice sheets, as well as the GIA during and after the MIS 5e until the present day. Overall, the three ice-sheet models are very different and are characterized by very different eustatic elevations and temporal durations of the last interglacial phase. The three models are the following:

1. ICE-5G (Peltier, 2004): This model describes the ice-sheet thickness variations over North America, Eurasia, Greenland and Antarctica from 26 ka to present. For this time span, ICE-5G was constrained by the means of geological RSL data and modern geodetical observations (Peltier, 2004). Prior to 26 ka, the ice-sheet growth is tuned to the delta-18O curve (Lisieki and Raymo, 2005) and is not glaciologically realistic (Peltier, 2004). The chronology starts at 123 ka, when the global ice-sheet volume was smaller than it is today and resulted in a eustatic sea level of ~0.9 m above the present level (mostly due to a smaller GrIS; to be specified). In order to capture the GIA contribution to the MIS 5.5 highstand, we combined in time two consecutive ICE-5G chronologies. This allowed us to simulate the ice-sheet growth towards the MIS 6 glacial maximum and the subsequent retreat during the period from MIS 6 to MIS 5.5 Therefore, after the MIS 5e, the ice-sheet chronology is repeated towards the present day (including the last glacial maximum LGM, of course). However, we do not claim that the MIS 6 glacial maximum was the same as the LGM. According to our reconstructed chronology, the MIS 5.5 interglacial starts at 129.5 ka, which corresponds to the end of the initial cycle, and ends at 122 ka. The maximum peak of 0.9 m equivalent sea level (ESL) starts at 125 ka and ends at 123 ka, therefore resulting in a 2 kyr-long (late) highstand (see red dashed curves in **Figs. 6 and 7**).

2. ICE-6G (Argus et al., 2014; Peltier et al., 2015): This model represents the latest improvement of the ICE-5G (see previous entry). We apply the same time discretization and chronology of the ICE-5G. According to the ICE-6G, the maximum MIS 5.5 eustatic highstand is ~3.1 m above present-day MSL as a consequence of the GrIS and AIS retreat and occurred from 125 to 123 ka (see blue dashed curves in Figs. 6 and 7).

3. ANICE-SELEN (de Boer et al., 2014, 2016): This model describes the global ice-sheet fluctuations that follow the delta-18O stack (Lisiecki and Raymo, 2004) and that dynamically account for all the GIA feedback. ANICE-SELEN, therefore, is the result of a fully and dynamically coupled system and, so far, has been ~~. ANICE-SELEN was~~ not constrained by means of RSL data.~~;~~ ~~hence, it is extremely realistic when it comes to the physical processes, but may be locally unrealistic in terms of ice margins and the location of domes.~~ We followed the original ANICE-SELEN chronology and, during the MIS 5e, forced the GrIS and AIS to release, respectively, 2 and 5 m of equivalent sea level (ESR) (see also Lorscheied et al., 2016; Rovere et al., 2016) Therefore,

under the eustatic approximation, this would result in 7.0 m ubiquitous sea-level highstand from 120 ka to 117 ka (see green dashed curves in Figs. 6 and 7).

Overall, the three ice sheet models are very different and they are expected, therefore, to result in different RSL changes not just in the proximity of the formerly glaciated areas, but also at ice distal or far-field sites such as the Mediterranean Sea. Also, it is interesting to compare the response of the Mediterranean basin to two different classes of ice sheet models: (i) ICE-5 and 6G, both the result of RSL data inversions, and (ii) ANICE-SELEN, the result of a pure process-based modeling approach. In fact, whicle ICE-5 and 6G are built to give an excellent fit with post LGM RSL data, ANICE-SELEN purely follows ice-flow physics and dynamics. Therefore, we expect large regional differences, but also a consistent signal in the Mediterranean. This could prove that, regardless of all the uncertainties in the ice sheet models (no model is perfect or 100% realistic), we can constrain the expected GIA response of the Mediterranean (lower to upper limit), and therefore provide better estimates of the absolute glacio-eustatic value at the MIS 5e (mostly Greenland and Antarctic ice sheets reduction).

~~We employ the three ice-sheet models to *(i)* investigate the sensitivity of the Mediterranean RSL sites to the GIA process and (ii) evaluate, albeit without recurring specific statistics, which glacio-eustatic scenario better represents the observations.~~

4. Results

4.1. FTN elevation

The mean elevation of all measurementss (Figs. 1, 2, 3, S2, S3, S4 and Figure S5; Tables 1 and 2) in the studied sites is 5.71 m with a maximum of 12.78 m at Monte d'Argento (southern Latium) and a minimum of 2.09 m (Palinuro, south of Naples). If we do not consider the values lower than 2.5 m (Palinuro, Capo Zafferano and Rosh Hanikra Israel) and higher than 10 m, the average elevation is 5.95 m. We added to the measured sites in Italy six measurements at sites elsewhere in the Mediterranean Sea (Abad et al., 2012, 2013; Rodriguez Vidal et al., 2007, 2015; **Table 3 and Figure S6),** but we did not use these observations for statistical analysis.

4.2 FTN width and comparison with PTN width

The mean width of MIS 5.5 FTN (Figs. 2 and 8; Table 1) is 0.74 m with a maximum of 1.20 m at Levanzo and a minimum of 0.38 m at Palinuro. The PTN mean width is 0.59 m with a maximum of 0.9 m at Levanzo and a minimum of 0.30 m at Palinuro. The FTN/PTN ratio width is 1.28. This value is always larger than 1 (Tables 1 and 2, column 4; Fig. 5). Compared with the PTN widths, the FTN widths are always wider by 10 to 25 cm (Table 1; Figs. 2, 5, S2, S3 and S4).

4.3 FTN depth and comparison with PTN depth

The mean depth of the FTNs (Tables 1 and 2; Figs. 2 and 3) is 0.9 m with a maximum of 1.20 m at Capo Caccia (site 2) and a minimum of 0.20 m at Capo Caccia (site 10). In the Orosei Gulf, near springs with a flow rate of thousands m^3/sec, the PTN has a width up to 4 m (Antonioli et al., 2015). The FTN/PTN ratio width is 0.92 (with a maximum of 1.40 at Levanzo, and a minimum of 0.16 m at Capo Caccia) (Tables 1 and 2, column 4). Compared with the PTN depths, the FTN depths are almost always smaller (Figs. 3, S3, S4 and S5). Regarding the FTN base (Figs. 2 and 3), the mean of our measures is 0.66 m, with a maximum of 1.80 m at Pedralonga (site 2) and a minimum of 0.15 m at San Vito Macari (site 72) (Tables 1 and 2).

4.4 Age of the fossil notch

Regarding the age of the fossil notch, for each site, we considered the distance between the notches and the nearest dated fossil deposit which can be correlated to it. The results (**Fig. 9; Table 1**) show a mean distance of 4.5 km with a maximum distance of 22.9 km (Pedralonga, site 44) and a minimum of 0.2 km (Capo Caccia, site 12). Regarding the quality of analyses or markers used, as explained in Table 1, we provide the references for each site. The dating techniques used for the FTN are the following: 1) U/Th analysis on Cladocora caespitosa or on speleothems; 2) OSL on sandy deposits; 3) Aminostratigraphy on marine shells; and 4) Correlation to fossil assemblages containing Persististrombus latus or other Senegalese fauna.

4.5 FTN older than MIS 5.5

Uplifted FTN older than MIS 5.5 were studied and measured in Sicily and Apulia **(Fig. 1; Table 2, Figure S5; sites 74–80)** at Custonaci, Grotta Racchio, Capo Zafferano, Sferracavallo and Grotta Romanelli (the elevation ranged from 9.2 m at Romanelli to 73 m at Custonaci). These notches show a width from 1.5 to 2.12 m, with a mean of 1.82 m and a FTN/PTN ratio of notch depth always higher than 1 (Fig. 10; Tables 1 and 2).

4.6 Glacial- and hydro-isostatic adjustment

Within the Mediterranean Basin, the predicted GIA-modulated RSL curves for all the three ice-sheet models are significantly different from the eustatic curves (see Figs. 6 and 7). There are significant differences between the predicted RSL curves in the central regions of the basin, such as Italy (Fig. 6) and France (Fig. 7), and the marginal areas, such as Morocco and Israel, respectively, in the western and eastern Mediterranean Sea (Fig. 7a and c). In the central areas, in fact, the RSL curves are characterized by a monotonous RSL rise that lags behind the eustatic signal and that eventually results in a higher than eustatic highstand by the end of the MIS 5.5 temporal window (see solid curves w.r.t. dashed curves of Fig. 6). This holds for all three ice-sheet models that, albeit different, are combined in the same mantle viscosity profile. Interestingly, differences between GIA-modulated and eustatic signal are larger for the ANICE-SELEN (see green curves). The predicted RSL curves at the Italian sites all show a relatively fast RSL increase (about 0.5–1.0 m) from 125 ka to 123 ka, while the eustatic signal is flat for this time span.

The sites at the western and eastern boundaries (Fig. 7a and c) are characterized by earlier highstand, which is then followed by a relative sea level drop. This holds in particular for the ICE-5G and ICE-6G, while the signal is only visible for ANICE-SELEN within the 125–123 ka time window. The latter, in fact, is characterized by a local RSL drop as opposed to the rise at the Italian sites.

The GIA-driven regional contribution to RSL rise is related to the maximum peak from 1–2.5 m within the whole Mediterranean Basin. Notably, higher values are only reached at sites 1–4 for ICE-5G, and the rest of the estimates are within 1.5 m (Fig. 11; Table 5). This implies that GIA alone (leaving out the extra GrIS and AIS glacio-eustatic components) is capable of driving a 1–1.5 m (locally 2.5 m) higher than present sea level during the MIS 5.5. Such a value is comparable to the expected glacio-eustatic contribution of GrIS during the MIS 5.5 The latter, however, shows up at different times according to the geographical location.

The GIA contribution to RSL rise (related to the maximum peak) along the coasts of Italy (including Sardinia and Sicily) is up to 1.5 m (Fig. 12). This holds for all the three ice-sheet models and, therefore, confirms that the GIA signal in the Mediterranean is quite consistent among different ice-sheet chronologies (Fig. 12).

Overall, the predicted maximum peaks according to ICE-5G and ICE-6G (Fig. 12 left) could explain the observed lower limits. On the other hand, the maximum peaks predicted according to ANICE-SELEN fit quite well with some observations and, in general, with the higher limits.

Following from the previous point, GIA results alone are a second-order contributor to variability when compared to the observations. Hence, they can only explain in part the observed regional variations in the maximum peak elevation (see also regional variability in Fig. 11 and Table 5).

5. Discussion

5.1 Notch morphometry: comparison with the PTN

This study has yielded unprecedented details on the MIS 5.5 notch morphometry that can be compared with the morphometry of the PTN studied by Antonioli et al. (2015). The three morphometric parameters (width, depth and base) of PTNs show small differences depending whether they are located in sheltered or exposed areas. Similar results were also achieved for the FTNs (Tables 1 and 2). Moreover, near large fresh water springs (as described for Sardinia's western coast in Antonioli et al., 2015), PTN depths are noticeably higher (more than 4 m), while FTN remain the same because the PTN so deeply carved tend to collapse.

The main difference between the PTN and the FTN is the width. The average FTN width recorded in 67 sites was 0.73 m, while the average width of the PTN in 59 sites was 0.59 m. The conclusion is that the average width of an FTN is 0.14 m wider than that of a PTN. This difference supports, based on a larger data set, the conclusions of Antonioli et al. (2015), derived from data collected in eight sites.

We explain the FTN width exceeding the PTN width by 0.14 m as a result of a combination of chemical and biological weathering of the carbonate bedrock. The aforementioned processes are responsible also of the lack of the biological rim (Vermetids, Corallinales algae) in the FTN. We argue that a biological rim was present at the base of the FTN during MIS 5.5, based on the morphology of its lower part. Antonioli et al. (2006) and Antonioli et al. (2015) describe a fossil vermetid reef in an uplifted FTN attributed to MIS 5.5 near Taormina. With the disappearance of the rim, the notch was also increasingly more exposed to erosion.

Dissolution rates measured on carbonate rocks in the Mediterranean area show values ranging from 0.01 mm/a to 1 mm/a (Furlani et al., 2014b), with higher rates in correspondence with the mid- or low-tide levels (Furlani et al., 2009; Furlani and Cucchi, 2013). The longest data set covers about 40 years (Furlani et al., 2009; Stephenson et al., 2012). Taking into account significant approximations in the extrapolation of erosion rates for the long-term period, such as hundred thousand years or more, due to the complete lacking of instrumental data older than half century or morphometric proxies, a linear extrapolation over 125,000 years, implies a total amount of erosion of Mesozoic limestones hosting FTNs ranging from 0.125 m to 5 m (**Table 4**). Uncertainties can be due to the effects of past local climate setting, that could have affected past erosion rates or different geological conditions, such as the shedding of the notch by younger sediments that have now been stripped off. In some cases, limestone lowering rates can be also higher, such as at Mallorca Island (Gomez-Pujol et al., 2006), with the result of the complete disappearance of MIS 5.5 notches. Softer limestones, such as Miocene calcarenites, have higher dissolution rates, with a total estimated erosion of 100 m (**Table 4**). The latter is not the case for the observed FTNs. The relatively low average difference in width (0.14 m) between FTNs and PTNs calls for erosion rates at the lower boundary of the estimate. The other measured morphometric dimensions of FTNs do not show any systematic difference from those of PTNs.

On the other hand, the preservation of the FTNs at some or several sites and the minimal difference in width with respect to the PTNs could be explained by taking into account subsequent deposition processes which preserved the FTNs, even in the presence of higher dissolution rates. The sediments could have protected the buried forms, at least until their post-LGM exhumation. Many examples of this occurrence have been recorded in many sites in the Orosei Gulf and at Tavolara Island, where traces of LGM eolianites are still found inside the FTNs (Fig. 5i–j).

An FTN changes its morphology and morphometry depending on whether it is covered and preserved by sediments (aeolianites and/or other continental deposits) or not. The final morphometric shape (especially the width) may have a significant enlargement due to karst solution processes, with rates that (on carbonate lithologies) may reach 0.04 mm per year (Furlani et al., 2009, 2010; Furlani and Cucchi, 2013) outside the tidal zone. This is confirmed by the FTN/PTN ratio width that is always greater than 1. The other measured morphometric dimensions of an FTN do not show any peculiar difference from those of a PTN.

5.2. Glacial- and hydro-isostatic adjustment

The departures from the eustasy and the regional variability of the predicted RSL curves (in particular the differences between the central areas and the marginal regions) stem from the ice-induced crustal variations (mostly from Fennoscandia) and the sea-bottom deformations driven by the ocean loading term.

In particular, the monotonous RSL rise and late highstand that are predicted at the Italian sites (Fig. 6) stem from the subsidence of the solid Earth in response to the collapse of the peripheral forebulge (around Fennoscandia) and to ocean load-driven subsidence of the crust. The predicted early highstand in the marginal sites (Fig. 7a and c), which is then followed by an RSL drop, is the result of two processes that are related to both meltwater redistribution and solid Earth deformations. The first is the so-called continental levering, which stems from the lithospheric flexure in response to the loading of the basins and which results in coastal uplift. The second is the migration of meltwater towards the collapsing forebulges. Together, these two processes result in an early highstand (w.r.t. the eustatic signal), which is opposed to the later highstand that is predicted in the central areas (Fig. 6), and the GIA signal is consistent regardless of the ice-sheet models (the predicted GIA variability is smaller if compared to the observations).

Overall, the maximum predicted highstand for the three ice-sheet models do show and confirm that the GIA signal in the Mediterranean is of the order of 1–2.5 m and is quite consistent, regardless of the shape and chronology of the MIS 6 glaciation and deglaciation.

5.3 Notch elevation distribution and comparison with GIA predictions

Measurements of the MIS 5.5 FTN elevation at 74 sites in areas of Italy that are considered tectonically stable in the literature (Table 1; Figure 4, Figures S3, S4, S5) show an average value of 5.73 m, with a maximum of 12.78 m and a minimum of 2.09 m.

The studied sites are far from tectonically or volcanic active zones. Elsewhere in Italy, active tectonic or volcanic processes account for a marked positive or negative departure of the observed MIS 5.5 FTN elevation from the predicted GIA-eustatic elevation, most notably in the northwestern Adriatic Sea and in the Ionian and Tyrrhenian sides of Calabria (Ferranti et al., 2006, 2010). Nevertheless, we suspect that some of the minor scatter between values at stable sites presented in this paper derives from unaccounted albeit slow local tectonic or volcanic processes.

In order to place further constraints on the accurate elevation of the MIS 5.5 FTN, we selected, from the total 74 observed sites in Italy, the 13 sites that we considered less affected by local land motion. Within these 13 sites, we retained only one elevation datum when multiple observations are available at sites that are few tens of meters to few kilometers apart within a geologically coherent area (Table 6). We selected this representative datum based on the ascertained (or suspected) slow tectonic process acting in each area and on the resulting sign of vertical land motion. When the prevailing process is normal faulting or aseismic subsidence related to a passive continental margin development, we considered the highest elevation found in the area as the most accurate. On the other hand, when arching related to magmatic processes controls coastal deformation and the land motion is uplift, we selected the lowest value (Table 6). Similarly, in areas where folding and thrusting produce uplift parallel to the coastline, the lowest FTN elevation is considered as most reliable. When faulting or folding is at a high angle to the coast, the resulting process is tilting and, thus, an intermediate FTN elevation, as close as possible to the tilt axis, represents the most accurate estimate.

We analysed the selected sites' distribution along a regional scale (~850 km long) E-W transect from the western Sardinia margin to the western Adriatic margin in Apulia, with a manually traced trend line of the observed MIS 5.5 highstand elevation (Fig. 13 All the sites but Talamone in Tuscany and Marettimo in Sicily lay very close to the trace of the transect (yellow dots in Fig. 13). Because the two sites in Tuscany and Sicily are far from the trace compared to all the others, we showed these two sites in a different way (white dots in Fig. 13).

In NW Sardinia, we selected the FTN found at the maximum elevation (5.5 m) out of the 20 measurements in the area of Capo Caccia and Punta Giglio (Fig. 1D). As pointed out by Ferranti et al. (2006), NW Sardinia faces the Balearic continental margin of the western Mediterranean Sea, and the decrease in elevation of the FTN from east to west may be the result of fault- or creep-related subsidence (Table 6). Continental margin downthrow is also suspected in SW Sardinia (Buggerru-Masua and S. Antico sectors), so we picked the maximum elevation (3.5 m) as well. It is interesting to note that, on this continental margin, the selected FTN progressively loses 2.5 m of elevation from N (Capo Caccia-Punta Giglio) to S (Buggerru-Masua-S.Antioco) over a distance of 180 km. Whether this occurrence is fortuitous or reflects the process of a southward tilt of the whole of western Sardinia has not been established. However, being at a prominent continental margin, we chose to start the trend line at the maximum elevation in the north.

In respect to eastern Sardinia, Ferranti et al. (2006) suggested the presence of residual volcanic activity to explain the northward increase in elevation pattern of the FTN over a 25 km distance in the Orosei Gulf (sites 37–44; Fig. 1D). Mariani et al. (2009) modelled this deformation with a magmatic intrusion that post-dates the MIS 5.5 notch, as documented by minor explosive breccia flows that locally cover the notch. Based on this argument, the elevation increase is related to tilting ensuing from intrusion. Because the prevailing land motion is an uplift, we selected the minimum elevation (7.0 m) of the FTN observed at the Pedralonga site (Table 6). In NE Sardinia, the MIS 5.5 notch shows about 2 m difference in elevation from Tavolara (6–7 m) in the south to Capo Figari (4.5–5 m) in the north, over a distance of less than 10 km. Regional NE-SW striking left transcurrent faults that cross the interposed bay could be responsible for the coast-parallel tilt, but they are retained as inactive (Oggiano et al., 2009). With the existing uncertainty, we included in the selection both the lowest elevation at Capo Figari and the highest elevation at Tavolara, assuming a tilt axis lies in between. The trend line crosses the eastern Sardinia margin midway between the observations at Capo Caccia, Tavolara and Capo Figari (Fig 13).

On the eastern Tyrrhenian margin, only an FTN observation (Talamone, 4.8 m elevation) is available from Tuscany in the north. This site is projected 250 km southward on the transect and, as for the Capo Figari site, has an elevation residing under the trend line, suggesting it could have been lowered by unaccounted processes.

South of Talamone, sites in Latium show a 3.4 m south-eastward decrease in elevation from 9.3 m (Circeo) to 5.9 m (Gaeta) along 50 km of coast which at this location has an E-W trend (Fig. 1B). We discarded from selection the site of Minturno, which displays the highest measured elevation in this study (12.48 m, site 54, Figures 11 and S4), because we considered it affected by processes related to the now extinct Roccamonfina volcano. The last documented activity of the volcano was at 150 Ka BP, but younger activity could have occurred (Rouchon et al., 2008). We also suspected that the continental margin rebound affected the 9.3 m elevation of the FTN at Circeo, and, thus, we excluded this site as well. The remaining three sites have elevations ranging from 6–6.5 m (Gaeta-Sperlonga) to 8 m (Terracina). The Terracina site lies close to a post-MIS 5.5 extensional fault, and, thus, the footwall uplift may have contributed to a fraction of the observed elevation. Fortunately, a borehole in the nearby Fondi Plain, located in the immediate hanging wall of the fault, which has revealed MIS 5.5 deposits at –6 m, allowed making a predictive estimation of the footwall uplift. By using a ratio of hanging-wall subsidence to footwall uplift of 1:10, supported by theoretical modelling and observational data (King et al., 1988; Armijo et al., 1996), the 14 m difference between the FTN at Terracina in the fault footwall and the drilled deposit in its hanging-wall results in 1.4 m footwall uplift. In terms of difference, the estimated GIA-eustatic position of the FTN at Terracina is 6.6 m (Table 6). This estimate is strikingly similar to observations in nearby Sperlonga and Gaeta, suggesting that the trend line passes through the corrected elevation at Terracina.

Several FTNs have been measured between Capri Island and Sorrento Peninsula (Campania). As pointed out by Ferranti and Antonioli (2007), the elevation of the notch at Capri decreases progressively from southeast (8.0 m) to northwest (5.2 m). The pattern of down-dropping of the tidal notch is consistent with the active subsidence with a maximum occurring in the Gulf of Naples, located north of Capri Island, and monocline tilting of the island and the nearby Sorrento Peninsula. We argue that the axis of tilting at Capri is at an elevation of 7.0 m, which is the most represented FTN elevation (Tables 1 and 6).

Further south, in Cilento, contrasting observations come from Palinuro (FTN at 2.1 m) and from nearby Marina di Camerota - Bulgheria site (FTN at 6.7 m) (Table 1, Figure S4, site 54). In line with the reasoning for continental margin faults, we regard the higher measurement as the most accurate.

The group of FTN sites measured in NW Sicily (Fig. 1E) is placed over an active collisional margin, where the convergence between Sardinia and Sicily in response to African and European plate motion is accommodated by thrusting and folding and is expressed by seismicity and geodetic data (Ferranti et al., 2008; Palano et al., 2012; Serpelloni et al., 2007). Thus, we picked the lowest observed FTN elevation (8.1 m at Marettimo) as representative of this sector, after discarding the very low elevation data from Capo Zafferano which could have been affected by local subsidence. When we projected the Marettimo datum 200 km northward on the trend line, a positive mismatch of about 2 m with respect to the trend line is estimated (Fig. 13).

The easternmost observed notch was at an elevation of 8.2 m at Striare in Apulia, at the southward terminus of the Adriatic Sea. Southern Apulia lies at the eastern tip of the conspicuous regional uplift of the Calabrian Arc, related to Ionian plate subduction (Ferranti et al., 2006, 2010), and, thus the FTN elevation could be 1–2 m higher than the trend line because of a far-field tectonic residual (Fig. 13).

A comparison between the selected observations of the FTN elevations and the predicted values from the ANICE-SELEN GIA model reveals that the GIA signal is partly at odds with respect to the observed trend (Fig. 13). Along the E-W transect, shown in Fig. 13, the GIA signal has elevations that are up to 4 m higher than the observation points, and 1–3 m higher than the inferred observational trend. The discrepancy between the GIA predicted values and the observations is higher in western Sardinia (Buggerru) and at the northeastern Tyrrhenian margin (Talamone), and progressively decreases to 1–2 m towards the the southeastern Tyrrhenian (Capri) margins, and on the Adriatic margin (Striare), where it is minimal. The observed and predicted trends along this transect appears to be comparable in the sector between the Adriatic and Tyrrhenian margins, with a 1.5–2 m lower elevation for the observed trend. Only the observed FTN at Terracina has an elevation similar to the predicted value, but, as outlined above, the elevation at this site has been corrected to 6.6 m.

The lower-than-predicted observed values in western Sardinia, and possibly at Talamone, could have been affected by unaccounted marginal tectonic subsidence, and this could alleviate the discrepancy. On the other hand, the cluster of selected sites on the Latium-Campanian coast (Terracina, Sperlonga, Capri and Marina di Camerota) seems to define a 6.5 reference value as the most appropriate. Under this hypothesis, a 1.5 difference with predicted values still remains in the comparable part of the transect (Fig. 13). This observation allows us to argue that the glacio-eustatic contribution at the MIS 5.5 was probably lower than most recent estimates (Kopp et al., 2009).

5.4 Age of the FTN

In this section of the study, we define the age of FTN in areas of the Mediterranean that are considered tectonically stable on the basis of correlation to well-known dated sediments attributed to the MIS 5.5. The latter were dated due to the presence of *Senegalese* fauna or by means of U/Th on *Cladocora caespitosa* or on speleothems, OSL or aminostratigraphy age determinations (Table S7). In fact, many FTNs are dated at MIS 5.5 because they are correlated very closely and at similar elevations with fossiliferous deposits (Fig. 9; Table 1) which contain *Senegalese* fauna. This argument was debated at the end of the nineties, when some authors (Hillaire-Marcel et al., 1996; Zazo et al., 1999) indicated that, in fossiliferous deposits on the southern Spanish coast, there were various levels containing *Persististrombus latus*. The consequence of this would have been that *Persistrombus* entered the Mediterranean Sea in various isotopic stages (MIS 11, 7, 5.1 and 5.3). In 2009, Mauz and Antonioli denied this thesis, arguing that, in the Mediterranean, *Persististrombus* and correlated tropical Senegalese fauna had been found only in one level (or terrace in uplifted areas, i.e. Calabria). There are no doubts that the *Persististrombus* gives a precise dating of an FTN. Furthermore, in stable areas, the sea level related to MIS 9 and 11 transgressions (or older) has always remained at similar elevations, and the occurrence of subsequent transgressions at the same elevation has always obliterated the older ones. Finally, Antonioli and Ferranti (1992) in the Orosei Gulf, dated pulmonate molluscs found in the aeolianites that were inside the FTN to MIS 2. Thus confirming that an FTN can be ascribed only to the most recent phase of the high sea level preceding the MIS 2, namely the MIS 5.5. Figure 9 shows that at sites 41-44 the distance between the FTN and the dated deposit is more than 20 km. These sites are located within the gulf of Orosei (Sardinia, Italy) one of the remotest and least anthropized coasts of the central Mediterranean sea. It is, therefore, likely that the distance between the measured FTN and the dated deposit is, in this case, a result of the inaccessibility of this region for study. These sites are some of those where the FTN is longer and more continuous than anywhere in the entire Mediterranean: between sites 38 and the 44, the FTN is constantly exposed and visible. These sites are, therefore, reliably considered to represent the same FTN and be of robust MIS 5.5 age.

5.5 Notches older than MIS 5.5

Uplifted FTNs older than MIS 5.5 were measured in Sicily and Apulia (Fig. 1; Table 2; sites 75–80) at Custonaci and Grotta Racchio (Trapani), Capo Zafferano, Sferracavallo (Pa) and Grotta Romanelli (Lecce), (S4). These uplifted FTN show a mean width of 1.79 m, compared to a mean width of 0.74 m of the MIS 5.5 FTNs. This difference is significant and very obvious, as it is two and a half times wider than MIS 5.5; furthermore, these FTNs are uplifted at an elevation from 9 m and 73 m (in column 5 of Table 2). Although greater in width, these uplifted FTNs cannot be confused with the smoothed notch sensu of Antonioli et al. (2006) (Figs. 2 and 3), which is much wider at 4 m. Therefore, on the basis of the measurements of these FTNs, we hypothesize that the amplitude of the paleo-tide related to the sea level when these FTNs were carved had a larger range than the present and the MIS 5.5 tides.

The uplifted FTNs of Custonaci and Grotta Racchio are located 1 km from Grotta Rumena (Custonaci) where Stocchi et al. (2017) examined a speleothem (the oldest stalactite containing marine hiatuses ever studied) inside an uplifted cave. In this cave, four marine ingressions are preserved: three hiatuses in the speleothem section and the last one, the younger, is an overgrowth of coral on the speleothem and the roof cave. The authors provided the tectonic uplift rate for the last one million years, and, using a multidisciplinary approach (assuming a continuous vertical uplift tectonic at a rate of 0.81 mm/yr), provided the age of the fourth and last marine ingression based on scleractinian coral species (1.1 ± 0.2 Ma). The latter corresponds are related to MIS25 (Stocchi et al.,2017). The cave is presently located at the altitude of 97 ± 0.2 m. In Fig. 10, the blue curve is referred to the chronological attribution of the uplifted FTN (sea level curves in Lisiecki and Raymo [2005], corrected for GIA in Stocchi et al., [2017]); the red curve is corrected with tectonic movements (0.81 mm/y). Comparing the elevations of the studied FTNs, located at 73, 58 and 34 m, with the red curve, the FTNs (green arrows) corresponded with the highstands of

MIS 25, 21 and 11, respectively. These highstands refer to the last transgression in the Grotta Rumena (MIS 31), witnessed by corals covering the walls and some stalactites (comprising the studied hiatus, not the older hiatuses).

Regarding the FTNs located at 40 m and 23 m, respectively, at Sferracavallo and Arco di Zafferano, the comparison had less precision because the surrounding area of Palermo was certainly uplifted during the Middle-Lower Pleistocene, with vertical tectonic uplifting rates presumably lower than those of Custonaci.

In the area of Custonaci, the FTN studied at Grotta dei Cavalli (San Vito lo Capo, Table 2, S4, site 77), was located at an elevation of 34 m. Based on the curve corrected for tectonics in Fig. 10, this highstand could be attributed to MIS 11. Although the width of the FTN has been blunted by erosion, the measure (0.60 m in Table 2, S4) is fully compatible with the PTN or with the MIS 5.5 FTN. Therefore, this Middle Pleistocene FTN shows a width similar to MIS 5.5, while the other uplifted FTNs at higher elevations (showing an average width of 1.82 m) are placed in the lower Early Pleistocene. In this period the highstands and the lowstands (glacial-interglacial, Fig. 12) occurred with a mean period of 40,000 years, and not at a period of 100,000 years as occurred in the High and Middle Pleistocene (transgressions MIS 5, 7, 9 and 11). This obvious global climatic change (established by hundreds of global curves performed all over the world) could have determined higher tides in the Mediterranean, and the width of the FTN here described is a direct proof.

In summary, the red curve in Fig. 10, following Liesiki and Raymo (2005), allows us to attribute to the FTNs located at 73, 58 and 34 m an age of 950, 850 and 400 ka, respectively. For the FTNs located in the Palermo area at the elevations of 40 m and 23 m, we can hypothesize a lower or non-continuous uplift rate compared to what was found in Custonaci, and assess, on the basis of the width, that they are aged at the Lower Pleistocene. It is possible to hypothesize a sharp change of tide amplitude presumably during the transition to Middle-Lower Pleistocene (780 ka BP).

5.6 Tides

Antonioli et al. (2015) demostrated that the tidal notches are strictly connected with the local tide. But the width of the present tidal notch shows higher values when compared with the local tide (on average the notch has a width slightly less than twice in respect to the mean tidal range). Comparing the FTN width with the PTN width, our results show that the FTN width (mean 0.73 m) is wider by about 0.14 m than that of the PTN (mean 0.59 m); we interpret this greater amplitude as being due to the lack of the biological reef and to the chemical and mechanical erosion of the notch.

Therefore, we believe that the tides of the Mediterranean Sea during the MIS 5.5 highstand were the same as ~~. Temptatively~~ today. Tentatively, considering the mean width of PTNs as 0.59 m and 0.38 m as the current mean Mediterranean tide (Antonioli et al., 2015), we can extrapolate the palaeo-tide of MIS 25–21 (when the mean width of the uplifted tidal notches is 1.82 meters), resulting in a possible tide of 1.21 m, before 780 ka BP, more than three times that of today.

6. Conclusions

At 80 sites in Italy and subordinately in the eastern and western Mediterranean Sea (Tables 1 and 2), the MIS 5.5 and few older notches have been accurately measured. The main conclusions of this study are:

1. The morphometric parameters of the PTN and FTN are broadly similar, with only a slightly larger FTN width due to the lack of the biological reef and to the chemical/mechanical erosion of the cliff during later exposure. This result implies that tide amplitude has not changed in the last 125 ka.

2. In contrast, during the MIS 25–21 highstands (1.2–0.6 Ma BP), the Mediterranean tides had amplitude three times larger than today.

3. The GIA-driven RSL changes within the Mediterranean Basin are regionally varying and significantly different from the eustatic signal. Two main typologies of RSL curves can be expected: monotonous rise followed by a late highstand in the central areas and initial (early) highstand followed by an RSL drop in the marginal regions at the western and eastern borders. Overall, the variability of the maximum GIA elevation is between 1 and 2.5 m, i.e. comparable to the expected eustatic contribution of the GrIS. 10.

4. Provided that the notches represent the maximum peak of local RSL rise, which may occur at different times and with different elevations from place to place (as explained by GIA), the observed spatial variability of MIS 5.5 notches is 1–12. m. This implies that GIA plays a secondary role in driving the regional variability of the maximum MIS 5.5 RSL elevation, and other regionally varying signals, either geologic or oceanographic, are operating.

5. Geologic processes are represented by volcanic intrusions (e.g. at the Orosei Gulf in Sardinia and at Minturno in Latium), or by tectonic displacement (e.g. continental margin down-faulting in western Sardinia and on the eastern Tyrrhenian coast, or contractional uplift in northern Sicily). These low-rate processes cause a spread of up to 10 m in the FTN elevation, five times larger than the GIA variability, even at sites commonly regarded to be on stable crustal sectors.

6. The elevation of the MIS 5.5 notch at selected sites which are less affected by these low tectonic or volcanic movements has a trend that, along a regional E-W transect, mimics but is 1–2 m lower than the predicted values from the GIA ANICE-SELEN model. The 6.5 m elevated MIS 5.5 notch on the Tyrrhenian margin, which is assumed as a reference elevation, has a 1.5 m discrepancy with the model, thus casting doubt on the currently accepted amount of glacio-eustatic contribution to the RSL during the MIS 5.5.

Acknowledgements

We thank Ian Kendy, editor of Earth Science revue and two anonymous reviewers for comments and useful suggestions. We thank Kurt Lambeck who supplied us with the photograph *of the Calanques FTN. We thank* Joaquin Rodriguez Vidal who sent us the photographs used in Supplementary material S6. *This study has been produced in the framework of the Flagship Project RITMARE* and a contribution to the project IGCP 639 - International Geological Correlation Programme 'Sea-level change from minutes to millennia' by UNESCO-IUGS, We also thanks GEOSWIM project

FIGURE captions

Fig. 1. Location of the investigated sites along the Mediterranean coasts. A. The red rectangles indicate the studied areas. The numbers refer to the sites of Table 1. B. White numbers refer to the altitude of the FTN, see Table 1. C. White numbers refer to the site number indicated in Table 2. D. White numbers refer to the FTN of the sites studied in Sardinia. E. White numbers refer to the FTN of the sites studied in Sicily, see also Table 1, and the white numbers refer to the sea level share of the FTN of the sites studied in Sicily, see Table 1. The yellow dots refer to the uplifted FTN sites (Table 3). F. The white numbers refer to the sites in Israel, indicated in Table 2. G. The white numbers refer to the site number in Frace, indicated in Table 2.

Fig. 2. a) MIS 5.5 and PTN notches morphological sketch. b) Tidal and smoothed notch as is possible to observe today in some sections we studied. c) Evolution of the tidal and smoothed notch during MIS 5.5, the final coverage of fans or aeolianites deposits preserves the notches from the dissolution.

Fig. 3. Sections of fossil and present tidal notch morphology. The letters refer to the width (w), depth (d) and the base of the notch (c). On the right an overlap between the present and the fossil tidal notch (for the sites 52, 71 and 2 of Table 1) morphology highlights the marine and ~~aeolian~~ subaerial erosion that slightly modified the original morphology, but preserves a similar width.

Fig. 4. View of some representative morphology of the studied tidal notches. a) Site 5, Sardinia. b)Site 30, Sardinia. c) Site 38, Sardinia. d) Sites 40 and 48, Sardinia. f) Site 69, Sicily. g) Uplifted FTN site 76, Sicily. h) Uplifted FTN, site 78, Sicily. See also Tables 1 and 2.

Fig. 5. View of the different measurement methods. a) Using the telescopic measuring gauge on site 38. b) Using tape meter on site 39. c., d., e., f., g. and h. Using DGPS on sites 50, 51, 79 and 52. i. and j. In Sardinia, near Grotta Biddiriscottai, an FTN filled with aeolianite sediments aged MIS 2. k) a wall riddled by *Lithophaga* holes under the FTN of site 54. m. In Pianosa, a possible FTN that we did not use in our database due to a lack of geomorphological lateral continuity. Although we recorded day and time during each survey (see Tables 1 and 2), we did not applied tidal corrections because we referred to: a) the base of the PTN, b) the living vermetid reef, except for the FTN of Capri and Mitigliano whose measurements have been taken with respect to the corrected tide sea level, due to the lack of the PTN (Ferranti and Antonioli, 2007).

Fig. 6. Predicted MIS 5.5 RSL curves at sites along the Italian coastlines according to ICE-5G (red curves), ICE-6G (blue curves) and ANICE-SELEN (green curves) ice-sheet models. The dashed curves

represent the eustatic trend, while the solid curves represent the GIA-induced RSL changes. The RSL curves are computed at each investigated site and are plotted cumulatively for different sub-regions.

Fig. 7. Same as for Fig. 6, but for sites in Morocco (a), southern Spain (a), France (b) and Israel (c).

Fig. 8. The FTN width compared with the PTN width. The FTN widths are always a few cm larger due to limestone dissolution (see also Fig. 4). On the right, the larger 2 m width of the uplifted notches, older than last Interglacial period.

Fig. 9. Distance between the measured site and the nearest site dated using 1) U/th, 2) aminostratigraphy, 3) ESR/OSL, but above all, 4) presence of *Persististrombus latus* or Senegalese fauna. The sites are sorted as in Table 1.

Fig. 10. In blue, the Lisiecki and Raymo (2005) curve corrected by Stocchi et al. (2017) for GIA calculated for Custonaci, Sicily. In red, the same corrected curve for a rate of vertical tectonic movement of 0.81 mm/a. In yellow, the calculated age of the uplifted tidal notches of Table 3.

Fig. 11. Maximum predicted RSL highstands according to ICE-5G, ICE-6G and ANICE-SELEN at each site considered in this study. The sites are displayed and enumerated from left to right as a function of the longitude. The numbers in the x-axis correspond to the site number. The horizontal lines correspond to the maximum eustatic value of each ice-sheet model (0.91 m for ICE-5G; 3.1 m for ICE-6G; 7.0 m for ANICE-SELEN).

Fig. 12. Predicted "maximum" RSL elevation (w.r.t. present-day) between 120 kyr BP and 110.0 kyr BP (left) and predicted RSL elevation (w.r.t. present-day) exactly at 117 kyr BP (right). On the left figure we show the maximum RSL elevation predicted, for each element of the surface mesh, between 120 and 110 ka. Because of the viscous response of the mantle, in fact, RSL continues to change also without any further addition of meltwater to the oceans. Hence maximum elevations are reached at different times according to the geographical location and are followed by RSL drop. Comparing left with right reveal indeed that in areas such as Gibraltar and Israel, maximum elevation is reached at 117 ka, and is later followed by RSL drop while other areas experience a further increase. The RSL drop predicted at Gibraltar and Israel is a consequence of *(i)* continental levering (i.e. upward tilt of the continental margins) and *(ii)* meltwater syphoning (i.e. migration of sea water towards the surroundings of formerly glaciated areas in N and S hemisphere).

Fig. 13. Observed and predicted elevation of selected MIS 5.5 FTN sites along an ☐E-W transect from western Sardinia to southern Apulia. Predicted elevations are from the GIA ANICE-SELEN model. The trend across observed elevations is traced based on geological constraints (see text for further details).

TABLES

Table 1: MIS 5.5 and Present tidal notches data in the Mediterranean Sea

1) Site number; 2) Locality and site name; 3) Elevation, uncertain are explained in chapter 3.1 ; 4) Notch Morphometry; 5) Type of Notch: MTN= MIS 5.5 Tidal Notch; PTN= Present Tidal Notch; NM= Not Measured; NC= Not Carved; C= Consumed); 6) Distance (km) and *reference site name for the age of deposit: 1 Abate et al., 1996; 2 Antonioli, 1991; 3 Antonioli et al., 1994a; 4 Antonioli et al., 1994b; 5 Antonioli et al., 1999; 6 Antonioli et al., 2002; 7 Blanc and Segre, 1953; 8 Bosellini et al., 1999; 9 Brancaccio et al., 1986, 1990; 10 Cesaraccio and Puxeddu, 1986; 11 Delicato et al., 1999; 12 Durante, 1975; 13 Esposito et al., 2003; 14 Ferranti and Antonioli, 2007; 15 Hearty P.J., 1986, 1987; 16 Malatesta, 1954a, 1954b, 1970; 17 Mastronuzzi et al., 2007; 18 Orrù and Ulzega, 1986; 19 Orrù and Pasquini, 1992; 20 Orrù et al., 2011; 21 Palmerini and Ulzega, 1969; 22 Pascucci et al., 2014; 23 Porqueddu et al., 2011; 24 Sanna et al., 2010; 25 Segre, 1951; 26 Segre, 1957; 27 Ulzega and Ozer, 1980;

Table 2

FTNs older than the uplifted MIS 5.5. 1) Site number; 2) Locality and site name; 3) Coordinates; 4) Measures; 5) Elevation (m) uncertain is explained in the method section 3.1, as regard site 75, the 0.25 m uncertain was due the particular erosion of the base of the FTN ; 6) Average notch measures (m); 7) Notch Morphometry; 8) Kind of measurement (DGPS= Differential Global Positioning System; DT= Digital Altimeter) 9) MIS 5.5 elevation; 10) Reference for age; 11) Age MIS ka.

Table 3

Published FTN altitude in the Mediterranean Sea.

Table 4

Erosion rates in the intertidal and inner karst in the Mediterranean area. The total erosion for the last 125 Ka was evaluated considering a constant erosion rate.

Table 5

Comparison between GIA prediction with different models and geophysical parameters with the observed data (FTN elevations).

Table 6

Selected sites with MIS 5.5 FTN elevations less affected by tectonic displacement in Italy. See text for further details.

Supplementary material

S1 table Acronyms and definitions.

S2 File kmz of the geographical coordinates of all sites.

S3, S4, S5 Figures. A complete collection of images of all the studied notches (numbers refer to Table 1)

S6 Figures Notches measured in France, Gibiltrair and Morocco, by other authors (refer to Table 3). 1a, b, c: site 81; 2a and 2b: site 82, notch profile and Lithophaga holes; 3: site 83; 4: site 84, Caleta Hotel. MIS 5.5 FTN and its wave-cut-platform , MIS 5.5 FTN (close up) with borings and flowstone; 5a and 5b: site 85; 6a and 6b, site 86, from Sisma Ventura et al., 2017 redrowned. Photo 1, 2, 3, 4 courtesy prof.   , photo 5 courtesy prof. Kurt Lambeck. Photo 6 from redrowned from Sisma Ventura et al., 2016.

S7 Table 7: MIS 5.5 and Present tidal notches data in the Mediterranean Sea

1) Site number; 2) Locality and site name; 3) Coordinates; 4) Measures date; 5) Elevation with uncertain, m; 6) Type of Notch: MTN= MIS 5.5 Tidal Notch; PTN= Present Tidal Notch; NM= Not Measured; NC= Not Carved; C= Consumed; 8) Notch morphometry; 9) Kind of measurement: T: Telefix; M: Tape meter; DGPS: DGPS; 10) Faunal assemblage of the nearest aged fossil deposit; Distance (km) and reference site name for the age of deposit. 1) Site number; 2) Locality and site name; 3) Coordinates; 4) Notch Morphometry; 5) Elevation with uncertain, m; 6) Average notch measures, m; 7) Type of Notch: MTN= MIS 5.5 Tidal Notch; PTN= Present Tidal Notch; NM= Not Measured; NC= Not Carved; C= Consumed); 8) Notch morphometry; 9 Kind of measurement; 10) Faunal assemblages in aged fossil deposit; 11) Thechnique of chronological attribuition; 12 Distance (km) from the site used for give the age of deposit. References: 1 Abate et al., 1996; 2 Antonioli, 1991; 3 Antonioli et al., 1994a; 4 Antonioli et al., 1994b; 5 Antonioli et al., 1999; 6 Antonioli et al., 2002; 7 Blanc and Segre, 1953; 8 Bosellini et al., 1999; 9 Brancaccio et al., 1986, 1990; 10 Cesaraccio and Puxeddu, 1986; 11 Delicato et al., 1999; 12 Durante, 1975; 13 Esposito et al., 2003; 14 Ferranti and Antonioli, 2007; 15 Hearty P.J., 1986, 1987; 16 Malatesta, 1954a, 1954b, 1970; 17 Mastronuzzi et al., 2007; 18 Orrù and Ulzega, 1986; 19 Orrù and Pasquini, 1992; 20 Orrù et al., 2011; 21 Palmerini and Ulzega, 1969; 22 Pascucci et al., 2014; 23 Porqueddu et al., 2011; 24 Sanna et al., 2010; 25 Segre, 1951; 26 Segre, 1957; 27 Ulzega and Ozer, 1980.

REFERENCES

Abad, M., Rodríguez-Vidal, J., Aboumaria, K.,. Zaghloul, M.N., Cáceres, L.M., Ruiz F., Martínez-Aguirre, A., Izquierdo, T., Chamorro, S., 2013. Evidence of MIS 5 sea-level highstands in Gebel Mousa coast (Strait of Gibraltar, North of Africa). Geomorphology 182, 133–146.

Abate, B, Incandela, A, Renda, P., 1996. Lineamenti strutturali dell'Isola di Marettimo (Arcipelago delle Egadi, Sicilia N-O) Mem. Soc. Geol. It., 5, 23-33.

Amorosi, A., Antonioli, F., Bertini, A., Marabini, S., Mastronuzzi, G., Montagna, P., Negri, A., Rossi, V., Scarponi, D.,Taviani, M., Angeletti, L., Piva, A., Vai, G.B., 2014. The Middle–Upper Pleistocene Fronte Section (Taranto, Italy): An exceptionally preserved marine record of the Last Interglacial. Global and Planetary Change 119, 23–38.

Antonioli, F., 1991. Geomorfologia subacquea e costiera del litorale compreso tra Punta Stendardo e Torre S. Agostino (Gaeta). Il Quaternario 4 (2), 257–274.

Antonioli, F., Ferranti, L., 1992. Geomorfologia costiera e subacquea e considerazioni paleoclimatiche sul settore compreso tra S.M. in Navarrese e Punta Goloritzè (Golfo di Orosei, Sardegna). Il Giornale di Geologia 54, 2, 65-89.

Antonioli, F., Cinque, A., Ferranti, L., Romano, P., 1994a. Emerged and Submerged Quaternary marine terraces of Palinuro Cape (Southern Italy). Memorie Descrittive del Servizio Geologico Nazionale 52 237-260.

Antonioli, F., Belluomini, G., Ferranti, L., Improta, S., 1994b. Il sito preistorico dell'arco naturale di Capo Zafferano (Sicilia). Aspetti geomorfologici e relazione con le variazioni del livello del mare. Il Quaternario, Italian Journal of Quaternary Sciences 7(1) 109-118.

Antonioli, F., Reitano, G., Puglisi, C., Tusa, S., 1997. Evoluzione geomorfologica pleistocenica del settore costiero di S. Vito Lo Capo (Trapani): rapporti tra neotettonica, eustatismo e comunità preistoriche. Memorie Descrittive del Servizio Geologico Nazionale 52, 337-360.

Antonioli, F., Silenzi, S., Vittori, E., Villani, M., 1999. Sea level changes and tectonic stability: precise measurements in 3 coastlines of Italy considered stable during last 125 ky. Physics and Chemistry of the Earth (A) 24, 337-342.

Antonioli, F., Cremona, G., Immordino, F., Puglisi, C., Romagnoli, C., Silenzi, S., Valpreda, E., Verrubbi, V., 2002. New data on the Holocenic sea level rise in NW Sicily (central Mediterranean Sea). Global and Planetary Change 34, 121-140.

Antonioli, F., Ferranti, L., Kershaw, S., 2006. A glacial isostatic adjustment origin for double MIS 5.5 and Holocene marine notches in the coastline of Italy. Quaternary International 145–146, 19-29.

Antonioli, F., Anzidei, M., Lambeck, K., Auriemma, R., Gaddi, D., Furlani, S., Orrù, P., Solinas, E., Gaspari, A., Karinja, S., Kovačić, V., Surace, L., 2007. Sea level change in Italy during Holocene from archaeological and geomorphological data. Quat. Sci. Rev. 26, 2463-2486.

Antonioli, F., Ferranti, L., Fontana, A., Amorosi, A., Bondesan, A., Braitenberg, C., Dutton, A., Fontolan, G., Furlani, S., Lambeck, K., Mastronuzzi, G., Monaco, C., Spada, G., Stocchi, P., 2009. Holocene relative sea-level changes and vertical movements along the Italian and Istrian coastlines, Quaternary International 206, 102-133.

Antonioli, F., Lo Presti, V., Anzidei, M., Deiana, G., de Sabata, E., Ferranti, L., Furlani, S., Mastronuzzi G., Orru, P. E., Pagliarulo, R., Rovere, A., Sannino, G., Sansò, P., Scicchitano, G., Spampinato, C. R., Vacchi, M., Vecchio, A., 2015. Tidal notches in Mediterranean Sea: a comprehensive analysis. Quaternary Science review. Quaternary Science Reviews 119, 66-84.

Anzidei, M., Lambeck, K., Antonioli, F., Furlani, S., Mastronuzzi, G., Serpelloni, E., Vannucci, G., 2014. Coastal structure, sea-level changes and vertical motion of the land in the Mediterranean. Geological Society, London, Special Publications 388, 453-479. http://dx.doi.org/10.1144/SP388.20

Argus, D.F., Peltier WR, Drummond, R., Moore, A.W. 2014. The Antarctica component of postglacial rebound model ICE-6G_C (VM5a) based on GPS positioning, exposure age dating of ice thicknesses, and relative sea level histories. Geophysical Journal International, 198 (1), 537-563.

Armijo, R., Meyer, B., King, G.C.P., Rigo, A., Papanastassiou, D., 1996. Quaternary evolution of the Corinth Rift and its implications for the Late Cenozoic evolution of the Aegean. Geophysical Journal International 126, 11–53.

Austermann, J., Mitrovica, J. X., Huybers, P., Rovere, A., 2017. Detection of a dynamic topography signal in last interglacial sea-level records. Science Advances, 3(7), e1700457.

Bard, E., Hamelin, B., Fairbanks, R.G., 1990. U/Th ages obtained by mass spectrometry in corals from Barbados. Sea level during the past 130,000 years, Nature 346, 456-458.

Benac, C., Juracic, M., Bakran-Petricioli, T., 2004. Submerged tidal notches in the Rijeka Bay NE Adriatic Sea: indicators of relative sea-level change and of recent tectonic movements. Marine Geology 212, 21-33.

Benac, C., Juracic, M., Blaskovic, I., 2008. Tidal notches in Vinodol channel and Bakar bay, NE Adriatic Sea: indicators of recent tectonics. Marine Geology 248, 151-160.

Blanc, A. C., 1936. Una spiaggia pleistocenica a *Strombus bubonius* presso Palidoro (Roma). Accademia Nazionale dei Lincei, Rendiconti 23, 200-204.

Blanc, A. C., Segre, A., 1953. Le Quaternaire du Monte Circeo. Livret-Guide, IV Congr. INQUA, Roma, pp. 23-108.

Blanchon, P., Eisenhauer, A., Fietzke, J., Liebetrau, V. 2009. Rapid sea-level rise and reef back-stepping at the close of the last interglacial highstand. Nature 458 (7240), 881-884.

Bonifay, F., Mars, P., 1959. Le Tyrrhenien dans le cadre de la chronologie quaternaire mediterraneenne. Bulletin de Societé Geologique de France 7, 62–78.

Bosellini, A., Bosellini, F., Colalongo, ML., Parente, M., Russo, A., Vescogni, A., 1999. Stratigraphic architecture of the Salento coast from Capo d'Otranto to S. Maria di Leuca (Apulia, Southern Italy). Riv. Ital. Paleontol. Stratigr. 105, 397–416.

Boulton, S.J., Stewart, I.S., 2015. Holocene Coastal Notches in the Mediterranean Region: indicators of Palaeoseismic clustering? Geomorphology 237, 29-37

Brancaccio, L., Cinque, A., Belluomini, G., Branca, M., Delitala, L., 1986. Isoleucine epimerization dating and tectonic significance of Upper Pleistocene sea level features of the Sele plain (southern Italy). Zeitschrift für Geomorphologie N. F., Suppl.-Bd. 62, 159-166.

Brancaccio, L., Cinque, A., Russo, F., Belluomini, G., Branca, M., Delitala, L. 1990. Segnalazione e datazione di depositi marini tirreniani sulla costa campana. Bollettino Società Geologica Italiana 109, 259-265.

Carobene, L., 1972. Osservazioni sui solchi di battente attuali ed antichi nel golfo di Orosei in Sardegna. Boll. Soc. Geol. it. 91, 583-601

Cesaraccio, M., Puxeddu, C., Ulzega, A., 1986. Geomorfologia della fascia costiera tra Buggerru e Portixeddu nella Sardegna Sud- Occidentale. Rend. Sem. Fac. Sc. Univ. Cagliari, 56/1, 75-89.

Chappell, J., Omura, A., Esat, T., McCulloch, M., Pandolfi, J., Ota, Y., Pillans, B., 1996. Reconciliation of late Quaternary sea levels derived from coral terraces at Huon Peninsula with deep sea oxygen isotope records. Earth and Planetary Science Letters 141, 227-236.

Chen, J.H, Curran, H.A., White, B., Wasserburg, G.J., 1991. Precise chronology of the last interglacial period: 234U-230Th data from fossil coral reefs in the Bahamas, Geol. Soc. Am. Bull. 103, 82-97.

Creveling, J. R., Mitrovica, J. X., Hay, C. C., Austermann, J., Kopp, R. E., 2015. Revisiting tectonic corrections applied to Pleistocene sea-level highstands. Quaternary Science Reviews 111, 72-80.

Cucchi, F., Forti, F., Furlani, S. 2006. Erosion/Dissolution Rates Of Limestone Along The Western Istrian Shoreline And The Gulf Of Trieste. Geografia Fisica e Dinamica Quaternaria 29, 61-69.

de Boer, B., Lourens, L.J., Van de Wal, R.S.W., 2014. Persistent 400,000-year variability of Antarctic ice volume and the carbon cycle is revealed throughout the Plio-Pleistocene. Nat. Commun. 5, 2999.

de Boer, B., P. Stocchi, Whitehouse, P. L., van de Wal, R. S. W., 2017. Current state and future perspective on coupled ice-sheet - sea-level modeling. Quaternary Science Reviews 169, 13 - 28.

Delicato, M.A., 1999. Utilizzo di marker eutirreniani per l'assetto neotettonico di aree costiere tirreniche. L'esempio della piana del Garigliano. Unpublished Laurea Thesis, Università degli Studi di Roma 'La Sapienza', ENEA, A.A. 1-129.

De Mets, C., Laffaldano, G., Merkouriev, S., 2015. High-resolution Neogene and Quaternary estimates of Nubia-Eurasia-North America Plate motion. Geophys. J. Int. 203, 416-427.

Dépéret, C., 1918. Essai de coordination chronologique générale des temps quaternaires. Comptes Rendus de l'Accad!emie des Sciences, 167, 418–422.

Devoti, R., D'Agostino, N., Serpelloni, E., Galvani, A., Anzidei, M. et al., 2017. A combined velocity field of the Mediterranean region, Ann. Geophys., 60(2), doi:10.4401/ag-7059.

De Waele, J., Furlani, S. 2013. Seawater and biokarst effects on coastal karst. In: Shroeder, J.F., Frumkin A. (Eds), Treatise on Geomorphology, Vol. 6, Elsevier, Amsterdam, 341-350.

Durante, S., 1975. Sul Tirreniano e la malacofauna della Grotta del Fossellone (Circeo). Quaternaria 18, 331–347.

Dutton, A., Lambeck, K., 2012. Ice Volume and Sea Level During the Last Interglacial. Science, 337, 216-9.

Dutton, A., Webster, J.M., Zwartz, D., Lambeck, K., Wohlfarth, B., 2015. Tropical tales of polar ice: evidence of Last Interglacial polar ice sheet retreat recorded by fossil reefs of the granitic Seychelles islands. Quat. Sci. Rev. 107, 182–196.

Esposito, C., Filocamo, F., Marciano, R., Romano, P., Santangelo, N., Scarmiglia, F., Tuccimei, P., 2003. Late Quaternary shorelines in southern Cilento (Mt. Bulgheria): Morphostratigraphy and chronology. Il Quaternario 16 (1), 3-14.

Farrell, W. E., Clark, J.A., 1976. On postglacial sea level. Geophysical Journal of the Royal Astronomical Society 46, 647–667.

Ferranti, L., Antonioli, F., Amorosi, A., Dai Prà, G., Mastronuzzi, G., Mauz B., Monaco, C., Orrù P., Pappalardo M., Radtke U., Renda P., Romano P., Sansò P., Verrubbi V., 2006. Elevation of the last interglacial highstand in Sicily (Italy): a benchmark of coastal tectonics. Quaternary International 145-146, 30-54.

Ferranti, L., Antonioli, F., 2007. Misure del solco tirreniano (MIS 5.5) nell'isola di Capri: implicazioni su micro-dislocazioni e blocchi cinematici attivi negli ultimi 124 ka. Il Quaternario. 20(2), 125-136.

Ferranti, L., Oldow, J.S., D'Argenio, B., Catalano, R., Lewis, D., Marsella, E., Avellone, G., Maschio, L., Pappone, G., Pepe, F., Sulli, A., 2008. Active deformation in Southern Italy, Sicily and southern Sardinia from GPS velocities of the Peri-Tyrrhenian Geodetic Array (PTGA). Bollettino Della Società Geologica Italiana 127, 299-316.

Ferranti, L., Antonioli, F., Anzidei, M., Monaco, C., Stocchi, P., 2010. The timescale and spatial extent of vertical tectonic motions in Italy: insights from relative sea-level changes studies. J. Virtual Explorer 36, 1–34.

Furlani, S., Cucchi, F., Forti, F., Rossi, A., 2009. Comparison between coastal and inland Karst limestone lowering rates in the northeastern Adriatic Region (Italy and Croatia). Geomorphology 104, 73-81.

Furlani, S., Cucchi, F., Biolchi, S., Antonioli, F., Odorico, R., 2011. Notches in the Adriatic Sea: genesis and development, Quaternary International 232, 158-168.

Furlani, S., Cucchi, F., 2013. Downwearing rates of vertical limestone surfaces in the intertidal zone (Gulf of Trieste, Italy). Marine Geology 343, 92-98.

Furlani, S., Ninfo, A., Zavagno, E., Paganini, P., Zini, L., Biolchi, S., Antonioli, F., Coren, F., Cucchi, F., 2014a. Submerged notches in Istria and the Gulf of Trieste: results from the Geoswim Project. Quaternary International 332, 37-47.

Furlani, S., Pappalardo, M., Gomez-Pujol, L., Chelli, A., 2014b. The rocky coasts of the Mediterranean and Black Sea. In: Kennedy, D.M., Stephenson, W.J., Naylor, L.A. (Eds), Rock coast Geomorphology: A Global Synthesis. Geological Society, London, Memoirs 40, 89-123

Furlani, S., Antonioli, F., Gambin, T., Gauci, R., Ninfo, A., Zavagno, E., Micallef, A., Cucchi, F., 2017. Marine notches on the Maltese Islands (Central Mediterranean Sea). Quaternary International 39, 158-168.

Gignoux, M., 1911a. Les couches "a Strombus bubonius (Lmk.) dans la Mediterranée occidentale. Compte Rendus des Séances de l'Academie des Sciences, February 6th, 1911, 1–3.

Gignoux, M., 1911b. Resultats généraux d'une etude des anciens rivages dans la Méditerranée occidentale. Annales de l'Université de Grenoble XXIII (1), 1–21.

Gignoux, M., 1913. Les formations marines pliocenes et quaternaires de l'Italie du sud et de la Sicilie. Annales de l'Universite de Lyon 36, 693.

Gomez-Pujol, L., Fornos, J.J., Swantesson, J.O.H. 2006. Rock surface millimeter-scale roughnessand weathering of supratidal Mallrcan carbonate coasts (Balearic Islands).Earth Surface Processes and Landforms 31(14), 1792-1801.

Harmon, R.S., Land, L.S., Mitterer, R.M., Garrett, P., Schwarcz, H.P., Larson, G.J., 1981. Bermuda sea-level during the last interglacial. Nature 289, 481-483.

Hearty, P.J., 1986. An inventory of last interglacial (sensu lato) age deposits from the Mediterranean Basin: a study of Isoleucine epimerization and U-Series dating. Zeitschrift fur Geomorphologie N. F. Suppl. Bd. 62, 51– 69.

Hearty, P.J., 1987. New Data on the Pleistocene of Mallorca. Quaternary Sci Rev 6, 245-257.

Higgins, C.G., 1980. Nips, Notches, and the Solution of Coastal Limestone: an overview of the problem with examples from Greece. Estuar. Coast. Sci. 10, 15-30.

Hillaire-Marcel, C., Garièpy, C., Ghaleb, B., Goy, J. L., Zazo, C., Barcelos, C., 1996. U-series measurements in Tyhrrenian deposits from Mallorca — further evidence for two last-interglacial high sea levels in the Balearic Islands. Quaternary Science Reviews 15, 53–62.

Issel, A., 1914. Lembi fossiliferi quaternari e recenti osservati nella Sardegna meridionale dal prof. D. Lovisato. Atti della Reale Accademia dei Lincei, Rendiconti, Classe di Scienze Fisiche, Matematiche e Naturali, S. 5, CCCXI, 23, 759–770.

Kelletat, D.H., 2005. Notches. In: Schwartz, M.L. (Ed.), Encyclopedia of Coastal Science. Springer, Dordrecht, 728-729.

King, G.C., Stein, R.S., Rundle, J.B., 1988. The growth of geological structures by repeated earthquakes 1. Conceptual framework. Journal of Geophysical Research 93, 13307–13318.

Kopp, R.E., Simons, F.J., Mitrovica, J.X., Maloof, A.C., Oppenheimer, M., 2009. Probabilistic assessment of sea-level during the last interglacial stage. Nature 462, 863–867.

Kružić P. & Benković L., 2008. Bioconstructional features of the coral Cladocora caespitosa (Anthozoa, Scleractinia) in the AdriaticSea (Croatia). MarineEcology 29 (2008), 125–139.

Laborel, J. 1987. Marine biogenic costructionsin the Mediterranean a review. Scientific Reports of the Port-Cross National Park. 13, 97-126.

Lambeck, K., Bard, E., 2000. Sea-level change along the French Mediterranean coast since the time of the Last Glacial Maximum. Earth and Planetary Science Letters 175 (3–4), 202–222.

Lambeck, K., Antonioli, F., Anzidei, M., Ferranti, L., Leoni, G., Scicchitano, G., Silenzi, S., 2011. Sea level change along Italian coast during Holocene and a proiection for the future Quaternary International, 232, 1–2, 250–257.

Lisiecki, L., Raymo, M., 2005. A Pliocene-Pleistocene stack of 57 globally distributed benthic δ18O records. Paleoceanography 20, Issue 2.

Lorscheid, T., Stocchi, P., Casella, E., Gómez-Pujol, L., Vacchi, M., Mann, T., Rovere, A., 2017a. Paleo sea-level changes and relative sea-level indicators: Precise measurements, indicative meaning and glacial isostatic adjustment perspectives from Mallorca (Western Mediterranean). Palaeogeography, Palaeoclimatology, Palaeoecology 473, 94-107.

Lorscheid, T., Felis, T., Stocchi, P., J. Obert, J.C., Scholz, D., Rovere, A., 2017b. Tides in the Last Interglacial: insights from notch geometry and palaeo tidal models in Bonaire, Netherland Antilles. Scientific Reports 7, 16241.

Malatesta, A., 1954. Risultati del rilevamento del Foglio 192 (Alghero e Isola di Sardegna). II, Fossili delle spiagge tirreniane. Boll. del Serv. Geol. d'Italia 76, 9 e 17.

Malatesta, A., 1970. Cynotherium sardous Studiati: anextinct canid from the pleistocene of Sardinia. Mem. dell'Ist. Ital. Paleontol. Um.1, 1-72.

Malatesta, A., 1985. Geologia e paleobiologia dell'era glaciale. La Nuova Italia Scientifica, 282.

Mariani, P., Braitenberg, C., Antonioli, F., 2009. Sardinia coastal uplift and Volcanism. Pure and applied Geophysics 166, 1369-1402.

Mastronuzzi, G., Quinif, Y., Sansò, P., Selleri, G., 2007. Middle-Late Pleistocene polycyclic evolution of a geologically stable coastal area (southern Apulia, Italy). Geomorphology 86, 393–408.

Moses, C.A. 2013. Tropical rock coasts: Cliff, notch and platform erosion dynamics. Progress in Physical Geography 37(2), 206-226.

Moses, C.A., Robinson, D., Kazmer, M., Williams, R. 2015. Earth Surface Processes and Landforms 40(6), 771-782.

Muhs, D. R., Simmons, K. R. 2017. Taphonomic problems in reconstructing sea-level history from the late Quaternary marine terraces of Barbados. Quaternary Research 88, 4019-429.

Mitrovica, J.X., Peltier, W.R., 1991. On postglacial geoid subsidence over the equatorial oceans. Journal of Geophysical Research 96, 20053–20071.

Murray-Wallace, C. V., Woodroffe, C. D., 2014. Quaternary Sea-Level Changes: A Global Perspective. Cambridge, United Kingdom: Cambridge University Press.

Naylor, L.A., Viles, H.A., 2002. A new technique for evaluating short-term rates of coastal bioerosion and bioprotection. Geomorphology 47(1), 31-44.

Negri, A., Amorosi, A., Antonioli, F., Bertini, A., Florindo, F., Lurcok, P., Marabini, S., Mastronuzzi, S., Regattieri, E., Rossi, V., Scarponi, D., Taviani, M., Zanchetta, G., Vai G.B, 2015. A potential global boundary stratotype section and point (GSSP) for the Tarentian Stage, Upper Pleistocene, from the Taranto area (Italy): Results and future perspectives. Journal of Quat. Int. 383, 145-157.

Neumann, A.C., Hearty, P.J., 1996. Rapid sea-level changes at the close of the last interglacial (substage 5e) recorded in Bahamian island geology. Geology 24, 775–778.

Nisi, M.F., Antonioli, F., Dai Pra, G., Leoni, G., Silenzi, S., 2003. Coastal deformation between the Versilia and the Garigliano Plains (Italy) since the Last Interglacial stage. Journal of Quaternary Science 18(8), 709-721.

Oggiano, G., Funedda, A., Carmignani, L., Pasci, S., 2009. The Sardinia-Corsica microplate and its role in the Northern Apennine Geodynamics: new insights from the Tertiary intraplate strike-slip tectonics of Sardinia. Ital. J. Geosci. 128, 527-539.

Oldow, J. S., Ferranti, L., Lewis, D. S., Campbell, J. K., D'Argenio, B., Catalano, R., Pappone, G., Carmignani, L., P., Conti, Aiken, C. L. V., 2002. Active fragmentation of Adria based on Global Positioning System velocities and regional seismicity. Geology 30, 779-782.

Orrù, P., Ulzega, A., 1986. Geomorfologia costiera e sottomarina della baia di Funtanamare (Sardegna sud-occidentale). Geografia Fisica e Dinamica Quaternaria 9, 59-67.

Orrù, P., Pasquini, C., 1992. Rilevamento geomorfologico e sottomarino della Riserva Marina di Tavolara e di Capo Coda Cavallo (Sardegna nord-orientale). Atti del Conv. Naz. sulla Geologia Subacquea e Sottomarina - ENEA - Giornale di Geologia 54(2), 49-63.

Orrù, P., Antonioli, F., Hearty, P.J., Radtke, U., 2011 Chronostratigraphic confirmation of MIS 5 age of a baymouth bar at Is Arenas (Cagliari, Italy). Quat. Int. 232, 1-2, 169-178.

Palano, M., Ferranti, L., Monaco, C., Mattia, M., Aloisi, M., Bruno, V., Cannavò, F., Siligato, G., 2012. GPS velocity and strain fields in Sicily and southern Calabria, Italy: Updated geodetic constraints on tectonic block interaction in the central Mediterranean. Journal of Geophysical Research. Solid Earth 117, 1-12.

Palmerini, V., Ulzega, A., 1969. Sedimentologia e geomorfologia del settore costiero tra la foce del Rio Piscinas e Capo Pecora. Rend. Sem. Fac. Sc. Univ. Cagliari 39 (3-4), 1-38.

Pascucci, V., Sechi, D., Andreucci, S., 2014. Middle Pleistocene to Holocene coastal evolution of NW Sardinia (Mediterranean Sea, Italy). Quaternary International 328-329, 3-20.

Pedoja, K., Husson, L., Regard, V., Cobbold, P.R., Ostanciaux, E., Johnson, M.E., Kershaw, S.,Saillard, M., Martinod, J., Furgerot, L.,Weill, P., Delcaillau, B., 2011. Relative sea-level fall since the last interglacial stage: are coasts uplifting worldwide? Earth Sci. Rev. 108, 1–15. http://dx.doi.org/10.1016/j.earscirev.2011.05.002.

Peirano, A., Morri, C., Bianchi, C.N., Anguirre, J., Antonioli, F., Calzetta, G., Carobene, L., Mastronuzzi, G., Orrù, P., 2004. The Mediterranean coral Cladocora caespitosa; a proxy for past climate fluctuations? Global and Planetary Changes 40, 195-200.

Peirano, A., Kružić, P., Mastronuzzi, P., 2009. Growth of Mediterranean reef of Cladocora caespitosa (L.) in the Late Quaternary and climate inferences. Facies, 55, 325-333.

Peltier, W.R., 2004. Global Glacial Isostasy and the Surface of the Ice-Age Earth: The ICE-5G (VM2) model and GRACE. Annual Reviews of Earth and Planetary Sciences 32, 111–149.

Peltier, W.R., Argus, D. F., Drummond, R., 2015. Space geodesy constrains ice age terminal deglaciation, The global ICE-6G_C (VM5a) model. J. Geophys. Res. Solid Earth, 120, 450-487.

Pirazzoli, P.A., 1986. Marine notches. In: Van de Plassche, O (ed), Sea-level Research: a manual for the collection and evaluation of data. Geo Books, Norwich, 361-400.

Porqueddu, A., Antonioli, F., D’Oriano, R., Gavini, V., Trainito, E., Verrubbi, V., 2011. Relative sea level change in Olbia Gulf (Sardinia, Italy), an historically important Mediterranean harbour. Quaternary International 232(1-2), 21-30.

Rodríguez-Vidal, J., Abad, M., Cáceres, L.M., Ruiz, F., Fa, D., Finlayson, C., Finlayson, G., Martínez Aguirre, A., 2007. Evidencias erosivas y bioerosivas en la costa rocosa de Gibraltar al inicio del Último Interglaciar. Sociedad Española de Geomorfología, Mallorca (Spain), 4, 197–201.

Rodríguez Vidal, J., Zaghoul, M.N. Aboumaria K., Cáceres, L.M., Caceres L.M., Ruiz F., Abad M. Martinez-Aguirre A., Finlayson, C., Finlayson, G., Fa, D. 2010. Morphosedimentary evidence and U-Series dating of MIS 5 in Gebel Musa coast (Strait of Gibraltar, Morocco). Conference: Decoding the last Integlacial in western Mediterranean, INQUA Project 0911 cmp, Sardinia, Italy.

Rodríguez-Vidal, J., Cáceres, L.M., Gómez, P., Finlayson, C., Finlayson, G., 2015. Plio-Pleistocene archive of highstand sea-cave markers in the Rock of Gibraltar. Conference: Progress in Quaternary archives studies in the Iberian Peninsula, Seville, Spain.

Rosenbaum, G., Lister, G.S., Duboz, C., 2002. Relative motions of Africa, Iberia, and Europe during the Alpine orogeny. Tectonophysics 359, 117-129.

Rouchon, V., Gillot, PY., Quidelleur, X., Chiesa, S., Floris, B., 2008. Temporal evolution of the Roccamonfina complex (Pleistocene), central Italy. J Volcanol. Geotherm. Res. 177, 500–514.

Rovere, A., Raymo, M., Vacchi, M., Lorscheid, T., Stocchi, P., Gómez-Pujol, L., Harris, D., Casella, E., J. O'Leary, M., Hearty, P., 2016. The analysis of Last Interglacial (MIS 5e) relative sea-level indicators: Reconstructing sea-level in a warmer world. Earth-Science Reviews 159, 404-427.

Sanna, L., De Waele, J., Pasini, G., Pascucci, V., Andreucci, S., 2010. Sea level changes in the Gulf of Orosei based on continental and marine cave deposits. Rendiconti online della Società Geologica Italiana, 11 (1), 48-49.

Schellmann, G., and Radtke, U., 2004. A revised morpho- and chronostratigraphy of the Late and Middle Pleistocene coral reef terraces on Southern Barbados (West Indies). Earth Science Reviews, 64, 157–187.

Segre, A. G., 1951. Molluschi del Tirreniano di Porto Torres e di Golfo Aranci (Sardegna). Bollettino del Servizio Geologico d'Italia 73 (2), 269-290.

Segre, A.G.,1957. Nota sui rilevamenti eseguiti nel foglio 158, Latina, della carta geologica d'Italia. Bollettino del Servizio Geologico d'Italia 78, 569-5844.

Shackleton, N.J., Sanchez-Gon M. F., Pailler, D., Lancelot. Y. 2003. Marine Isotope Substage 5e and the Eemian Interglacial Global and Planetary Change 36, 151 – 155.

Shtober-Zisu, N., Amasha, H. and Frumkin, A., 2017. Inland notches: lithological characteristics and climatic implications of subaerial cavernous landforms in Israel. Earth Surface Processes and Landforms 42, 1820-1832.

Sisma-Ventura, G., Sivan, D., Shtienberg, G., Bialik, O. M., Filin, S., Greenbaum, N., 2017. Last interglacial sea level high-stand deduced from well-preserved abrasive notches exposed on the Galilee coast of northern Israel. Palaeogeography, Palaeoclimatology, Palaeoecology 470, 1–10.

Sivan, D., Sisma-Ventura, G., Greenbaum, N., Bialik, O.M., Williams, F.H., Tamisiea, M.E., Rohling, E.J., Frumkin, A., Avnaim-Katav, S., Shtienberg, G., Stein, M., 2016. Eastern Mediterranean Sea level through the last interglacial from a coastal-marine sequence in northern Israel. Quaternary Science Reviews 145, 204 -225.

Spada, G., Stocchi, P., 2007. SELEN: a Fortran 90 program for solving the "Sea Level Equation". Computers and Geosciences 33 (4), 538-562.

Spratt, T.A.B., 1865. Travels and Researches in Crete, J. van Voorst, London 2, pp 428.

Stearns, C.E., 1976. Estimates of the position of sea-level between 140,000 and 75,000 years ago. Quat. Res. 6, 445–449.

Stephenson, W.J., Kirk, R.M., Kennedy, D.M., Finlayson, B.L., Chen, Z., 2012. Long term shore platform surface lowering rates: Revisiting Gill and Lang after 32 years. Marine Geology, 299-302, 90-95.

Stirling, C. H., Esat, T. M., Lambeck, K., McCulloch, M.T., 1998. Timing and duration of the Last Interglacial: evidence for a restricted interval of widespread coral reef growth. Earth Planet Sci. Lett. 160, 745-762.

Stocchi, P., Antonioli, F., Montagna, P., Pepe, F., Lo Presti, V., Caruso, A., Corradino, M., Dardanelli, G., Renda, P., Frank, N., Douville, E., Thil, F., de Boer, B., Ruggieri, R., Sciortino, R., Pierre, C., 2017. A stalactite record of four relative sea-level highstands during the Middle Pleistocene Transition. Quaternary Science Reviews 173, 92-100.

Stocchi, P., Vacchi, M., Lorscheid, T., de Boer, B., Simms, A.S., van de Wal, R.W.S., Vermeersen, B.L.A., Pappalardo, M., Rovere, A., 2018. MIS 5e relative sea-level changes in the Mediterranean Sea: Contribution of isostatic disequilibrium. Quaternary Science Reviews, 185, 122 -134.

Swantesson, J.O.H., Moses, C.A., Berg, G.E., Jansson, K.M., 2006. Methods for measuring shore platform micro erosion: A comparison of the micro-erosion meter and laser scanner. Zeitschrift fur Geomorphologie N.F. Suppl. 144, 137-151.

Taborosi, D., Kazmer, M., 2013. Erosional and depositional textures and structures in coastal karst landscapes. Coastal Karst Landforms. Springer Science Netherlands,15-58.

Torunski, H., 1979. Biological erosion and its significance for the morphogenesis of limestone coasts and for nearshore sedimentation (northern Adriatic). Senckenberg. Maritima 11 3 (6), 193-265.

Trenhaile, A.S., 2002. Rock coasts, with particular emphasis on shore platform. Geomorphology 48, 7-22.

Trenhaile, A.S., 2014. Modelling marine notch formation by wetting and drying and salt weathering. Geomorphology 224, 139-151.

Trenhaile, A.S., 2015. Coastal notches: Their morphology, formation and function. Earth Science Review 150, 285-304.

Ulzega, A., Ozer, A., 1980. Comptes-rendus de l’Excursion Table Ronde sur le Tyrrhénien de Sardaigne. INQUA, Univ. Cagliari 110.

Zazo, C., Jose Luis Goy, J., Dabrio, J., Bardaj, T., Hillaire-Marcel, C., Ghaleb, B., Gonzalez-Delgado, J.A., Vicente, S., 1999. Pleistocene raised marine terraces of the Spanish Mediterranean and Atlantic coasts: records of coastal uplift, sea-level highstands and climate changes. Marine Geology 194, 103– 133.

ABSTRACT

We report detailed morphometric observations on several MIS 5.5 and a few older (MIS 11, 21, 25) fossil tidal notches shaped along carbonate coasts at 80 sites in the central Mediterranean Sea and at an additional six sites in the eastern and western Mediterranean. At each site, we performed precise measurements of the fossil tidal notch (FTN) width and depth, and of the elevation of its base relative to the base of the present tidal notch (PTN). The age of the fossil notches is obtained by correlation with biologic material associated with the notches at or very close to the site. This material was previously dated either through radiometric analysis or by its fossiliferous content.

The width (i.e. the difference in elevation between base and top) of the notches ranges from 1.20 to 0.38 m, with a mean of 0.74 m. Although the FTN is always a few centimetres wider than the PTN, probably because of the lack of the biological reef coupled with a small erosional enlargement in the FTN, the broadly comparable width suggests that tide amplitude has not changed since MIS 5.5 times. This result can be extended to the MIS 11 features because of a comparable notch width, but not to the MIS 21 and 25 epochs. Although observational control of these older notches is limited, we regard this result as suggesting that changes in tide amplitude broadly occurred at the Early-Middle Pleistocene transition.

The investigated MIS 5.5 notches are located in tectonically stable coasts, compared to other sectors of the central Mediterranean Sea where they are uplifted or subsided to ~100 m and over. In these stable areas, the elevation of the base of the MIS 5.5 notch ranges from 2.09 to 12.48 m, with a mean of 5.7 m. Such variability, although limited, indicates that small land movements, deriving from slow crustal processes, may have occurred in stable areas. We defined a number of sectors characterized by different geologic histories, where a careful evaluation of local vertical land motion allowed the selection of the best representative elevation of the MIS 5.5 peak highstand for each sector. This elevation has been compared against glacial isostatic adjustment (GIA) predictions drawn from a suite of ice-sheet models (ICE-G5, ICE-G6 and ANICE-SELEN) that are used in combination with the same solid Earth model and mantle viscosity parameters. Results indicate that the GIA signal is not the main cause of the observed highstand variability and that other mechanisms are needed. The GIA simulations show that, even within the Mediterranean Basin, the maximum highstand is reached at different times according to the geographical location. Our work shows that, besides GIA, even in areas considered tectonically stable, additional vertical tectonic movements may occur with a magnitude that is significantly larger than the GIA.

Morphometry and elevation of the Last Interglacial tidal notches in tectonically stable coasts of the Mediterranean Sea.

Antonioli F.[1], Ferranti L. [2], Stocchi P.[3], Deiana G. [4], Lo Presti V. [1], Furlani S. [5], Marino C. [2], Orru P. [4], Scicchitano G. [6], Trainito E. [7], Anzidei M. [8], Bonamini M. [9], Sansò P. [10], Mastronuzzi G. [11]

1 ENEA, Laboratory Climate Modelling and Impacts, Roma, Italy.

2 Dipartimento di Scienze della Terra, delle Risorse e dell'Ambiente, Università Federico II, Napoli, Italy.

3 NIOZ - Royal Netherlands Institute for Sea Research, Department of Coastal Systems (TX), and Utrecht University, P.O. Box 59, 1790 AB, Den Burg, Texel, The Netherlands.

4 Dipartimento di Scienze Chimiche e Geologiche - Università degli Studi di Cagliari, Italy.

5 Department of Mathematics and Geosciences, University of Trieste, Italy.

6 Studio Geologi Associati T.S.T. Misterbianco, Catania Italy.

7 Villaggio i Fari, Loiri Porto San Paolo, Italy.

8 Istituto Nazionale di Geofisica e Vulcanologia, Rome, Italy.

9 Marco Bonamini Palermo via Trinacria 4, Palermo, Italy

10 Dipartimento di Scienze e Tecnologie Biologiche e Ambientali, Università del Salento Ecotekne, Lecce, Italy.

11 Dipartimento di Scienze della Terra e Geoambientali, Università degli Studi di Bari "Aldo Moro", Bari, Italy.

Keywords

Fossil and Present Tidal Notches, glacial isostatic adjustment (GIA), Vertical tectonic movement

ABSTRACT

We report detailed morphometric observations on several MIS 5.5 and a few older (MIS 11, 21, 25) fossil tidal notches shaped along carbonate coasts at 80 sites in the central Mediterranean Sea and at an additional six sites in the eastern and western Mediterranean. At each site, we performed precise measurements of the fossil tidal notch (FTN) width and depth, and of the elevation of its base relative to the base of the present tidal notch (PTN). The age of the fossil notches is obtained by correlation with biologic material associated with the notches at or very close to the site. This material was previously dated either through radiometric analysis or by its fossiliferous content.

The width (i.e. the difference in elevation between base and top) of the notches ranges from 1.20 to 0.38 m, with a mean of 0.74 m. Although the FTN is always a few centimetres wider than the PTN, probably because of the lack of the biological reef coupled with a small erosional enlargement in the FTN, the broadly comparable width suggests that tide amplitude has not changed since MIS 5.5 times. This result can be extended to the MIS 11 features because of a comparable notch width, but not to the MIS 21 and 25 epochs. Although observational control of these older notches is limited, we regard this result as suggesting that changes in tide amplitude broadly occurred at the Early-Middle Pleistocene transition.

The investigated MIS 5.5 notches are located in tectonically stable coasts, compared to other sectors of the central Mediterranean Sea where they are uplifted or subsided to ~100 m and over. In these stable areas, the elevation of the base of the MIS 5.5 notch ranges from 2.09 to 12.48 m, with a mean of 5.7 m. Such variability, although limited, indicates that small land movements, deriving from slow crustal processes, may have occurred in stable areas. We defined a number of sectors characterized by different geologic histories, where a careful evaluation of local vertical land motion allowed the selection of the best representative elevation of the MIS 5.5 peak highstand for each sector. This elevation has been compared against glacial isostatic adjustment (GIA) predictions drawn from a suite of ice-sheet models (ICE-G5, ICE-G6 and ANICE-SELEN) that are used in combination with the same solid Earth model and mantle viscosity parameters. Results indicate that the GIA signal is not the main cause of the observed highstand variability and that other mechanisms are needed. The GIA simulations show that, even within the Mediterranean Basin, the maximum highstand is reached at different times according to the geographical location. Our work shows that, besides GIA, even in areas considered tectonically stable, additional vertical tectonic movements may occur with a magnitude that is significantly larger than the GIA.

Keywords

Fossil and Present Tidal Notches, glacial isostatic adjustment (GIA), Vertical tectonic movements

1. Introduction

1. Introduction

Quantifying the elevation and duration of the highstand that occurred during the Last interglacial, Marine Isotope Stage (MIS) 5.5, is of key importance as it allows the sensitivity of the Greenland and Antarctic Ice Sheets (GrIS and AIS, respectively) to climate conditions that are warmer than the present day to be assessed (all acronyms are defined in table S1). The MIS 5.5 highstand can, therefore, be used as an analogue for future scenarios of global warming, which is of key importance to 2100 sea-level projections. The elevation above the present sea level (p.s.l.) of the highstand, measured in globally stable areas (Rovere et al., 2016), has previously been estimated based on coral reefs using various methods (Bard et al., 1990; Chen et al., 1991; Chappel et al., 1996; Schellmann and Radtke, 2004; Blanchon et al., 2009; Dutton et al., 2015). These estimates show a significant uncertainty (some meters) in the assessment of the palaeo sea level (Muhs et al., 2017) because corals do not accurately mark the sea level but live in the photic zone. Furthermore, in many regions of the world coral reefs are absent and cannot be relied on to constrain the height of MIS 5.5 sea levels.

In tectonically stable areas of the Mediterranean Sea (Fig. 1A), fossil tidal notches (FTNs) of MIS 5.5 age are found at 6–8 m above present sea level (Ferranti et al., 2006; Lambeck et al., 2011, Present tidal notches or PTNs). The base of a tidal notch is considered the best and most precise marker of average palaeo sea level because its width is closely linked to the local tidal range (Antonioli et al., 2015; Rovere et al., 2016; Lorscheid et al., 2017a). The age of FTNs is constrained through correlation with adjacent marine deposits that are either; 1) radiometrically dated using the Th/U method or 2) contain the “Senegalese” fauna (a biostratigraphically distinct assemblage of marine mollusca the appearance of which, in the Mediterranean, is robustly constrained to MIS 5.5). The Mediterranean Sea is microtidal in character and many examples of late Holocene tidal notches formed in carbonate bedrock occur (e.g. Benac et al., 2004, 2008; Antonioli et al., 2007; Furlani et al., 2011, 2014a). These features allow the relationship between tidal notches and sea level elevation to be discussed and estimates of MIS 5.5 sea level to be assessed and corrected.

The aim of this study is to investigate the role of crustal movements in the height distribution of MIS 5.5 FTNs in the Mediterranean, primarily Italy but also from other locations across the basin. In this study we present a database of the morphometric measurements and height elevation of MIS 5.5 FTNs from across the Mediterranean as well as a summary of the chronological information that has been used to correlate these features to the Last Interglacial. The elevation and morphometric relationship between these MIS 5.5 FTNs and modern tidal notches is discussed and presented in order to make observations about crustal movements (furthermore a number of older TFNs are identified and discussed). The paper then maps the regional variability of the elevation of MIS 5.5 notches and compares this variability with predictions of specifically built GIA models that include different ice-sheet scenarios. The paper concludes by evaluating the residual difference between the measured heights of MIS 5.5 FTNs and the GIA-corrected elevation of notches in the light of tectonic movement.

2. Background setting

2.1. The tidal notch

Nearly half of the Mediterranean’s rocky coasts are generated on carbonate rocks (Furlani et al., 2014b). Such coasts are characterized by a typical set of landforms (Taborosi and Kazmer, 2013), which are related to a combination of mechanical (Trenhaile, 2002), chemical (Higgins, 1980; Furlani et al., 2014a) and biological processes (Torunski, 1979), although recently Trenhaile (2014) has argued that notches form also as a consequence of wetting and drying cycles. While bioerosion plays a role in the lowering of rocks in the intertidal zone, some hard bottom biological communities can protect the bedrock from erosion (Laborel, 1987; Naylor and Viles, 2002). Tidal notches are indentations or undercuttings that are mainly cut in steep carbonate cliffs at sea level; they are amongst the most common landforms along the Mediterranean’s coasts and range from a few centimetres to several meters in width. Antonioli et al. (2015) defined a tidal notch as the undercutting found at, or near, the tidal level on carbonate sea cliffs shaped with characteristic morphology. Tidal notches have been widely used as sea level indicators for more than 150 years, and many authors have suggested that they are cut by complex and polygenetic processes (Spratt et al., 1895; Carobene, 1972; Higgins, 1980; Pirazzoli, 1986; Antonioli et al., 2004, 2006; Kelletat, 2005; Furlani et al., 2011, 2014a; Trenhaile, 2014, 2015; Moses, 2013; Moses et al., 2015). Antonioli et al. (2015) measured the morphometric parameters of notches at 73 sites in the central Mediterranean Sea, together with the occurrence and features of the biological rims at their bases, and they correlated these parameters with wave energy, tidal range and rock lithology. Their conclusions were that *'tidal notches in the Mediterranean are, rather than the effect of a single process, the result of several processes that co-occur with different rates'*(pag. 81).

When the floor is lacking, a tidal notch is defined as a marine notch (Pirazzoli, 1986; Kelletat, 2005; Boulton and Stewart, 2015; Trenhaile, 2015), although some authors still call it a tidal notch (e.g. Antonioli et al., 2015; Furlani et al., 2017) in order to distinguish it from an inland notch (Shtober-Zisu et al., 2017). Its shape is, in fact, affected by the local tidal range, with a maximum width, *sensu* Antonioli et al. (2015), up to 400 cm (Trenhaile, 2015). In the Mediterranean Sea, present day notch width ranges from 13 to 95 cm. When the floor is lacking, we define the notch as a roof notch. A notch which develops near the sea floor, with sand and pebbles that mechanically erode the rock, is defined as an abrasional notch. It has no correlation with sea level, as it shows a depth and width which are different from the local tidal regime (Antonioli et al., 2015).

2.2. Geotectonic setting of the central Mediterranean Sea

The indented coasts of the Mediterranean Basin and the present configuration of the coastal landscape are the result of the interaction between tectonic and morphoclimatic processes that acted during the long-lasting convergence, active since the Late Cretaceous, between the African and European plates along an east-west boundary (Rosenbaum et al., 2002). The region is characterized by narrow as well as broader zones of seismicity and geodetic deformation, which highlight the position of the major plate boundary and of the boundaries of minor plates whose interiors appear to be largely aseismic (Anzidei et al., 2014; De Mets et al., 2015).

The basins of the central Mediterranean Sea are the result of different tectonic processes (Oldow et al., 2002; Rosenbaum et al., 2002; Anzidei et al., 2014). The Adriatic Sea and the surrounding promontories are the remaining parts of the Adriatic continental lithospheric block, caught between Europe and Africa, which served as the foreland domain for the southern Alpine, Dinarid-Hellenid and Apennine thrust belts. The Tyrrhenian Sea is a back-arc basin that opened behind the Apennines in the wake of the retreating Adriatic-Ionian slab and is partially floored by oceanic crust. The Ionian Sea is a remnant of the old Ionian oceanic lithosphere, closed between the Calabria and Hellenic subductions. The result of this tectonic evolution is a complex mosaic in which, during the Late Pleistocene and the Holocene, areas of recognized tectonic stability

(Sardinia, western and southeastern Sicily, Campania, southern Apulia, Ligury and Tuscany) alternated with areas marked by often large vertical movements (eastern Sicily, Calabria, Basilicata, Veneto and Friuli, Ferranti et al., 2006, 2010; Antonioli et al., 2009). This pattern of vertical stability or deformation is supported by the analysis of seismicity and of global positioning system (GPS) data (Oldow et al., 2002; Devoti et al., 2017; Serpelloni et al., 2014).

In addition to tectonic processes, glacio-eustatic sea level changes induced the extensive reshaping of the coastal areas during the Quaternary. Terraced marine deposits and landforms, such as notches, sea caves, inner margins and paleocliffs, mark the past sea-level stands, which are found below and above present-day sea level. The study of these geomorphological features has allowed the recognition of the regional tectonic behavior and the long-term sea-level trend, which have been summarized in recent papers by Ferranti et al. (2006; 2010), Antonioli et al. (2009) and Furlani et al. (2014a).

2.3. The MIS 5.5 highstand

The marine isotope substage (MIS) 5.5 corresponds to the last interglacial period. Its geochronology is based on orbital tuning of high-resolution deep-sea oxygen isotope stratigraphy. The geochronological subunit MIS 5.5 occurred between Termination II (end of MIS 6) and the onset of MIS 5.4 and lasted from 132 to 116 ka (Stirling et al., 1998; Shackleton et al., 2003; Kopp et al., 2009; Murray-Wallace and Woodroffe, 2014). The study of Last Interglacial shorelines dates back at least a century (Gignoux, 1913), and sea level indicators that formed during MIS 5.5 have been reported from over one thousand sites worldwide (Pedoja et al., 2011).

With respect to the Mediterranean Sea, since the identification and definition of the *Tirreniano* interglacial stage (effectively MIS 5.5) by Blanc in Sardinia at Cala Mosca in 1908, numerous studies have identified and dated hundreds of Last Interglacial, or 'Tyrrhenian', sites throughout the Mediterranean (Blanc, 1936; Malatesta, 1985; Hearty 1986, 1987; Zazo et al., 1999; Lambeck and Bard, 2000; Nisi et al., 2003). Using a compilation of 246 sites, all attributed to the MIS 5.5, Ferranti et al. (2006) found a significant alongshore difference in site elevation from +175 to −125 m in respect to the present sea level, which they attributed to the interplay of regional and local tectonic processes, including faulting and volcanic deformation.

A recent integrated study (Amorosi et al., 2014; Negri et al., 2015) of *Fronte Section* near Taranto, Italy detailed one of the most representative and extensive MIS 5.5 sequences to be found in the Mediterranean. Facies analysis, detailed macro- and microfaunal characterization and sequence stratigraphy (using Senegalese fauna and ten U-series dates on *Cladocora caespitosa* samples) permitted an unequivocal MIS 5.5 age (132–116 ka) to be attributed to these deposits. These results portray the composite section as a very promising candidate (named Tarentiano) in the search for the Upper Pleistocene global boundary stratotype section and point (GSSP).

In the Mediterranean Sea, *Cladocora caespitosa* is one of the few scleractinian corals that build extended bioherms and the only one that does so at the present time. Its presence is recorded at depths of a 4-10 m as well as down to 30–40 m (Peirano et al., 2004; Silenzi et al., 2005; Peirano et al., 2009). Existing banks of *Cladocora* are reported in Croatia (Kruzĭć and Benković, 2008), where the most extensive one that is known in the Mediterranean covers an area of more than 650 m^2. The depth of the Croatians banks ranges between 6 and 21 m. Hence, the presence of this coral as fossil allows for the age determination of the past sea-level stands, but it is definitely not a reliable indicator of paleo water depth. The presence in fossil deposits of *Persististrombus latus* (= *Strombus bubonius*) and other Senegalese fauna have allowed the dating of thousands of deposits, giving a precise chronological attribution.

Finally, Hearty (1986) used available U\th dates and the presence of Senegalese fauna on some MIS 5.5 fossil deposits to calibrate the amino acid ratio of shells from these sediments and landforms across the whole Mediterranean area (in particular, *Arca*, *Glicymeris* and *Cerastoderma*). Using this approach, he was able to use the amino acid ratios to infer a MIS 5.5 age of undated or barren deposits from elsewher in the region.

2.4 "Senegalese fauna"

In the Mediterranean geological context, the term Senegalese fauna indicates a fossil faunistic assemblage consisting of warm species, from the Atlantic (Gignoux, 1911a, b) where ‘‘the most famous and common is *Strombus bubonius* Lamarck 1791’’ (Gignoux, 1913). Other warm water species are represented by *Patella ferruginea*, *Conus ermineus*, *Gemophos viverratus*, *Cardita calyculata senegalensis* and *Hyotissa hyotis*. The gastropod *Persististrombus latus* (Gmelin, 1791) (named until 2010 *S. bubonius*) entered in the Mediterranean sea only during the Tyrrhenian time corresponding to the Last Interglacial Time ; this last term - in the form "Tirreno" - has been proposed for the first time by Issel (1914) and then by Dépéret (1918) for indicating the age of raised marine terraced deposits characterised by the presence of Senegalese fauna with or without *P. latus*.

It is generally correlated to the last interglacial (MIS 5.5), which occurred between 132 and 116 ka roughly, but generally extended up to 80k a; this lap of time has been defined thanks to different age determinations performed by means of U/Th analysis on the coral *Cladocora caespitosa* and amino acid racemization analyses on mollusc shells as *Glycymeris sp*, *Arca sp* and *Cerastoderma sp.* associated to the before mentioned taxa (e.g.: Amorosi et al., 2014; Negri et al., 2015 and references therein).

Bonifay and Mars (1963) affirmed that the *S. bubonius* (today *P. latus*) is not the characteristic element of the Tyrrhenian and Senegalese deposits. In fact, it is very important to underline that the presence of this tropical gastropod defines only a fossil facies and not all Tyrrhenian deposits ("Tirreno" in Issel, 1914) with warm fauna of Atlantic origin (sensu Gignoux, 1911a,b; 1913) or Senegalese (sensu Bonifay and Mars, 1963).

2.5. Glacial- and hydro-isostatic adjustment

Quantifying the melting of the GrIS and AIS during the MIS 5.5 on the basis of paleo RSL indicators from tectonically stable areas requires that the GIA process is accounted for (Dutton and Lambeck, 2012). This is usually accomplished by means of numerical modelling. The latter demands that an ice-sheet model, which describes the forcing function (i.e. the surface loading variation), is combined with a solid Earth model, which describes the response function (i.e. solid Earth and geoid deformations). The outcome yields the space- and time-dependant RSL changes that accompany and follow the ice-sheet fluctuations. The GIA-driven RSL changes incorporate all the solid Earth and geoid deformations that stem from the pre-MIS 5.5 glacial-interglacial cycles (in particular the melting of MIS 6 ice sheets) as well as from the retreat of the GrIS and AIS during the actual MIS 5.5 interglacial period. The predicted local RSL change can be very different from the eustatic signal, the difference being a function of the distance with respect to the ice sheets and of the shape and size of the ocean basins. It is expected that, even within an enclosed basin such as the Mediterranean Sea, the MIS 5.5 highstand reached different elevations at different times as a function of the geographical location (Lorscheid et al., 2017a; Stocchi et al., 2018).

Neglecting the GIA might significantly hamper the quantification of the eustatic sea-level peak, which mostly stems from GrIS and AIS melting. In fact, as discussed by Rovere et al. (2016), early global-scale studies did not (properly) take GIA into account and resulted in estimates of 3–6 m above mean sea level (MSL) (Stearns, 1976; Harmon et al., 1981; Neumann and Hearty, 1996; Stirling et al., 1998). However, more recent studies have incorporated state-of-the-art GIA modelling and independently estimated values from 5 to 9.5 m above MSL (Kopp et al., 2009; Dutton and Lambeck, 2012). These recent results suggest that not only did the GrIS and West AIS collapse, but also the East AIS might have contributed to global sea level at this time.

In the Mediterranean, few studies up to this point have explicitly included the GIA contribution to the MIS 5.5 RSL fluctuations. As highlighted by Sivan et al. (2016), the local GIA-driven RSL highstand in Israel could contribute from 2–2.5 m to the highstand. Creveling et al. 2015 also show that the GIA contribution is significant and cannot be neglected when investigating the tectonic rates of deformation. Rovere et al. (2016), Lorscheid et al. (2017b) and Stocchi et al. (2018) show that the GIA signal is not uniform within the Mediterranean Basin and can contribute from 1–2.5 m of RSL highstand without accounting for extra melting from Greenland and Antarctica. For the latter ice sheets, several chronologies of melting have been proposed so far, but it is still uncertain whether there was a single peak, a two-stand peak or actual fluctuations (see Kopp et al., 2009). Furthermore, Austermann et al. (2017) show that dynamic topography could contribute quite significant subsidence in the Mediterranean that could explain 1–2 m of RSL change at the MIS 5.5. However, these results are not accurate enough for the Mediterranean Basin given the low-resolution model used by the authors. Finally, while the timing of the onset of the MIS 5.5 acme is relatively simultaneous, mostly taking place from 129 ka to 126 ka, the timing of the demise of the LIG acme is more variable and ranges from 122 ka to 113 ka (Rovere et al., 2016).

3. Materials and Methods

We selected and re-measured the features of a set of FTNs from areas that are located in the central Mediterranean Sea (S2, Fig. 1) and that are considered stable since the MIS 5.5 (Ferranti et al., 2006, 2010; Antonioli et al., 2015). The stable areas as well as the 80 surveyed sites are portrayed, respectively, in Fig. 1 A and Fig.1 B-E. Six additional sites from other regions such as Morocco, Gibraltar and France (Fig. 1 F–G) (Rodriguez Vidal et al., 2007, 2010; Abad et al., 2012, 2013) were considered because they show carved FTNs along coasts that are considered stable since the MIS 5.5. All of these were then included in a database (Tables 1, 2, 3 and S7) that included only well-carved FTNs on limestone rocks which presented morphological continuity. We established that a tidal notch can be defined continuous when it can be followed laterally for at least 50 meters.

3.1 Measures

The measurements of the FTNs were performed from the base of the FTN to the base of the PTN (**Figs. 2, 3, 4 and 5**). The measure was corrected by 3 cm because it corresponds to the average width of the biological rim once formed and currently eroded at the base of an FTN (Vermetids, Corallinaes Algae and others living at Present sea level). This is the reason why no correction has been introduced about sea level, unless in rare cases where a roof notch and an FTN are present (Circeo and Capri, sites 50 and 55), and therefore a PTN base is lacking (Ferranti and Antonioli, 2007). Even though we recorded the date and time for all measurements, these are the only cases where the measurements of the base of the FTN were referred to the local sea level, corrected for tides.

The measurements of the 80 studied sites (**Tables 1 and 2 and table S7**) were performed using different tools and with an estimated error ranging from ±1 up to ± 5 cm along the vertical error depending on both the tool and the adopted reference level (MSL, vermetid reef etc., see **Fig. 5 and S5**). All measurements were referred to the base of the PTN or zones where the vermetid reef was present and considered as representative of the MSL (H = 0). Vertical profiles along the notch sections were realized through several measurements. An uncertainty of ± 2.5 cm was assumed to account for the identification of the marker.

The tools we used and related instrumental uncertainty are the following:

a) Global Positioning System/Real Time Kinematic (GPS/RTK) technique. In eight sites (50, 51, 52, 54, 74, 75, 79 and 80, respectively, in **Figs. 4 and 5; Tables 1 and 2, table S7**), we used the GPS/RTK technique which has an accuracy better than ± 3 cm along the vertical. This depends on both the tool and the adopted measurement base (MSL, vermetid reef etc., see **S5**), but it often depends on the setting of MSL. An accuracy of ± 5 cm was estimated.

b) Levelling surveys. Sites 50, 51, 52 and 54 were surveyed by a levelling technique, using a Leica Runner4 instrument. Elevation data were referred to the local sea level at the time of the surveys and corrected for tides by the nearest tide station (**Fig. 5)**. An accuracy of ± 5 cm was estimated

c) Total station. Sites 79 and 80 were surveyed with a Total Station Leica TCRP 1203, equipped with an infrared laser beam, capable of capturing targets at a distance up to one km. For the measurements in the range of about 700 m, we used the laser beam without a prism, keeping a precision of a few mm along the distance. (**Fig. 5**). An accuracy of ± 5 cm along the vertical was estimated

d) Telescopic rod. In 19 sites (**Figs. 4 and 5; Tables 1 and 2, table S7**), a 10 m long telescopic measuring gauge was used (Telefix). This device provides direct readings on a graduated tape and is built with non-extensible material which ensures an accuracy of about 3 mm when fully extended to 10 m. We estimated an error comprised from 1 to 5 cm depending on the morphological conditions of the PTN and on the position of the MIS 5.5 FTN (**Figure in S5**). This is always used when the FTN is orthogonal above the PTN. Otherwise, when a few degrees of inclination occurred (1–6°) between the platforms of the PTN and the FTN, the top of the instrument was placed a few cm from the FTN base. The level was defined by an operator located on a nearby boat and were taken photos to roughly verify the positioning of the rod with respect to the significant morphologies. An accuracy of ± 1 cm along the vertical was estimated.

d) Tape. In 46 sites (**Figs. 4 and 5; Tables 1 and 2, Table S7**), we used a 20 m long measuring tape, positioned on morphological markers by two operators. This measurement tool was used in sites where the cliff was not back drawn and the tape could therefore be positioned vertically or with an acceptable slant (**Figure S5**) . The use of the tape was done with an operator on the FTN and one on the PTN that is in the sea. Because of the presence of some vertical offset in the position of the two markers, and resulting tilt of the tape from the vertical, these measurements have been assigned an error bar of ± 15 cm.

e) Digital altimeter: In three sites (**Figs. 4 and 5; Tables 1, 2 and Figure S5, Table S7**) where uplifted notches were far from the present day coast, position and elevation measurements were performed by a digital altimeter (Garmin Oregon 650) with a vertical accuracy of 50 cm and were calibrated with respect to the sea level along the nearby coast. Measurements were taken at the base of the FTN and at the vermetid platform. An accuracy of ± 50 cm along the vertical was estimated. When the Vermetid rim was lacking, an uncertain ty of ± 10 cm was summed to the marker identification and instrumental error. Any other specifications about the formation, morphology and spatial variations of the morphological measurements of the PTN can be found in Antonioli et al. (2015).

3.2 Glacial- and hydro-isostatic adjustment

In this paper we investigated the role of GIA in modulating the elevation of the MIS 5 sea-level highstand across the Mediterranean Sea by means of process-based numerical modelling. We employed three different ice-sheet models to *(i)* quantify the sensitivity of the Mediterranean RSL sites to the GIA process and (ii) evaluate, albeit without recurring specific statistics, which glacio-eustatic scenario better represents the observations.

To evaluate the contribution of GIA to the observed RSL changes from the MIS 5.5, we solved the gravitationally self-consistent sea level equation (SLE) (Farrell and Clark, 1976). The SLE incorporates all the GIA feedbacks and yields RSL changes that accompany and follow continental (i.e. land-based) ice-sheet thickness variations. We make use of of the SELEN Fortran 90 program (Spada and Stocchi, 2007), which solves the SLE by means of the pseudo-spectral approach (Mitrovica and Peltier, 1991). Accordingly, the SLE solution consists of spatio-temporal convolutions where ice-sheets thickness variations are coupled to solid Earth responses and propagated through time in order to account for the time-dependent viscous relaxation of the mantle. At the core of the SLE formalism is the concept that, at any time *t* since the beginning of the ice-sheet model chronology, the RSL changes of each point of the Earth's surface stem from the solid Earth and geoid deformations induced by all the ice- and water-loading variations that have occurred since the initial time t^0. Accordingly, the solid Earth is assumed to be spherically symmetric, radially stratified, self-gravitating, rotating and deformable, but not compressible (Spada et al., 2003). We assume an elastic lithosphere and a Maxwell viscoelastic mantle. We devide the latter into three layers: upper mantle, transition zone and lower mantle. The core of the Earth is considered inviscid.

We consider three global ice-sheet models that describe the last 240 kyrs of fluctuations (i.e. two glacial-interglacial cycles). This is necessary in order to accurately account for the GIA which accompanies and follows the melting of the MIS 6 ice sheets, as well as the GIA during and after the MIS 5e until the present day. Overall, the three ice-sheet models are very different and are characterized by very different eustatic elevations and temporal durations of the last interglacial phase. The three models are the following:

1. ICE-5G (Peltier, 2004): This model describes the ice-sheet thickness variations over North America, Eurasia, Greenland and Antarctica from 26 ka to present. For this time span, ICE-5G was constrained by the means of geological RSL data and modern geodetical observations (Peltier, 2004). Prior to 26 ka, the ice-sheet growth is tuned to the delta-18O curve (Lisieki and Raymo, 2005) and is not glaciologically realistic (Peltier, 2004). The chronology starts at 123 ka, when the global ice-sheet volume was smaller than it is today and resulted in a eustatic sea level of ~0.9 m above the present level (mostly due to a smaller GrIS; to be specified). In order to capture the GIA contribution to the MIS 5.5 highstand, we combined in time two consecutive ICE-5G chronologies. This allowed us to simulate the ice-sheet growth towards the MIS 6 glacial maximum and the subsequent retreat during the period from MIS 6 to MIS 5.5 Therefore, after the MIS 5e, the ice-sheet chronology is repeated towards the present day (including the last glacial maximum LGM, of course). However, we do not claim that the MIS 6 glacial maximum was the same as the LGM. According to our reconstructed chronology, the MIS 5.5 interglacial starts at 129.5 ka, which corresponds to the end of the initial cycle, and ends at 122 ka. The maximum peak of 0.9 m equivalent sea level (ESL) starts at 125 ka and ends at 123 ka, therefore resulting in a 2 kyr-long (late) highstand (see red dashed curves in **Figs. 6 and 7**).

2. ICE-6G (Argus et al., 2014; Peltier et al., 2015): This model represents the latest improvement of the ICE-5G (see previous entry). We apply the same time discretization and

chronology of the ICE-5G. According to the ICE-6G, the maximum MIS 5.5 eustatic highstand is ~3.1 m above present-day MSL as a consequence of the GrlS and AIS retreat and occurred from 125 to 123 ka (see blue dashed curves in Figs. 6 and 7).

3. ANICE-SELEN (de Boer et al., 2014, 2016): This model describes the global ice-sheet fluctuations that follow the delta-18O stack (Lisiecki and Raymo, 2004) and that dynamically account for all the GIA feedback. ANICE-SELEN, therefore, is the result of a fully and dynamically coupled system and, so far, has been not constrained by means of RSL data. We followed the original ANICE-SELEN chronology and, during the MIS 5e, forced the GrIS and AIS to release, respectively, 2 and 5 m of equivalent sea level (ESR) (see also Lorscheied et al., 2016; Rovere et al., 2016) Therefore, under the eustatic approximation, this would result in 7.0 m ubiquitous sea-level highstand from 120 ka to 117 ka (see green dashed curves in Figs. 6 and 7).

Overall, the three ice sheet models are very different and they are expected, therefore, to result in different RSL changes not just in the proximity of the formerly glaciated areas, but also at ice distal or far-field sites such as the Mediterranean Sea. Also, it is interesting to compare the response of the Mediterranean basin to two different classes of ice sheet models: (i) ICE-5 and 6G, both the result of RSL data inversions, and (ii) ANICE-SELEN, the result of a pure process-based modeling approach. In fact, whicle ICE-5 and 6G are built to give an excellent fit with post LGM RSL data, ANICE-SELEN purely follows ice-flow physics and dynamics. Therefore, we expect large regional differences, but also a consistent signal in the Mediterranean. This could prove that, regardless of all the uncertainties in the ice sheet models (no model is perfect or 100% realistic), we can constrain the expected GIA response of the Mediterranean (lower to upper limit), and therefore provide better estimates of the absolute glacio-eustatic value at the MIS 5e (mostly Greenland and Antarctic ice sheets reduction).

4. Results

4.1. FTN elevation

The mean elevation of all measurementss (Figs. 1, 2, 3, S2, S3, S4 and Figure S5; Tables 1 and 2) in the studied sites is 5.71 m with a maximum of 12.78 m at Monte d’Argento (southern Latium) and a minimum of 2.09 m (Palinuro, south of Naples). If we do not consider the values lower than 2.5 m (Palinuro, Capo Zafferano and Rosh Hanikra Israel) and higher than 10 m, the average elevation is 5.95 m. We added to the measured sites in Italy six measurements at sites elsewhere in the Mediterranean Sea (Abad et al., 2012, 2013; Rodriguez Vidal et al., 2007, 2015; **Table 3 and Figure S6),** but we did not use these observations for statistical analysis.

4.2 FTN width and comparison with PTN width

The mean width of MIS 5.5 FTN (Figs. 2 and 8; Table 1) is 0.74 m with a maximum of 1.20 m at Levanzo and a minimum of 0.38 m at Palinuro. The PTN mean width is 0.59 m with a maximum of 0.9 m at Levanzo and a minimum of 0.30 m at Palinuro. The FTN/PTN ratio width is 1.28. This value is always larger than 1 (Tables 1 and 2, column 4; Fig. 5). Compared with the PTN widths, the FTN widths are always wider by 10 to 25 cm (Table 1; Figs. 2, 5, S2, S3 and S4).

4.3 FTN depth and comparison with PTN depth

The mean depth of the FTNs (Tables 1 and 2; Figs. 2 and 3) is 0.9 m with a maximum of 1.20 m at Capo Caccia (site 2) and a minimum of 0.20 m at Capo Caccia (site 10). In the Orosei Gulf, near springs with a flow rate of thousands m^3/sec, the PTN has a width up to 4 m (Antonioli et al., 2015). The FTN/PTN ratio width is 0.92 (with a maximum of 1.40 at Levanzo, and a minimum of 0.16 m at Capo Caccia) (Tables 1 and 2, column 4). Compared with the PTN depths, the FTN depths are almost always smaller (Figs. 3, S3, S4 and S5). Regarding the FTN base (Figs. 2 and 3), the mean of our measures is 0.66 m, with a maximum of 1.80 m at Pedralonga (site 2) and a minimum of 0.15 m at San Vito Macari (site 72) (Tables 1 and 2).

4.4 Age of the fossil notch

Regarding the age of the fossil notch, for each site, we considered the distance between the notches and the nearest dated fossil deposit which can be correlated to it. The results (**Fig. 9; Table 1**) show a mean distance of 4.5 km with a maximum distance of 22.9 km (Pedralonga, site 44) and a minimum of 0.2 km (Capo Caccia, site 12). Regarding the quality of analyses or markers used, as explained in Table 1, we provide the references for each site. The dating techniques used for the FTN are the following: 1) U/Th analysis on Cladocora caespitosa or on speleothems; 2) OSL on sandy deposits; 3) Aminostratigraphy on marine shells; and 4) Correlation to fossil assemblages containing Persististrombus latus or other Senegalese fauna.

4.5 FTN older than MIS 5.5

Uplifted FTN older than MIS 5.5 were studied and measured in Sicily and Apulia **(Fig. 1; Table 2, Figure S5; sites 74–80)** at Custonaci, Grotta Racchio, Capo Zafferano, Sferracavallo and Grotta Romanelli (the elevation ranged from 9.2 m at Romanelli to 73 m at Custonaci). These notches show a width from 1.5 to 2.12 m, with a mean of 1.82 m and a FTN/PTN ratio of notch depth always higher than 1 (Fig. 10; Tables 1 and 2).

4.6 Glacial- and hydro-isostatic adjustment

Within the Mediterranean Basin, the predicted GIA-modulated RSL curves for all the three ice-sheet models are significantly different from the eustatic curves (see Figs. 6 and 7). There are significant differences between the predicted RSL curves in the central regions of the basin, such as Italy (Fig. 6) and France (Fig. 7), and the marginal areas, such as Morocco and Israel, respectively, in the western and eastern Mediterranean Sea (Fig. 7a and c). In the central areas, in fact, the RSL curves are characterized by a monotonous RSL rise that lags behind the eustatic signal and that eventually results in a higher than eustatic highstand by the end of the MIS 5.5 temporal window (see solid curves w.r.t. dashed curves of Fig. 6). This holds for all three ice-sheet models that, albeit different, are combined in the same mantle viscosity profile. Interestingly, differences between GIA-modulated and eustatic signal are larger for the ANICE-SELEN (see green curves). The predicted RSL curves at the Italian sites all show a relatively fast RSL increase (about 0.5–1.0 m) from 125 ka to 123 ka, while the eustatic signal is flat for this time span.

The sites at the western and eastern boundaries (Fig. 7a and c) are characterized by earlier highstand, which is then followed by a relative sea level drop. This holds in particular for the ICE-5G and ICE-6G, while the signal is only visible for ANICE-SELEN within the 125–123 ka time window. The latter, in fact, is characterized by a local RSL drop as opposed to the rise at the Italian sites.

The GIA-driven regional contribution to RSL rise is related to the maximum peak from 1–2.5 m within the whole Mediterranean Basin. Notably, higher values are only reached at sites 1–4 for ICE-5G, and the rest of the estimates are within 1.5 m (**Fig. 11**; Table 5). This implies that GIA alone (leaving out the extra GrIS and AIS glacio-eustatic components) is capable of driving a 1–1.5 m (locally 2.5 m) higher than present sea level during the MIS 5.5. Such a value is comparable to the expected glacio-eustatic contribution of GrIS during the MIS 5.5 The latter, however, shows up at different times according to the geographical location.

The GIA contribution to RSL rise (related to the maximum peak) along the coasts of Italy (including Sardinia and Sicily) is up to 1.5 m (Fig. 12). This holds for all the three ice-sheet models and, therefore, confirms that the GIA signal in the Mediterranean is quite consistent among different ice-sheet chronologies (Fig. 12).

Overall, the predicted maximum peaks according to ICE-5G and ICE-6G (Fig. 12 left) could explain the observed lower limits. On the other hand, the maximum peaks predicted according to ANICE-SELEN fit quite well with some observations and, in general, with the higher limits.

Following from the previous point, GIA results alone are a second-order contributor to variability when compared to the observations. Hence, they can only explain in part the observed regional variations in the maximum peak elevation (see also regional variability in Fig. 11 and **Table 5)**.

5. Discussion

5.1 Notch morphometry: comparison with the PTN

This study has yielded unprecedented details on the MIS 5.5 notch morphometry that can be compared with the morphometry of the PTN studied by Antonioli et al. (2015). The three morphometric parameters (width, depth and base) of PTNs show small differences depending whether they are located in sheltered or exposed areas. Similar results were also achieved for the FTNs (Tables 1 and 2). Moreover, near large fresh water springs (as described for Sardinia's western coast in Antonioli et al., 2015), PTN depths are noticeably higher (more than 4 m), while FTN remain the same because the PTN so deeply carved tend to collapse.

The main difference between the PTN and the FTN is the width. The average FTN width recorded in 67 sites was 0.73 m, while the average width of the PTN in 59 sites was 0.59 m. The conclusion is that the average width of an FTN is 0.14 m wider than that of a PTN. This difference supports, based on a larger data set, the conclusions of Antonioli et al. (2015), derived from data collected in eight sites.

We explain the FTN width exceeding the PTN width by 0.14 m as a result of a combination of chemical and biological weathering of the carbonate bedrock. The aforementioned processes are responsible also of the lack of the biological rim (Vermetids, Corallinales algae) in the FTN. We argue that a biological rim was present at the base of the FTN during MIS 5.5, based on the morphology of its lower part. Antonioli et al. (2006) and Antonioli et al. (2015) describe a fossil vermetid reef in an uplifted FTN attributed to MIS 5.5 near Taormina. With the disappearance of the rim, the notch was also increasingly more exposed to erosion.

Dissolution rates measured on carbonate rocks in the Mediterranean area show values ranging from 0.01 mm/a to 1 mm/a (Furlani et al., 2014b), with higher rates in correspondence with the mid- or low-tide levels (Furlani et al., 2009; Furlani and Cucchi, 2013). The longest data set covers about 40 years (Furlani et al., 2009; Stephenson et al., 2012). Taking into account significant approximations in the extrapolation of erosion rates for the long-term period, such as hundred thousand years or more, due to the complete lacking of instrumental data older than half century or morphometric proxies, a linear extrapolation over 125,000 years, implies a total amount of erosion of Mesozoic limestones hosting FTNs ranging from 0.125 m to 5 m (**Table 4**). Uncertainties can be due to the effects of past local climate setting, that could have affected past erosion rates or different geological conditions, such as the shedding of the notch by younger sediments that have now been stripped off. In some cases, limestone lowering rates can be also higher, such as at Mallorca Island (Gomez-Pujol et al., 2006), with the result of the complete disappearance of MIS 5.5 notches. Softer limestones, such as Miocene calcarenites, have higher dissolution rates, with a total estimated erosion of 100 m (**Table 4**). The latter is not the case for the observed FTNs. The relatively low average difference in width (0.14 m) between FTNs and PTNs calls for erosion rates at the lower boundary of the estimate. The other measured morphometric dimensions of FTNs do not show any systematic difference from those of PTNs.

On the other hand, the preservation of the FTNs at some or several sites and the minimal difference in width with respect to the PTNs could be explained by taking into account subsequent deposition processes which preserved the FTNs, even in the presence of higher dissolution rates. The sediments could have protected the buried forms, at least until their post-LGM exhumation. Many examples of this occurrence have been recorded in many sites in the Orosei Gulf and at Tavolara Island, where traces of LGM eolianites are still found inside the FTNs (Fig. 5i–j).

An FTN changes its morphology and morphometry depending on whether it is covered and preserved by sediments (aeolianites and/or other continental deposits) or not. The final morphometric shape (especially the width) may have a significant enlargement due to karst solution processes, with rates that (on carbonate lithologies) may reach 0.04 mm per year (Furlani et al., 2009, 2010; Furlani and Cucchi, 2013) outside the tidal zone. This is confirmed by the FTN/PTN ratio width that is always greater than 1. The other measured morphometric dimensions of an FTN do not show any peculiar difference from those of a PTN.

5.2. Glacial- and hydro-isostatic adjustment

The departures from the eustasy and the regional variability of the predicted RSL curves (in particular the differences between the central areas and the marginal regions) stem from the ice-induced crustal variations (mostly from Fennoscandia) and the sea-bottom deformations driven by the ocean loading term.

In particular, the monotonous RSL rise and late highstand that are predicted at the Italian sites (Fig. 6) stem from the subsidence of the solid Earth in response to the collapse of the peripheral forebulge (around Fennoscandia) and to ocean load-driven subsidence of the crust. The predicted early highstand in the marginal sites (Fig. 7a and c), which is then followed by an RSL drop, is the result of two processes that are related to both meltwater redistribution and solid Earth deformations. The first is the so-called continental levering, which stems from the lithospheric flexure in response to the loading of the basins and which results in coastal uplift. The second is the migration of meltwater towards the collapsing forebulges. Together, these two processes result in an early highstand (w.r.t. the eustatic signal), which is opposed to the later highstand that is predicted in the central areas (Fig. 6), and the GIA signal is consistent regardless of the ice-sheet models (the predicted GIA variability is smaller if compared to the observations).

Overall, the maximum predicted highstand for the three ice-sheet models do show and confirm that the GIA signal in the Mediterranean is of the order of 1–2.5 m and is quite consistent, regardless of the shape and chronology of the MIS 6 glaciation and deglaciation.

5.3 Notch elevation distribution and comparison with GIA predictions

Measurements of the MIS 5.5 FTN elevation at 74 sites in areas of Italy that are considered tectonically stable in the literature (Table 1; Figure 4, Figures S3, S4, S5) show an average value of 5.73 m, with a maximum of 12.78 m and a minimum of 2.09 m.

The studied sites are far from tectonically or volcanic active zones. Elsewhere in Italy, active tectonic or volcanic processes account for a marked positive or negative departure of the observed MIS 5.5 FTN elevation from the predicted GIA-eustatic elevation, most notably in the northwestern Adriatic Sea and in the Ionian and Tyrrhenian sides of Calabria (Ferranti et al., 2006, 2010). Nevertheless, we suspect that some of the minor scatter between values at stable sites presented in this paper derives from unaccounted albeit slow local tectonic or volcanic processes.

In order to place further constraints on the accurate elevation of the MIS 5.5 FTN, we selected, from the total 74 observed sites in Italy, the 13 sites that we considered less affected by local land motion. Within these 13 sites, we retained only one elevation datum when multiple observations are available at sites that are few tens of meters to few kilometers apart within a geologically coherent area (**Table 6**). We selected this representative datum based on the ascertained (or suspected) slow tectonic process acting in each area and on the resulting sign of vertical land motion. When the prevailing process is normal faulting or aseismic subsidence related to a passive continental margin development, we considered the highest elevation found in the area as the most accurate. On the other hand, when arching related to magmatic processes controls coastal deformation and the land motion is uplift, we selected the lowest value (Table 6). Similarly, in areas where folding and thrusting produce uplift parallel to the coastline, the lowest FTN elevation is considered as most reliable. When faulting or folding is at a high angle to the coast, the resulting process is tilting and, thus, an intermediate FTN elevation, as close as possible to the tilt axis, represents the most accurate estimate.

We analysed the selected sites' distribution along a regional scale (~850 km long) E-W transect from the western Sardinia margin to the western Adriatic margin in Apulia, with a manually traced trend line of the observed MIS 5.5 highstand elevation (**Fig. 13** All the sites but Talamone in Tuscany and Marettimo in Sicily lay very close to the trace of the transect (yellow dots in Fig. 13). Because the two sites in Tuscany and Sicily are far from the trace compared to all the others, we showed these two sites in a different way (white dots in Fig. 13).

In NW Sardinia, we selected the FTN found at the maximum elevation (5.5 m) out of the 20 measurements in the area of Capo Caccia and Punta Giglio (Fig. 1D). As pointed out by Ferranti et al. (2006), NW Sardinia faces the Balearic continental margin of the western Mediterranean Sea, and the decrease in elevation of the FTN from east to west may be the result of fault- or creep-related subsidence (Table 6). Continental margin downthrow is also suspected in SW Sardinia (Buggerru-Masua and S. Antico sectors), so we picked the maximum elevation (3.5 m) as well. It is interesting to note that, on this continental margin, the selected FTN progressively loses 2.5 m of elevation from N (Capo Caccia-Punta Giglio) to S (Buggerru-Masua-S.Antioco) over a distance of 180 km. Whether this occurrence is fortuitous or reflects the process of a southward tilt of the whole of western Sardinia has not been established. However, being at a prominent continental margin, we chose to start the trend line at the maximum elevation in the north.

In respect to eastern Sardinia, Ferranti et al. (2006) suggested the presence of residual volcanic activity to explain the northward increase in elevation pattern of the FTN over a 25 km distance in the Orosei Gulf (sites 37–44; Fig. 1D). Mariani et al. (2009) modelled this deformation with a magmatic intrusion that post-dates the MIS 5.5 notch, as documented by minor explosive breccia flows that locally cover the notch. Based on this argument, the elevation increase is related to tilting ensuing from intrusion. Because the prevailing land motion is an uplift, we selected the minimum elevation (7.0 m) of the FTN observed at the Pedralonga site (Table 6). In NE Sardinia, the MIS 5.5 notch shows about 2 m difference in elevation from Tavolara (6–7 m) in the south to Capo Figari (4.5–5 m) in the north, over a distance of less than 10 km. Regional NE-

SW striking left transcurrent faults that cross the interposed bay could be responsible for the coast-parallel tilt, but they are retained as inactive (Oggiano et al., 2009). With the existing uncertainty, we included in the selection both the lowest elevation at Capo Figari and the highest elevation at Tavolara, assuming a tilt axis lies in between. The trend line crosses the eastern Sardinia margin midway between the observations at Capo Caccia, Tavolara and Capo Figari (Fig 13).

On the eastern Tyrrhenian margin, only an FTN observation (Talamone, 4.8 m elevation) is available from Tuscany in the north. This site is projected 250 km southward on the transect and, as for the Capo Figari site, has an elevation residing under the trend line, suggesting it could have been lowered by unaccounted processes.

South of Talamone, sites in Latium show a 3.4 m south-eastward decrease in elevation from 9.3 m (Circeo) to 5.9 m (Gaeta) along 50 km of coast which at this location has an E-W trend (Fig. 1B). We discarded from selection the site of Minturno, which displays the highest measured elevation in this study (12.48 m, site 54, Figures 11 and S4), because we considered it affected by processes related to the now extinct Roccamonfina volcano. The last documented activity of the volcano was at 150 Ka BP, but younger activity could have occurred (Rouchon et al., 2008). We also suspected that the continental margin rebound affected the 9.3 m elevation of the FTN at Circeo, and, thus, we excluded this site as well. The remaining three sites have elevations ranging from 6–6.5 m (Gaeta-Sperlonga) to 8 m (Terracina). The Terracina site lies close to a post-MIS 5.5 extensional fault, and, thus, the footwall uplift may have contributed to a fraction of the observed elevation. Fortunately, a borehole in the nearby Fondi Plain, located in the immediate hanging wall of the fault, which has revealed MIS 5.5 deposits at –6 m, allowed making a predictive estimation of the footwall uplift. By using a ratio of hanging-wall subsidence to footwall uplift of 1:10, supported by theoretical modelling and observational data (King et al., 1988; Armijo et al., 1996), the 14 m difference between the FTN at Terracina in the fault footwall and the drilled deposit in its hanging-wall results in 1.4 m footwall uplift. In terms of difference, the estimated GIA-eustatic position of the FTN at Terracina is 6.6 m (Table 6). This estimate is strikingly similar to observations in nearby Sperlonga and Gaeta, suggesting that the trend line passes through the corrected elevation at Terracina.

Several FTNs have been measured between Capri Island and Sorrento Peninsula (Campania). As pointed out by Ferranti and Antonioli (2007), the elevation of the notch at Capri decreases progressively from southeast (8.0 m) to northwest (5.2 m). The pattern of down-dropping of the tidal notch is consistent with the active subsidence with a maximum occurring in the Gulf of Naples, located north of Capri Island, and monocline tilting of the island and the nearby Sorrento Peninsula. We argue that the axis of tilting at Capri is at an elevation of 7.0 m, which is the most represented FTN elevation (Tables 1 and 6).

Further south, in Cilento, contrasting observations come from Palinuro (FTN at 2.1 m) and from nearby Marina di Camerota - Bulgheria site (FTN at 6.7 m) (Table 1, Figure S4, site 54). In line with the reasoning for continental margin faults, we regard the higher measurement as the most accurate.

The group of FTN sites measured in NW Sicily (Fig. 1E) is placed over an active collisional margin, where the convergence between Sardinia and Sicily in response to African and European plate motion is accommodated by thrusting and folding and is expressed by seismicity and geodetic data (Ferranti et al., 2008; Palano et al., 2012; Serpelloni et al., 2007). Thus, we picked the lowest observed FTN elevation (8.1 m at Marettimo) as representative of this sector, after discarding the very low elevation data from Capo Zafferano which could have been affected by local subsidence. When we projected the Marettimo datum 200 km northward on the trend line, a positive mismatch of about 2 m with respect to the trend line is estimated (Fig. 13).

The easternmost observed notch was at an elevation of 8.2 m at Striare in Apulia, at the southward terminus of the Adriatic Sea. Southern Apulia lies at the eastern tip of the conspicuous regional uplift of the Calabrian Arc, related to Ionian plate subduction (Ferranti et al., 2006, 2010), and, thus the FTN elevation could be 1–2 m higher than the trend line because of a far-field tectonic residual (Fig. 13).

A comparison between the selected observations of the FTN elevations and the predicted values from the ANICE-SELEN GIA model reveals that the GIA signal is partly at odds with respect to the observed trend (Fig. 13). Along the E-W transect, shown in Fig. 13, the GIA signal has elevations that are up to 4 m higher than the observation points, and 1–3 m higher than the inferred observational trend. The discrepancy between the GIA predicted values and the observations is higher in western Sardinia (Buggerru) and at the northeastern Tyrrhenian margin (Talamone), and progressively decreases to 1–2 m towards the the southeastern Tyrrhenian (Capri) margins, and on the Adriatic margin (Striare), where it is minimal. The observed and predicted trends along this transect appears to be comparable in the sector between the Adriatic and Tyrrhenian margins, with a 1.5–2 m lower elevation for the observed trend. Only the observed FTN at Terracina has an elevation similar to the predicted value, but, as outlined above, the elevation at this site has been corrected to 6.6 m.

The lower-than-predicted observed values in western Sardinia, and possibly at Talamone, could have been affected by unaccounted marginal tectonic subsidence, and this could alleviate the discrepancy. On the other hand, the cluster of selected sites on the Latium-Campanian coast (Terracina, Sperlonga, Capri and Marina di Camerota) seems to define a 6.5 reference value as the most appropriate. Under this hypothesis, a 1.5 difference with predicted values still remains in the comparable part of the transect (Fig. 13). This observation allows us to argue that the glacio-eustatic contribution at the MIS 5.5 was probably lower than most recent estimates (Kopp et al., 2009).

5.4 Age of the FTN

In this section of the study, we define the age of FTN in areas of the Mediterranean that are considered tectonically stable on the basis of correlation to well-known dated sediments attributed to the MIS 5.5. The latter were dated due to the presence of *Senegalese* fauna or by means of U/Th on *Cladocora caespitosa* or on speleothems, OSL or aminostratigraphy age determinations (Table S7). In fact, many FTNs are dated at MIS 5.5 because they are correlated very closely and at similar elevations with fossiliferous deposits (**Fig. 9**; Table 1) which contain *Senegalese* fauna. This argument was debated at the end of the nineties, when some authors (Hillaire-Marcel et al., 1996; Zazo et al., 1999) indicated that, in fossiliferous deposits on the southern Spanish coast, there were various levels containing *Persististrombus latus*. The consequence of this would have been that *Persistrombus* entered the Mediterranean Sea in various isotopic stages (MIS 11, 7, 5.1 and 5.3). In 2009, Mauz and Antonioli denied this thesis, arguing that, in the Mediterranean, *Persististrombus* and correlated tropical Senegalese fauna had been found only in one level (or terrace in uplifted areas, i.e. Calabria). There are no doubts that the *Persististrombus* gives a precise dating of an FTN. Furthermore, in stable areas, the sea level related to MIS 9 and 11 transgressions (or older) has always remained at similar elevations, and the occurrence of subsequent transgressions at the same elevation has always obliterated the older ones. Finally, Antonioli and Ferranti (1992) in the Orosei Gulf, dated pulmonate molluscs found in the aeolianites that were inside the FTN to MIS 2. Thus confirming that an FTN can be ascribed only to the most recent phase of the high sea level preceding the MIS 2, namely the MIS 5.5. Figure 9 shows that at sites 41-44 the distance between the FTN and the dated deposit is more than 20 km. These sites are located within the gulf of Orosei (Sardinia, Italy) one of the remotest and least anthropized coasts of the central Mediterranean sea. It is, therefore, likely that the distance between the measured FTN and the dated deposit is, in this case, a result of the inaccessibility of this region for study. These sites are some of those where the FTN is longer and more continuous than anywhere in the entire Mediterranean: between sites 38 and the 44, the FTN is constantly exposed and visible. These sites are, therefore, reliably considered to represent the same FTN and be of robust MIS 5.5 age.

5.5 Notches older than MIS 5.5

Uplifted FTNs older than MIS 5.5 were measured in Sicily and Apulia (Fig. 1; Table 2; sites 75–80) at Custonaci and Grotta Racchio (Trapani), Capo Zafferano, Sferracavallo (Pa) and Grotta Romanelli (Lecce), (S4). These uplifted FTN show a mean width of 1.79 m, compared to a mean width of 0.74 m of the MIS 5.5 FTNs. This difference is significant and very obvious, as it is two and a half times wider than MIS 5.5; furthermore, these FTNs are uplifted at an elevation from 9 m and 73 m (in column 5 of Table 2). Although greater in width, these uplifted FTNs cannot be confused with the smoothed notch sensu of Antonioli et al. (2006) (Figs. 2 and 3), which is much wider at 4 m. Therefore, on the basis of the measurements of these FTNs, we hypothesize that the amplitude of the paleo-tide related to the sea level when these FTNs were carved had a larger range than the present and the MIS 5.5 tides.

The uplifted FTNs of Custonaci and Grotta Racchio are located 1 km from Grotta Rumena (Custonaci) where Stocchi et al. (2017) examined a speleothem (the oldest stalactite containing marine hiatuses ever studied) inside an uplifted cave. In this cave, four marine ingressions are preserved: three hiatuses in the speleothem section and the last one, the younger, is an overgrowth of coral on the speleothem and the roof cave. The authors provided the tectonic uplift rate for the last one million years, and, using a multidisciplinary approach (assuming a continuous vertical uplift tectonic at a rate of 0.81 mm/yr), provided the age of the fourth and last marine ingression based on scleractinian coral species (1.1 ± 0.2 Ma). The latter corresponds are related to MIS25 (Stocchi et al.,2017). The cave is presently located at the altitude of 97 ± 0.2 m. In **Fig. 10,** the blue curve is referred to the chronological attribution of the uplifted FTN (sea level curves in Lisiecki and Raymo [2005], corrected for GIA in Stocchi et al., [2017]); the red curve is corrected with tectonic movements (0.81 mm/y). Comparing the elevations of the studied FTNs, located at 73, 58 and 34 m, with the red curve, the FTNs (green arrows) corresponded with the highstands of MIS 25, 21 and 11, respectively. These highstands refer to the last transgression in the Grotta Rumena (MIS 31), witnessed by corals covering the walls and some stalactites (comprising the studied hiatus, not the older hiatuses).

Regarding the FTNs located at 40 m and 23 m, respectively, at Sferracavallo and Arco di Zafferano, the comparison had less precision because the surrounding area of Palermo was certainly uplifted during the Middle-Lower Pleistocene, with vertical tectonic uplifting rates presumably lower than those of Custonaci.

In the area of Custonaci, the FTN studied at Grotta dei Cavalli (San Vito lo Capo, Table 2, S4, site 77), was located at an elevation of 34 m. Based on the curve corrected for tectonics in Fig. 10, this highstand could be attributed to MIS 11. Although the width of the FTN has been blunted by erosion, the measure (0.60 m in Table 2, S4) is fully compatible with the PTN or with the MIS 5.5 FTN. Therefore, this Middle Pleistocene FTN shows a width similar to MIS 5.5, while the other uplifted FTNs at higher elevations (showing an average width of 1.82 m) are placed in the lower Early Pleistocene. In this period the highstands and the lowstands (glacial-interglacial, Fig. 12) occurred with a mean period of 40,000 years, and not at a period of 100,000 years as occurred in the High and Middle Pleistocene (transgressions MIS 5, 7, 9 and 11). This obvious global climatic change (established by hundreds of global curves performed all over the world) could have determined higher tides in the Mediterranean, and the width of the FTN here described is a direct proof.

In summary, the red curve in Fig. 10, following Liesiki and Raymo (2005), allows us to attribute to the FTNs located at 73, 58 and 34 m an age of 950, 850 and 400 ka, respectively. For the FTNs located in the Palermo area at the elevations of 40 m and 23 m, we can hypothesize a lower or non-continuous uplift rate compared to what was found in Custonaci, and assess, on the basis of the width, that they are aged at the Lower Pleistocene. It is possible to hypothesize a sharp change of tide amplitude presumably during the transition to Middle-Lower Pleistocene (780 ka BP).

5.6 Tides

Antonioli et al. (2015) demostrated that the tidal notches are strictly connected with the local tide. But the width of the present tidal notch shows higher values when compared with the local tide (on average the notch has a width slightly less than twice in respect to the mean tidal range). Comparing the FTN width with the PTN width, our results show that the FTN width (mean 0.73 m) is wider by about 0.14 m than that of the PTN (mean 0.59 m); we interpret this greater amplitude as being due to the lack of the biological reef and to the chemical and mechanical erosion of the notch.

Therefore, we believe that the tides of the Mediterranean Sea during the MIS 5.5 highstand were the same as ~~. Temptatively~~ today. Tentatively, considering the mean width of PTNs as 0.59 m and 0.38 m as the current mean Mediterranean tide (Antonioli et al., 2015), we can extrapolate the palaeo-tide of MIS 25–21 (when the mean width of the uplifted tidal notches is 1.82 meters), resulting in a possible tide of 1.21 m, before 780 ka BP, more than three times that of today.

6. Conclusions

At 80 sites in Italy and subordinately in the eastern and western Mediterranean Sea (**Tables 1 and 2**), the MIS 5.5 and few older notches have been accurately measured. The main conclusions of this study are:

1. The morphometric parameters of the PTN and FTN are broadly similar, with only a slightly larger FTN width due to the lack of the biological reef and to the chemical/mechanical erosion of the cliff during later exposure. This result implies that tide amplitude has not changed in the last 125 ka.

2. In contrast, during the MIS 25–21 highstands (1.2–0.6 Ma BP), the Mediterranean tides had amplitude three times larger than today.

3. The GIA-driven RSL changes within the Mediterranean Basin are regionally varying and significantly different from the eustatic signal. Two main typologies of RSL curves can be expected: monotonous rise followed by a late highstand in the central areas and initial (early) highstand followed by an RSL drop in the marginal regions at the western and eastern borders. Overall, the variability of the maximum GIA elevation is between 1 and 2.5 m, i.e. comparable to the expected eustatic contribution of the GrIS. 10.

4. Provided that the notches represent the maximum peak of local RSL rise, which may occur at different times and with different elevations from place to place (as explained by GIA), the observed spatial variability of MIS 5.5 notches is 1–12. m. This implies that GIA plays a secondary role in driving the regional variability of the maximum MIS 5.5 RSL elevation, and other regionally varying signals, either geologic or oceanographic, are operating.

5. Geologic processes are represented by volcanic intrusions (e.g. at the Orosei Gulf in Sardinia and at Minturno in Latium), or by tectonic displacement (e.g. continental margin down-faulting in western Sardinia and on the eastern Tyrrhenian coast, or contractional uplift in northern Sicily).

These low-rate processes cause a spread of up to 10 m in the FTN elevation, five times larger than the GIA variability, even at sites commonly regarded to be on stable crustal sectors.

6. The elevation of the MIS 5.5 notch at selected sites which are less affected by these low tectonic or volcanic movements has a trend that, along a regional E-W transect, mimics but is 1–2 m lower than the predicted values from the GIA ANICE-SELEN model. The 6.5 m elevated MIS 5.5 notch on the Tyrrhenian margin, which is assumed as a reference elevation, has a 1.5 m discrepancy with the model, thus casting doubt on the currently accepted amount of glacio-eustatic contribution to the RSL during the MIS 5.5.

Acknowledgements

We thank Ian Kendy, editor of Earth Science revue and two anonymous reviewers for comments and useful suggestions. We thank Kurt Lambeck who supplied us with the photograph *of the Calanques FTN. We thank* Joaquin Rodriguez Vidal who sent us the photographs used in Supplementary material S6. *This study has been produced in the framework of the Flagship Project RITMARE* and a contribution to the project IGCP 639 - International Geological Correlation Programme 'Sea-level change from minutes to millennia' by UNESCO-IUGS, We also thanks GEOSWIM project

FIGURE captions

Fig. 1. Location of the investigated sites along the Mediterranean coasts. A. The red rectangles indicate the studied areas. The numbers refer to the sites of Table 1. B. White numbers refer to the altitude of the FTN, see Table 1. C. White numbers refer to the site number indicated in Table 2. D. White numbers refer to the FTN of the sites studied in Sardinia. E. White numbers refer to the FTN of the sites studied in Sicily, see also Table 1, and the white numbers refer to the sea level share of the FTN of the sites studied in Sicily, see Table 1. The yellow dots refer to the uplifted FTN sites (Table 3). F. The white numbers refer to the sites in Israel, indicated in Table 2. G. The white numbers refer to the site number in Frace, indicated in Table 2.

Fig. 2. a) MIS 5.5 and PTN notches morphological sketch. b) Tidal and smoothed notch as is possible to observe today in some sections we studied. c) Evolution of the tidal and smoothed notch during MIS 5.5, the final coverage of fans or aeolianites deposits preserves the notches from the dissolution.

Fig. 3. Sections of fossil and present tidal notch morphology. The letters refer to the width (w), depth (d) and the base of the notch (c). On the right an overlap between the present and the fossil tidal notch (for the sites 52, 71 and 2 of Table 1) morphology highlights the marine and ~~aeolian~~ subaerial erosion that slightly modified the original morphology, but preserves a similar width.

Fig. 4. View of some representative morphology of the studied tidal notches. a) Site 5, Sardinia. b)Site 30, Sardinia. c) Site 38, Sardinia. d) Sites 40 and 48, Sardinia. f) Site 69, Sicily. g) Uplifted FTN site 76, Sicily. h) Uplifted FTN, site 78, Sicily. See also Tables 1 and 2.

Fig. 5. View of the different measurement methods. a) Using the telescopic measuring gauge on site 38. b) Using tape meter on site 39. c., d., e., f., g. and h. Using DGPS on sites 50, 51, 79 and 52. i. and j. In Sardinia, near Grotta Biddiriscottai, an FTN filled with aeolianite sediments aged MIS 2. k) a wall riddled by *Lithophaga* holes under the FTN of site 54. m. In Pianosa, a possible FTN that we did not use in our database due to a lack of geomorphological lateral continuity. Although we recorded day and time during each survey (see Tables 1 and 2), we did not applied tidal corrections because we referred to: a) the base of the PTN, b) the living vermetid reef, except for the FTN of Capri and Mitigliano whose measurements have been taken with respect to the corrected tide sea level, due to the lack of the PTN (Ferranti and Antonioli, 2007).

Fig. 6. Predicted MIS 5.5 RSL curves at sites along the Italian coastlines according to ICE-5G (red curves), ICE-6G (blue curves) and ANICE-SELEN (green curves) ice-sheet models. The dashed curves represent the eustatic trend, while the solid curves represent the GIA-induced RSL changes. The RSL curves are computed at each investigated site and are plotted cumulatively for different sub-regions.

Fig. 7. Same as for Fig. 6, but for sites in Morocco (a), southern Spain (a), France (b) and Israel (c).

Fig. 8. The FTN width compared with the PTN width. The FTN widths are always a few cm larger due to limestone dissolution (see also Fig. 4). On the right, the larger 2 m width of the uplifted notches, older than last Interglacial period.

Fig. 9. Distance between the measured site and the nearest site dated using 1) U/th, 2) aminostratigraphy, 3) ESR/OSL, but above all, 4) presence of *Persististrombus latus* or Senegalese fauna. The sites are sorted as in Table 1.

Fig. 10. In blue, the Lisiecki and Raymo (2005) curve corrected by Stocchi et al. (2017) for GIA calculated for Custonaci, Sicily. In red, the same corrected curve for a rate of vertical tectonic movement of 0.81 mm/a. In yellow, the calculated age of the uplifted tidal notches of Table 3.

Fig. 11. Maximum predicted RSL highstands according to ICE-5G, ICE-6G and ANICE-SELEN at each site considered in this study. The sites are displayed and enumerated from left to right as a function of the longitude. The numbers in the x-axis correspond to the site number. The horizontal lines correspond to the maximum eustatic value of each ice-sheet model (0.91 m for ICE-5G; 3.1 m for ICE-6G; 7.0 m for ANICE-SELEN).

Fig. 12. Predicted "maximum" RSL elevation (w.r.t. present-day) between 120 kyr BP and 110.0 kyr BP (left) and predicted RSL elevation (w.r.t. present-day) exactly at 117 kyr BP (right). On the left figure we show the maximum RSL elevation predicted, for each element of the surface mesh, between 120 and 110 ka. Because of the viscous response of the mantle, in fact, RSL continues to change also without any further addition of meltwater to the oceans. Hence maximum elevations are reached at different times according to the geographical location and are followed by RSL drop. Comparing left with right reveal indeed that in areas such as Gibraltar and Israel, maximum

elevation is reached at 117 ka, and is later followed by RSL drop while other areas experience a further increase. The RSL drop predicted at Gibraltar and Israel is a consequence of *(i)* continental levering (i.e. upward tilt of the continental margins) and *(ii)* meltwater syphoning (i.e. migration of sea water towards the surroundings of formerly glaciated areas in N and S hemisphere).

Fig. 13. Observed and predicted elevation of selected MIS 5.5 FTN sites along an ☐E-W transect from western Sardinia to southern Apulia. Predicted elevations are from the GIA ANICE-SELEN model. The trend across observed elevations is traced based on geological constraints (see text for further details).

TABLES

Table 1: MIS 5.5 and Present tidal notches data in the Mediterranean Sea

1) Site number; 2) Locality and site name; 3) Elevation, uncertain are explained in chapter 3.1 ; 4) Notch Morphometry; 5) Type of Notch: MTN= MIS 5.5 Tidal Notch; PTN= Present Tidal Notch; NM= Not Measured; NC= Not Carved; C= Consumed); 6) Distance (km) and *reference site name for the age of deposit: 1 Abate et al., 1996; 2 Antonioli, 1991; 3 Antonioli et al., 1994a; 4 Antonioli et al., 1994b; 5 Antonioli et al., 1999; 6 Antonioli et al., 2002; 7 Blanc and Segre, 1953; 8 Bosellini et al., 1999; 9 Brancaccio et al., 1986, 1990; 10 Cesaraccio and Puxeddu, 1986; 11 Delicato et al., 1999; 12 Durante, 1975; 13 Esposito et al., 2003; 14 Ferranti and Antonioli, 2007; 15 Hearty P.J., 1986, 1987; 16 Malatesta, 1954a, 1954b, 1970; 17 Mastronuzzi et al., 2007; 18 Orrù and Ulzega, 1986; 19 Orrù and Pasquini, 1992; 20 Orrù et al., 2011; 21 Palmerini and Ulzega, 1969; 22 Pascucci et al., 2014; 23 Porqueddu et al., 2011; 24 Sanna et al., 2010; 25 Segre, 1951; 26 Segre, 1957; 27 Ulzega and Ozer, 1980;

Table 2

FTNs older than the uplifted MIS 5.5. 1) Site number; 2) Locality and site name; 3) Coordinates; 4) Measures; 5) Elevation (m) uncertain is explained in the method section 3.1, as regard site 75, the 0.25 m uncertain was due the particular erosion of the base of the FTN ; 6) Average notch measures (m); 7) Notch Morphometry; 8) Kind of measurement (DGPS= Differential Global Positioning System; DT= Digital Altimeter) 9) MIS 5.5 elevation; 10) Reference for age; 11) Age MIS ka.

Table 3

Published FTN altitude in the Mediterranean Sea.

Table 4

Erosion rates in the intertidal and inner karst in the Mediterranean area. The total erosion for the last 125 Ka was evaluated considering a constant erosion rate.

Table 5

Comparison between GIA prediction with different models and geophysical parameters with the observed data (FTN elevations).

Table 6

Selected sites with MIS 5.5 FTN elevations less affected by tectonic displacement in Italy. See text for further details.

Supplementary material

S1 table Acronyms and definitions.

S2 File kmz of the geographical coordinates of all sites.

S3, S4, S5 Figures. A complete collection of images of all the studied notches (numbers refer to Table 1)

S6 Figures Notches measured in France, Gibiltrair and Morocco, by other authors (refer to Table 3). 1a, b, c: site 81; 2a and 2b: site 82, notch profile and Lithophaga holes; 3: site 83; 4: site 84, Caleta Hotel. MIS 5.5 FTN and its wave-cut-platform , MIS 5.5 FTN (close up) with borings and flowstone; 5a and 5b: site 85; 6a and 6b, site 86, from Sisma Ventura et al., 2017 redrowned. Photo 1, 2, 3, 4 courtesy prof. , photo 5 courtesy prof. Kurt Lambeck. Photo 6 from redrowned from Sisma Ventura et al., 2016.

S7 Table 7: MIS 5.5 and Present tidal notches data in the Mediterranean Sea

1) Site number; 2) Locality and site name; 3) Coordinates; 4) Measures date; 5) Elevation with uncertain, m; 6) Type of Notch: MTN= MIS 5.5 Tidal Notch; PTN= Present Tidal Notch; NM= Not Measured; NC= Not Carved; C= Consumed; 8) Notch morphometry; 9) Kind of measurement: T: Telefix; M: Tape meter; DGPS: DGPS; 10) Faunal assemblage of the nearest aged fossil deposit; Distance (km) and reference site name for the age of deposit. 1) Site number; 2) Locality and site name; 3) Coordinates; 4) Notch Morphometry; 5) Elevation with uncertain, m; 6) Average notch measures, m; 7) Type of Notch: MTN= MIS 5.5 Tidal Notch; PTN= Present Tidal Notch; NM= Not Measured; NC= Not Carved; C= Consumed); 8) Notch morphometry; 9 Kind of measurement; 10) Faunal assemblages in aged fossil deposit; 11) Thechnique of chronological attribuition; 12

Distance (km) from the site used for give the age of deposit. References: 1 Abate et al., 1996; 2 Antonioli, 1991; 3 Antonioli et al., 1994a; 4 Antonioli et al., 1994b; 5 Antonioli et al., 1999; 6 Antonioli et al., 2002; 7 Blanc and Segre, 1953; 8 Bosellini et al., 1999; 9 Brancaccio et al., 1986, 1990; 10 Cesaraccio and Puxeddu, 1986; 11 Delicato et al., 1999; 12 Durante, 1975; 13 Esposito et al., 2003; 14 Ferranti and Antonioli, 2007; 15 Hearty P.J., 1986, 1987; 16 Malatesta, 1954a, 1954b, 1970; 17 Mastronuzzi et al., 2007; 18 Orrù and Ulzega, 1986; 19 Orrù and Pasquini, 1992; 20 Orrù et al., 2011; 21 Palmerini and Ulzega, 1969; 22 Pascucci et al., 2014; 23 Porqueddu et al., 2011; 24 Sanna et al., 2010; 25 Segre, 1951; 26 Segre, 1957; 27 Ulzega and Ozer, 1980.

REFERENCES

Abad, M., Rodríguez-Vidal, J., Aboumaria, K.,. Zaghloul, M.N., Cáceres, L.M., Ruiz F., Martínez-Aguirre, A., Izquierdo, T., Chamorro, S., 2013. Evidence of MIS 5 sea-level highstands in Gebel Mousa coast (Strait of Gibraltar, North of Africa). Geomorphology 182, 133–146.

Abate, B, Incandela, A, Renda, P., 1996. Lineamenti strutturali dell'Isola di Marettimo (Arcipelago delle Egadi, Sicilia N-O) Mem. Soc. Geol. It., 5, 23-33.

Amorosi, A., Antonioli, F., Bertini, A., Marabini, S., Mastronuzzi, G., Montagna, P., Negri, A., Rossi, V., Scarponi, D.,Taviani, M., Angeletti, L., Piva, A., Vai, G.B., 2014. The Middle–Upper Pleistocene Fronte Section (Taranto, Italy): An exceptionally preserved marine record of the Last Interglacial. Global and Planetary Change 119, 23–38.

Antonioli, F., 1991. Geomorfologia subacquea e costiera del litorale compreso tra Punta Stendardo e Torre S. Agostino (Gaeta). Il Quaternario 4 (2), 257–274.

Antonioli, F., Ferranti, L., 1992. Geomorfologia costiera e subacquea e considerazioni paleoclimatiche sul settore compreso tra S.M. in Navarrese e Punta Goloritzè (Golfo di Orosei, Sardegna). Il Giornale di Geologia 54, 2, 65-89.

Antonioli, F., Cinque, A., Ferranti, L., Romano, P., 1994a. Emerged and Submerged Quaternary marine terraces of Palinuro Cape (Southern Italy). Memorie Descrittive del Servizio Geologico Nazionale 52 237-260.

Antonioli, F., Belluomini, G., Ferranti, L., Improta, S., 1994b. Il sito preistorico dell'arco naturale di Capo Zafferano (Sicilia). Aspetti geomorfologici e relazione con le variazioni del livello del mare. Il Quaternario, Italian Journal of Quaternary Sciences 7(1) 109-118.

Antonioli, F., Reitano, G., Puglisi, C., Tusa, S., 1997. Evoluzione geomorfologica pleistocenica del settore costiero di S. Vito Lo Capo (Trapani): rapporti tra neotettonica, eustatismo e comunità preistoriche. Memorie Descrittive del Servizio Geologico Nazionale 52, 337-360.

Antonioli, F., Silenzi, S., Vittori, E., Villani, M., 1999. Sea level changes and tectonic stability: precise measurements in 3 coastlines of Italy considered stable during last 125 ky. Physics and Chemistry of the Earth (A) 24, 337-342.

Antonioli, F., Cremona, G., Immordino, F., Puglisi, C., Romagnoli, C., Silenzi, S., Valpreda, E., Verrubbi, V., 2002. New data on the Holocenic sea level rise in NW Sicily (central Mediterranean Sea). Global and Planetary Change 34, 121-140.

Antonioli, F., Ferranti, L., Kershaw, S., 2006. A glacial isostatic adjustment origin for double MIS 5.5 and Holocene marine notches in the coastline of Italy. Quaternary International 145–146, 19-29.

Antonioli, F., Anzidei, M., Lambeck, K., Auriemma, R., Gaddi, D., Furlani, S., Orrù, P., Solinas, E., Gaspari, A., Karinja, S., Kovačić, V., Surace, L., 2007. Sea level change in Italy during Holocene from archaeological and geomorphological data. Quat. Sci. Rev. 26, 2463-2486.

Antonioli, F., Ferranti, L., Fontana, A., Amorosi, A., Bondesan, A., Braitenberg, C., Dutton, A., Fontolan, G., Furlani, S., Lambeck, K., Mastronuzzi, G., Monaco, C., Spada, G., Stocchi, P., 2009. Holocene relative sea-level changes and vertical movements along the Italian and Istrian coastlines, Quaternary International 206, 102-133.

Antonioli, F., Lo Presti, V., Anzidei, M., Deiana, G., de Sabata, E., Ferranti, L., Furlani, S., Mastronuzzi G., Orru, P. E., Pagliarulo, R., Rovere, A., Sannino, G., Sansò, P., Scicchitano, G., Spampinato, C. R., Vacchi, M., Vecchio, A., 2015. Tidal notches in Mediterranean Sea: a comprehensive analysis. Quaternary Science review. Quaternary Science Reviews 119, 66-84.

Anzidei, M., Lambeck, K., Antonioli, F., Furlani, S., Mastronuzzi, G., Serpelloni, E., Vannucci, G., 2014. Coastal structure, sea-level changes and vertical motion of the land in the Mediterranean. Geological Society, London, Special Publications 388, 453-479. http://dx.doi.org/10.1144/SP388.20

Argus, D.F., Peltier WR, Drummond, R., Moore, A.W. 2014. The Antarctica component of postglacial rebound model ICE-6G_C (VM5a) based on GPS positioning, exposure age dating of ice thicknesses, and relative sea level histories. Geophysical Journal International, 198 (1), 537-563.

Armijo, R., Meyer, B., King, G.C.P., Rigo, A., Papanastassiou, D., 1996. Quaternary evolution of the Corinth Rift and its implications for the Late Cenozoic evolution of the Aegean. Geophysical Journal International 126, 11–53.

Austermann, J., Mitrovica, J. X., Huybers, P., Rovere, A., 2017. Detection of a dynamic topography signal in last interglacial sea-level records. Science Advances, 3(7), e1700457.

Bard, E., Hamelin, B., Fairbanks, R.G., 1990. U/Th ages obtained by mass spectrometry in corals from Barbados. Sea level during the past 130,000 years, Nature 346, 456-458.

Benac, C., Juracic, M., Bakran-Petricioli, T., 2004. Submerged tidal notches in the Rijeka Bay NE Adriatic Sea: indicators of relative sea-level change and of recent tectonic movements. Marine Geology 212, 21-33.

Benac, C., Juracic, M., Blaskovic, I., 2008. Tidal notches in Vinodol channel and Bakar bay, NE Adriatic Sea: indicators of recent tectonics. Marine Geology 248, 151-160.

Blanc, A. C., 1936. Una spiaggia pleistocenica a *Strombus bubonius* presso Palidoro (Roma). Accademia Nazionale dei Lincei, Rendiconti 23, 200-204.

Blanc, A. C., Segre, A., 1953. Le Quaternaire du Monte Circeo. Livret-Guide, IV Congr. INQUA, Roma, pp. 23-108.

Blanchon, P., Eisenhauer, A., Fietzke, J., Liebetrau, V. 2009. Rapid sea-level rise and reef back-stepping at the close of the last interglacial highstand. Nature 458 (7240), 881-884.

Bonifay, F., Mars, P., 1959. Le Tyrrhenien dans le cadre de la chronologie quaternaire mediterraneenne. Bulletin de Societé Geologique de France 7, 62–78.

Bosellini, A., Bosellini, F., Colalongo, ML., Parente, M., Russo, A., Vescogni, A., 1999. Stratigraphic architecture of the Salento coast from Capo d'Otranto to S. Maria di Leuca (Apulia, Southern Italy). Riv. Ital. Paleontol. Stratigr. 105, 397–416.

Boulton, S.J., Stewart, I.S., 2015. Holocene Coastal Notches in the Mediterranean Region: indicators of Palaeoseismic clustering? Geomorphology 237, 29-37

Brancaccio, L., Cinque, A., Belluomini, G., Branca, M., Delitala, L., 1986. Isoleucine epimerization dating and tectonic significance of Upper Pleistocene sea level features of the Sele plain (southern Italy). Zeitschrift für Geomorphologie N. F., Suppl.-Bd. 62, 159-166.

Brancaccio, L., Cinque, A., Russo, F., Belluomini, G., Branca, M., Delitala, L. 1990. Segnalazione e datazione di depositi marini tirreniani sulla costa campana. Bollettino Società Geologica Italiana 109, 259-265.

Carobene, L., 1972. Osservazioni sui solchi di battente attuali ed antichi nel golfo di Orosei in Sardegna. Boll. Soc. Geol. it. 91, 583-601

Cesaraccio, M., Puxeddu, C., Ulzega, A., 1986. Geomorfologia della fascia costiera tra Buggerru e Portixeddu nella Sardegna Sud- Occidentale. Rend. Sem. Fac. Sc. Univ. Cagliari, 56/1, 75-89.

Chappell, J., Omura, A., Esat, T., McCulloch, M., Pandolfi, J., Ota, Y., Pillans, B., 1996. Reconciliation of late Quaternary sea levels derived from coral terraces at Huon Peninsula with deep sea oxygen isotope records. Earth and Planetary Science Letters 141, 227-236.

Chen, J.H, Curran, H.A., White, B., Wasserburg, G.J., 1991. Precise chronology of the last interglacial period: 234U-230Th data from fossil coral reefs in the Bahamas, Geol. Soc. Am. Bull. 103, 82-97.

Creveling, J. R., Mitrovica, J. X., Hay, C. C., Austermann, J., Kopp, R. E., 2015. Revisiting tectonic corrections applied to Pleistocene sea-level highstands. Quaternary Science Reviews 111, 72-80.

Cucchi, F., Forti, F., Furlani, S. 2006. Erosion/Dissolution Rates Of Limestone Along The Western Istrian Shoreline And The Gulf Of Trieste. Geografia Fisica e Dinamica Quaternaria 29, 61-69.

de Boer, B., Lourens, L.J., Van de Wal, R.S.W., 2014. Persistent 400,000-year variability of Antarctic ice volume and the carbon cycle is revealed throughout the Plio-Pleistocene. Nat. Commun. 5, 2999.

de Boer, B., P. Stocchi, Whitehouse, P. L., van de Wal, R. S. W., 2017. Current state and future perspective on coupled ice-sheet - sea-level modeling. Quaternary Science Reviews 169, 13 - 28.

Delicato, M.A., 1999. Utilizzo di marker eutirreniani per l'assetto neotettonico di aree costiere tirreniche. L'esempio della piana del Garigliano. Unpublished Laurea Thesis, Università degli Studi di Roma 'La Sapienza', ENEA, A.A. 1-129.

De Mets, C., Laffaldano, G., Merkouriev, S., 2015. High-resolution Neogene and Quaternary estimates of Nubia-Eurasia-North America Plate motion. Geophys. J. Int. 203, 416-427.

Dépéret, C., 1918. Essai de coordination chronologique générale des temps quaternaires. Comptes Rendus de l'Accad!emie des Sciences, 167, 418–422.

Devoti, R., D'Agostino, N., Serpelloni, E., Galvani, A., Anzidei, M. et al., 2017. A combined velocity field of the Mediterranean region, Ann. Geophys., 60(2), doi:10.4401/ag-7059.

De Waele, J., Furlani, S. 2013. Seawater and biokarst effects on coastal karst. In: Shroeder, J.F., Frumkin A. (Eds), Treatise on Geomorphology, Vol. 6, Elsevier, Amsterdam, 341-350.

Durante, S., 1975. Sul Tirreniano e la malacofauna della Grotta del Fossellone (Circeo). Quaternaria 18, 331–347.

Dutton, A., Lambeck, K., 2012. Ice Volume and Sea Level During the Last Interglacial. Science, 337, 216-9.

Dutton, A., Webster, J.M., Zwartz, D., Lambeck, K., Wohlfarth, B., 2015. Tropical tales of polar ice: evidence of Last Interglacial polar ice sheet retreat recorded by fossil reefs of the granitic Seychelles islands. Quat. Sci. Rev. 107, 182–196.

Esposito, C., Filocamo, F., Marciano, R., Romano, P., Santangelo, N., Scarmiglia, F., Tuccimei, P., 2003. Late Quaternary shorelines in southern Cilento (Mt. Bulgheria): Morphostratigraphy and chronology. Il Quaternario 16 (1), 3-14.

Farrell, W. E., Clark, J.A., 1976. On postglacial sea level. Geophysical Journal of the Royal Astronomical Society 46, 647–667.

Ferranti, L., Antonioli, F., Amorosi, A., Dai Prà, G., Mastronuzzi, G., Mauz B., Monaco, C., Orrù P., Pappalardo M., Radtke U., Renda P., Romano P., Sansò P., Verrubbi V., 2006. Elevation of the last interglacial highstand in Sicily (Italy): a benchmark of coastal tectonics. Quaternary International 145-146, 30-54.

Ferranti, L., Antonioli, F., 2007. Misure del solco tirreniano (MIS 5.5) nell'isola di Capri: implicazioni su micro-dislocazioni e blocchi cinematici attivi negli ultimi 124 ka. Il Quaternario. 20(2), 125-136.

Ferranti, L., Oldow, J.S., D'Argenio, B., Catalano, R., Lewis, D., Marsella, E., Avellone, G., Maschio, L., Pappone, G., Pepe, F., Sulli, A., 2008. Active deformation in Southern Italy, Sicily and southern Sardinia from GPS velocities of the Peri-Tyrrhenian Geodetic Array (PTGA). Bollettino Della Società Geologica Italiana 127, 299-316.

Ferranti, L., Antonioli, F., Anzidei, M., Monaco, C., Stocchi, P., 2010. The timescale and spatial extent of vertical tectonic motions in Italy: insights from relative sea-level changes studies. J. Virtual Explorer 36, 1–34.

Furlani, S., Cucchi, F., Forti, F., Rossi, A., 2009. Comparison between coastal and inland Karst limestone lowering rates in the northeastern Adriatic Region (Italy and Croatia). Geomorphology 104, 73-81.

Furlani, S., Cucchi, F., Biolchi, S., Antonioli, F., Odorico, R., 2011. Notches in the Adriatic Sea: genesis and development, Quaternary International 232, 158-168.

Furlani, S., Cucchi, F., 2013. Downwearing rates of vertical limestone surfaces in the intertidal zone (Gulf of Trieste, Italy). Marine Geology 343, 92-98.

Furlani, S., Ninfo, A., Zavagno, E., Paganini, P., Zini, L., Biolchi, S., Antonioli, F., Coren, F., Cucchi, F., 2014a. Submerged notches in Istria and the Gulf of Trieste: results from the Geoswim Project. Quaternary International 332, 37-47.

Furlani, S., Pappalardo, M., Gomez-Pujol, L., Chelli, A., 2014b. The rocky coasts of the Mediterranean and Black Sea. In: Kennedy, D.M., Stephenson, W.J., Naylor, L.A. (Eds), Rock coast Geomorphology: A Global Synthesis. Geological Society, London, Memoirs 40, 89-123

Furlani, S., Antonioli, F., Gambin, T., Gauci, R., Ninfo, A., Zavagno, E., Micallef, A., Cucchi, F., 2017. Marine notches on the Maltese Islands (Central Mediterranean Sea). Quaternary International 39, 158-168.

Gignoux, M., 1911a. Les couches "a Strombus bubonius (Lmk.) dans la Mediterranée occidentale. Compte Rendus des Séances de l'Academie des Sciences, February 6th, 1911, 1–3.

Gignoux, M., 1911b. Resultats généraux d'une etude des anciens rivages dans la Méditerranée occidentale. Annales de l'Université de Grenoble XXIII (1), 1–21.

Gignoux, M., 1913. Les formations marines pliocenes et quaternaires de l'Italie du sud et de la Sicilie. Annales de l'Universite de Lyon 36, 693.

Gomez-Pujol, L., Fornos, J.J., Swantesson, J.O.H. 2006. Rock surface millimeter-scale roughnessand weathering of supratidal Mallrcan carbonate coasts (Balearic Islands).Earth Surface Processes and Landforms 31(14), 1792-1801.

Harmon, R.S., Land, L.S., Mitterer, R.M., Garrett, P., Schwarcz, H.P., Larson, G.J., 1981. Bermuda sea-level during the last interglacial. Nature 289, 481-483.

Hearty, P.J., 1986. An inventory of last interglacial (sensu lato) age deposits from the Mediterranean Basin: a study of Isoleucine epimerization and U-Series dating. Zeitschrift fur Geomorphologie N. F. Suppl. Bd. 62, 51– 69.

Hearty, P.J., 1987. New Data on the Pleistocene of Mallorca. Quaternary Sci Rev 6, 245-257.

Higgins, C.G., 1980. Nips, Notches, and the Solution of Coastal Limestone: an overview of the problem with examples from Greece. Estuar. Coast. Sci. 10, 15-30.

Hillaire-Marcel, C., Garièpy, C., Ghaleb, B., Goy, J. L., Zazo, C., Barcelos, C., 1996. U-series measurements in Tyhrrenian deposits from Mallorca — further evidence for two last-interglacial high sea levels in the Balearic Islands. Quaternary Science Reviews 15, 53–62.

Issel, A., 1914. Lembi fossiliferi quaternari e recenti osservati nella Sardegna meridionale dal prof. D. Lovisato. Atti della Reale Accademia dei Lincei, Rendiconti, Classe di Scienze Fisiche, Matematiche e Naturali, S. 5, CCCXI, 23, 759–770.

Kelletat, D.H., 2005. Notches. In: Schwartz, M.L. (Ed.), Encyclopedia of Coastal Science. Springer, Dordrecht, 728-729.

King, G.C., Stein, R.S., Rundle, J.B., 1988. The growth of geological structures by repeated earthquakes 1. Conceptual framework. Journal of Geophysical Research 93, 13307–13318.

Kopp, R.E., Simons, F.J., Mitrovica, J.X., Maloof, A.C., Oppenheimer, M., 2009. Probabilistic assessment of sea-level during the last interglacial stage. Nature 462, 863–867.

Kruzǐć P. & Benković L., 2008. Bioconstructional features of the coral Cladocora caespitosa (Anthozoa, Scleractinia) in the AdriaticSea (Croatia). MarineEcology 29 (2008), 125–139.

Laborel, J. 1987. Marine biogenic costructionsin the Mediterranean a review. Scientific Reports of the Port-Cross National Park. 13, 97-126.

Lambeck, K., Bard, E., 2000. Sea-level change along the French Mediterranean coast since the time of the Last Glacial Maximum. Earth and Planetary Science Letters 175 (3–4), 202–222.

Lambeck, K., Antonioli, F., Anzidei, M., Ferranti, L., Leoni, G., Scicchitano, G., Silenzi, S., 2011. Sea level change along Italian coast during Holocene and a proiection for the future Quaternary International, 232, 1–2, 250–257.

Lisiecki, L., Raymo, M., 2005. A Pliocene-Pleistocene stack of 57 globally distributed benthic δ18O records. Paleoceanography 20, Issue 2.

Lorscheid, T., Stocchi, P., Casella, E., Gómez-Pujol, L., Vacchi, M., Mann, T., Rovere, A., 2017a. Paleo sea-level changes and relative sea-level indicators: Precise measurements, indicative meaning and glacial isostatic adjustment perspectives from Mallorca (Western Mediterranean). Palaeogeography, Palaeoclimatology, Palaeoecology 473, 94-107.

Lorscheid, T., Felis, T., Stocchi, P., J. Obert, J.C., Scholz, D., Rovere, A., 2017b. Tides in the Last Interglacial: insights from notch geometry and palaeo tidal models in Bonaire, Netherland Antilles. Scientific Reports 7, 16241.

Malatesta, A., 1954. Risultati del rilevamento del Foglio 192 (Alghero e Isola di Sardegna). II, Fossili delle spiagge tirreniane. Boll. del Serv. Geol. d'Italia 76, 9 e 17.

Malatesta, A., 1970. Cynotherium sardous Studiati: anextinct canid from the pleistocene of Sardinia. Mem. dell'Ist. Ital. Paleontol. Um.1, 1-72.

Malatesta, A., 1985. Geologia e paleobiologia dell'era glaciale. La Nuova Italia Scientifica, 282.

Mariani, P., Braitenberg, C., Antonioli, F., 2009. Sardinia coastal uplift and Volcanism. Pure and applied Geophysics 166, 1369-1402.

Mastronuzzi, G., Quinif, Y., Sansò, P., Selleri, G., 2007. Middle-Late Pleistocene polycyclic evolution of a geologically stable coastal area (southern Apulia, Italy). Geomorphology 86, 393–408.

Moses, C.A. 2013. Tropical rock coasts: Cliff, notch and platform erosion dynamics. Progress in Physical Geography 37(2), 206-226.

Moses, C.A., Robinson, D., Kazmer, M., Williams, R. 2015. Earth Surface Processes and Landforms 40(6), 771-782.

Muhs, D. R., Simmons, K. R. 2017. Taphonomic problems in reconstructing sea-level history from the late Quaternary marine terraces of Barbados. Quaternary Research 88, 4019-429.

Mitrovica, J.X., Peltier, W.R., 1991. On postglacial geoid subsidence over the equatorial oceans. Journal of Geophysical Research 96, 20053–20071.

Murray-Wallace, C. V., Woodroffe, C. D., 2014. Quaternary Sea-Level Changes: A Global Perspective. Cambridge, United Kingdom: Cambridge University Press.

Naylor, L.A., Viles, H.A., 2002. A new technique for evaluating short-term rates of coastal bioerosion and bioprotection. Geomorphology 47(1), 31-44.

Negri, A., Amorosi, A., Antonioli, F., Bertini, A., Florindo, F., Lurcok, P., Marabini, S., Mastronuzzi, S., Regattieri, E., Rossi, V., Scarponi, D., Taviani, M., Zanchetta, G., Vai G.B, 2015. A potential global boundary stratotype section and point (GSSP) for the Tarentian Stage, Upper Pleistocene, from the Taranto area (Italy): Results and future perspectives. Journal of Quat. Int. 383, 145-157.

Neumann, A.C., Hearty, P.J., 1996. Rapid sea-level changes at the close of the last interglacial (substage 5e) recorded in Bahamian island geology. Geology 24, 775–778.

Nisi, M.F., Antonioli, F., Dai Pra, G., Leoni, G., Silenzi, S., 2003. Coastal deformation between the Versilia and the Garigliano Plains (Italy) since the Last Interglacial stage. Journal of Quaternary Science 18(8), 709-721.

Oggiano, G., Funedda, A., Carmignani, L., Pasci, S., 2009. The Sardinia-Corsica microplate and its role in the Northern Apennine Geodynamics: new insights from the Tertiary intraplate strike-slip tectonics of Sardinia. Ital. J. Geosci. 128, 527-539.

Oldow, J. S., Ferranti, L., Lewis, D. S., Campbell, J. K., D'Argenio, B., Catalano, R., Pappone, G., Carmignani, L., P., Conti, Aiken, C. L. V., 2002. Active fragmentation of Adria based on Global Positioning System velocities and regional seismicity. Geology 30, 779-782.

Orrù, P., Ulzega, A., 1986. Geomorfologia costiera e sottomarina della baia di Funtanamare (Sardegna sud-occidentale). Geografia Fisica e Dinamica Quaternaria 9, 59-67.

Orrù, P., Pasquini, C., 1992. Rilevamento geomorfologico e sottomarino della Riserva Marina di Tavolara e di Capo Coda Cavallo (Sardegna nord-orientale). Atti del Conv. Naz. sulla Geologia Subacquea e Sottomarina - ENEA - Giornale di Geologia 54(2), 49-63.

Orrù, P., Antonioli, F., Hearty, P.J., Radtke, U., 2011 Chronostratigraphic confirmation of MIS 5 age of a baymouth bar at Is Arenas (Cagliari, Italy). Quat. Int. 232, 1-2, 169-178.

Palano, M., Ferranti, L., Monaco, C., Mattia, M., Aloisi, M., Bruno, V., Cannavò, F., Siligato, G., 2012. GPS velocity and strain fields in Sicily and southern Calabria, Italy: Updated geodetic constraints on tectonic block interaction in the central Mediterranean. Journal of Geophysical Research. Solid Earth 117, 1-12.

Palmerini, V., Ulzega, A., 1969. Sedimentologia e geomorfologia del settore costiero tra la foce del Rio Piscinas e Capo Pecora. Rend. Sem. Fac. Sc. Univ. Cagliari 39 (3-4), 1-38.

Pascucci, V., Sechi, D., Andreucci, S., 2014. Middle Pleistocene to Holocene coastal evolution of NW Sardinia (Mediterranean Sea, Italy). Quaternary International 328-329, 3-20.

Pedoja, K., Husson, L., Regard, V., Cobbold, P.R., Ostanciaux, E., Johnson, M.E., Kershaw, S.,Saillard, M., Martinod, J., Furgerot, L.,Weill, P., Delcaillau, B., 2011. Relative sea-level fall since the last interglacial stage: are coasts uplifting worldwide? Earth Sci. Rev. 108, 1–15. http://dx.doi.org/10.1016/j.earscirev.2011.05.002.

Peirano, A., Morri, C., Bianchi, C.N., Anguirre, J., Antonioli, F., Calzetta, G., Carobene, L., Mastronuzzi, G., Orrù, P., 2004. The Mediterranean coral Cladocora caespitosa; a proxy for past climate fluctuations? Global and Planetary Changes 40, 195-200.

Peirano, A., Kružić, P., Mastronuzzi, P., 2009. Growth of Mediterranean reef of Cladocora caespitosa (L.) in the Late Quaternary and climate inferences. Facies, 55, 325-333.

Peltier, W.R., 2004. Global Glacial Isostasy and the Surface of the Ice-Age Earth: The ICE-5G (VM2) model and GRACE. Annual Reviews of Earth and Planetary Sciences 32, 111–149.

Peltier, W.R., Argus, D. F., Drummond, R., 2015. Space geodesy constrains ice age terminal deglaciation, The global ICE-6G_C (VM5a) model. J. Geophys. Res. Solid Earth, 120, 450-487.

Pirazzoli, P.A., 1986. Marine notches. In: Van de Plassche, O (ed), Sea-level Research: a manual for the collection and evaluation of data. Geo Books, Norwich, 361-400.

Porqueddu, A., Antonioli, F., D'Oriano, R., Gavini, V., Trainito, E., Verrubbi, V., 2011. Relative sea level change in Olbia Gulf (Sardinia, Italy), an historically important Mediterranean harbour. Quaternary International 232(1-2), 21-30.

Rodríguez-Vidal, J., Abad, M., Cáceres, L.M., Ruiz, F., Fa, D., Finlayson, C., Finlayson, G., Martínez Aguirre, A., 2007. Evidencias erosivas y bioerosivas en la costa rocosa de Gibraltar al inicio del Último Interglaciar. Sociedad Española de Geomorfología, Mallorca (Spain), 4, 197–201.

Rodríguez Vidal, J., Zaghoul, M.N. Aboumaria K., Cáceres, L.M., Caceres L.M., Ruiz F., Abad M. Martinez-Aguirre A., Finlayson, C., Finlayson, G., Fa, D. 2010. Morphosedimentary evidence and U-Series dating of MIS 5 in Gebel Musa coast (Strait of Gibraltar, Morocco). Conference: Decoding the last Integlacial in western Mediterranean, INQUA Project 0911 cmp, Sardinia, Italy.

Rodríguez-Vidal, J., Cáceres, L.M., Gómez, P., Finlayson, C., Finlayson, G., 2015. Plio-Pleistocene archive of highstand sea-cave markers in the Rock of Gibraltar. Conference: Progress in Quaternary archives studies in the Iberian Peninsula, Seville, Spain.

Rosenbaum, G., Lister, G.S., Duboz, C., 2002. Relative motions of Africa, Iberia, and Europe during the Alpine orogeny. Tectonophysics 359, 117-129.

Rouchon, V., Gillot, PY., Quidelleur, X., Chiesa, S., Floris, B., 2008. Temporal evolution of the Roccamonfina complex (Pleistocene), central Italy. J Volcanol. Geotherm. Res. 177, 500–514.

Rovere, A., Raymo, M., Vacchi, M., Lorscheid, T., Stocchi, P., Gómez-Pujol, L., Harris, D., Casella, E., J. O'Leary, M., Hearty, P., 2016. The analysis of Last Interglacial (MIS 5e) relative sea-level indicators: Reconstructing sea-level in a warmer world. Earth-Science Reviews 159, 404-427.

Sanna, L., De Waele, J., Pasini, G., Pascucci, V., Andreucci, S., 2010. Sea level changes in the Gulf of Orosei based on continental and marine cave deposits. Rendiconti online della Società Geologica Italiana, 11 (1), 48-49.

Schellmann, G., and Radtke, U., 2004. A revised morpho- and chronostratigraphy of the Late and Middle Pleistocene coral reef terraces on Southern Barbados (West Indies). Earth Science Reviews, 64, 157–187.

Segre, A. G., 1951. Molluschi del Tirreniano di Porto Torres e di Golfo Aranci (Sardegna). Bollettino del Servizio Geologico d'Italia 73 (2), 269-290.

Segre, A.G.,1957. Nota sui rilevamenti eseguiti nel foglio 158, Latina, della carta geologica d'Italia. Bollettino del Servizio Geologico d'Italia 78, 569-5844.

Shackleton, N.J., Sanchez-Gon M. F., Pailler, D., Lancelot. Y. 2003. Marine Isotope Substage 5e and the Eemian Interglacial Global and Planetary Change 36, 151 – 155.

Shtober-Zisu, N., Amasha, H. and Frumkin, A., 2017. Inland notches: lithological characteristics and climatic implications of subaerial cavernous landforms in Israel. Earth Surface Processes and Landforms 42, 1820-1832.

Sisma-Ventura, G., Sivan, D., Shtienberg, G., Bialik, O. M., Filin, S., Greenbaum, N., 2017. Last interglacial sea level high-stand deduced from well-preserved abrasive notches exposed on the Galilee coast of northern Israel. Palaeogeography, Palaeoclimatology, Palaeoecology 470, 1–10.

Sivan, D., Sisma-Ventura, G., Greenbaum, N., Bialik, O.M., Williams, F.H., Tamisiea, M.E., Rohling, E.J., Frumkin, A., Avnaim-Katav, S., Shtienberg, G., Stein, M., 2016. Eastern Mediterranean Sea level through the last interglacial from a coastal-marine sequence in northern Israel. Quaternary Science Reviews 145, 204 -225.

Spada, G., Stocchi, P., 2007. SELEN: a Fortran 90 program for solving the "Sea Level Equation". Computers and Geosciences 33 (4), 538-562.

Spratt, T.A.B., 1865. Travels and Researches in Crete, J. van Voorst, London 2, pp 428.

Stearns, C.E., 1976. Estimates of the position of sea-level between 140,000 and 75,000 years ago. Quat. Res. 6, 445–449.

Stephenson, W.J., Kirk, R.M., Kennedy, D.M., Finlayson, B.L., Chen, Z., 2012. Long term shore platform surface lowering rates: Revisiting Gill and Lang after 32 years. Marine Geology, 299-302, 90-95.

Stirling, C. H., Esat, T. M., Lambeck, K., McCulloch, M.T., 1998. Timing and duration of the Last Interglacial: evidence for a restricted interval of widespread coral reef growth. Earth Planet Sci. Lett. 160, 745-762.

Stocchi, P., Antonioli, F., Montagna, P., Pepe, F., Lo Presti, V., Caruso, A., Corradino, M., Dardanelli, G., Renda, P., Frank, N., Douville, E., Thil, F., de Boer, B., Ruggieri, R., Sciortino, R., Pierre, C., 2017. A stalactite record of four relative sea-level highstands during the Middle Pleistocene Transition. Quaternary Science Reviews 173, 92-100.

Stocchi, P., Vacchi, M., Lorscheid, T., de Boer, B., Simms, A.S., van de Wal, R.W.S., Vermeersen, B.L.A., Pappalardo, M., Rovere, A., 2018. MIS 5e relative sea-level changes in the Mediterranean Sea: Contribution of isostatic disequilibrium. Quaternary Science Reviews, 185, 122 -134.

Swantesson, J.O.H., Moses, C.A., Berg, G.E., Jansson, K.M., 2006. Methods for measuring shore platform micro erosion: A comparison of the micro-erosion meter and laser scanner. Zeitschrift fur Geomorphologie N.F. Suppl. 144, 137-151.

Taborosi, D., Kazmer, M., 2013. Erosional and depositional textures and structures in coastal karst landscapes. Coastal Karst Landforms. Springer Science Netherlands,15-58.

Torunski, H., 1979. Biological erosion and its significance for the morphogenesis of limestone coasts and for nearshore sedimentation (northern Adriatic). Senckenberg. Maritima 11 3 (6), 193-265.

Trenhaile, A.S., 2002. Rock coasts, with particular emphasis on shore platform. Geomorphology 48, 7-22.

Trenhaile, A.S., 2014. Modelling marine notch formation by wetting and drying and salt weathering. Geomorphology 224, 139-151.

Trenhaile, A.S., 2015. Coastal notches: Their morphology, formation and function. Earth Science Review 150, 285-304.

Ulzega, A., Ozer, A., 1980. Comptes-rendus de l'Excursion Table Ronde sur le Tyrrhénien de Sardaigne. INQUA, Univ. Cagliari 110.

Zazo, C., Jose Luis Goy, J., Dabrio, J., Bardaj, T., Hillaire-Marcel, C., Ghaleb, B., Gonzalez-Delgado, J.A., Vicente, S., 1999. Pleistocene raised marine terraces of the Spanish Mediterranean and Atlantic coasts: records of coastal uplift, sea-level highstands and climate changes. Marine Geology 194, 103– 133.

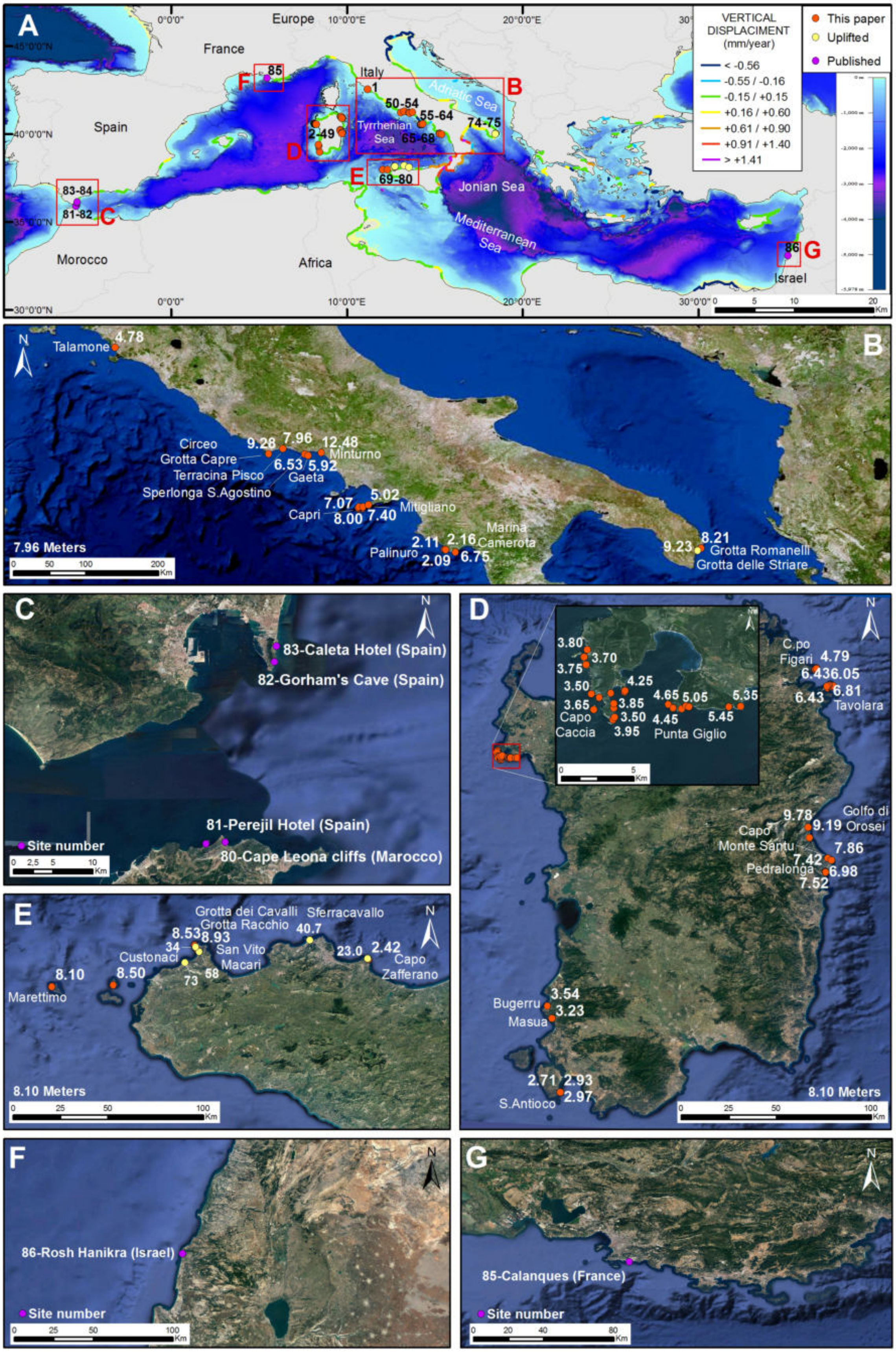
A
Europe
France
Italy
Spain
Morocco
Africa
Israel
Adriatic Sea
Tyrrhenian Sea
Jonian Sea
Mediterranean Sea
VERTICAL DISPLACIMENT (mm/year)
< -0.56
-0.55 / -0.16
-0.15 / +0.15
+0.16 / +0.60
+0.61 / +0.90
+0.91 / +1.40
> +1.41
This paper
Uplifted
Published
85
1
50-54
55-64
65-68
74-75
2-49
69-80
83-84
81-82
86
B
Talamone 4.78
Circeo 9.28
Grotta Capre
Terracina Pisco
Sperlonga S.Agostino
7.96
12.48
Minturno
6.53
5.92
Gaeta
7.07
5.02
Mitigliano
Capri
8.00
7.40
Palinuro
2.11
2.16
Marina Camerota
2.09
6.75
9.23
8.21
Grotta Romanelli
Grotta delle Striare
7.96 Meters
C
83-Caleta Hotel (Spain)
82-Gorham's Cave (Spain)
81-Perejil Hotel (Spain)
80-Cape Leona cliffs (Marocco)
Site number
D
3.80
3.70
3.75
3.50
4.25
3.65
3.85
Capo Caccia
3.50
3.95
4.65
5.05
5.35
4.45
5.45
Punta Giglio
C.po Figari
4.79
6.43
6.05
6.81
6.43
Tavolara
9.78
9.19
Golfo di Orosei
Capo Monte Santu
7.86
7.42
Pedralonga
6.98
7.52
Bugerru
3.54
Masua
3.23
2.71
2.93
S.Antioco
2.97
8.10 Meters
E
Grotta dei Cavalli
Grotta Racchio
Sferracavallo
8.53
8.93
40.7
34
San Vito
Custonaci
Macari
23.0
2.42
Capo Zafferano
8.10
8.50
73
58
Marettimo
8.10 Meters
F
86-Rosh Hanikra (Israel)
Site number
G
85-Calanques (France)
Site number

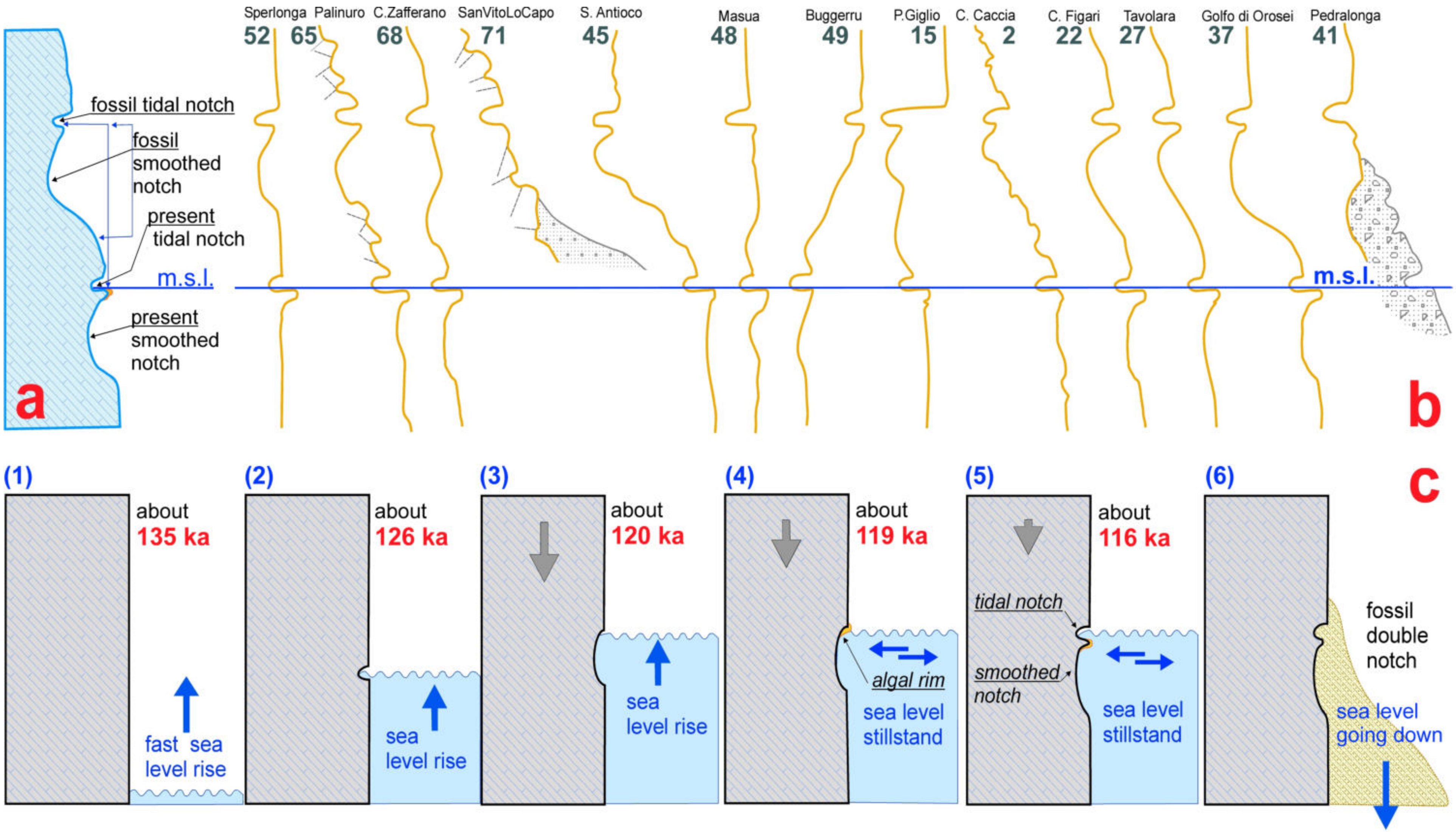

fossil tidal notch
fossil smoothed notch
present tidal notch
m.s.l.
present smoothed notch
a
Sperlonga 52
Palinuro 65
C.Zafferano 68
SanVitoLoCapo 71
S. Antioco 45
Masua 48
Buggerru 49
P.Giglio 15
C. Caccia 2
C. Figari 22
Tavolara 27
Golfo di Orosei 37
Pedralonga 41
m.s.l.
b
(1)
about 135 ka
fast sea level rise
(2)
about 126 ka
sea level rise
(3)
about 120 ka
sea level rise
(4)
about 119 ka
algal rim
sea level stillstand
(5)
about 116 ka
tidal notch
smoothed notch
sea level stillstand
(6)
fossil double notch
sea level going down
c

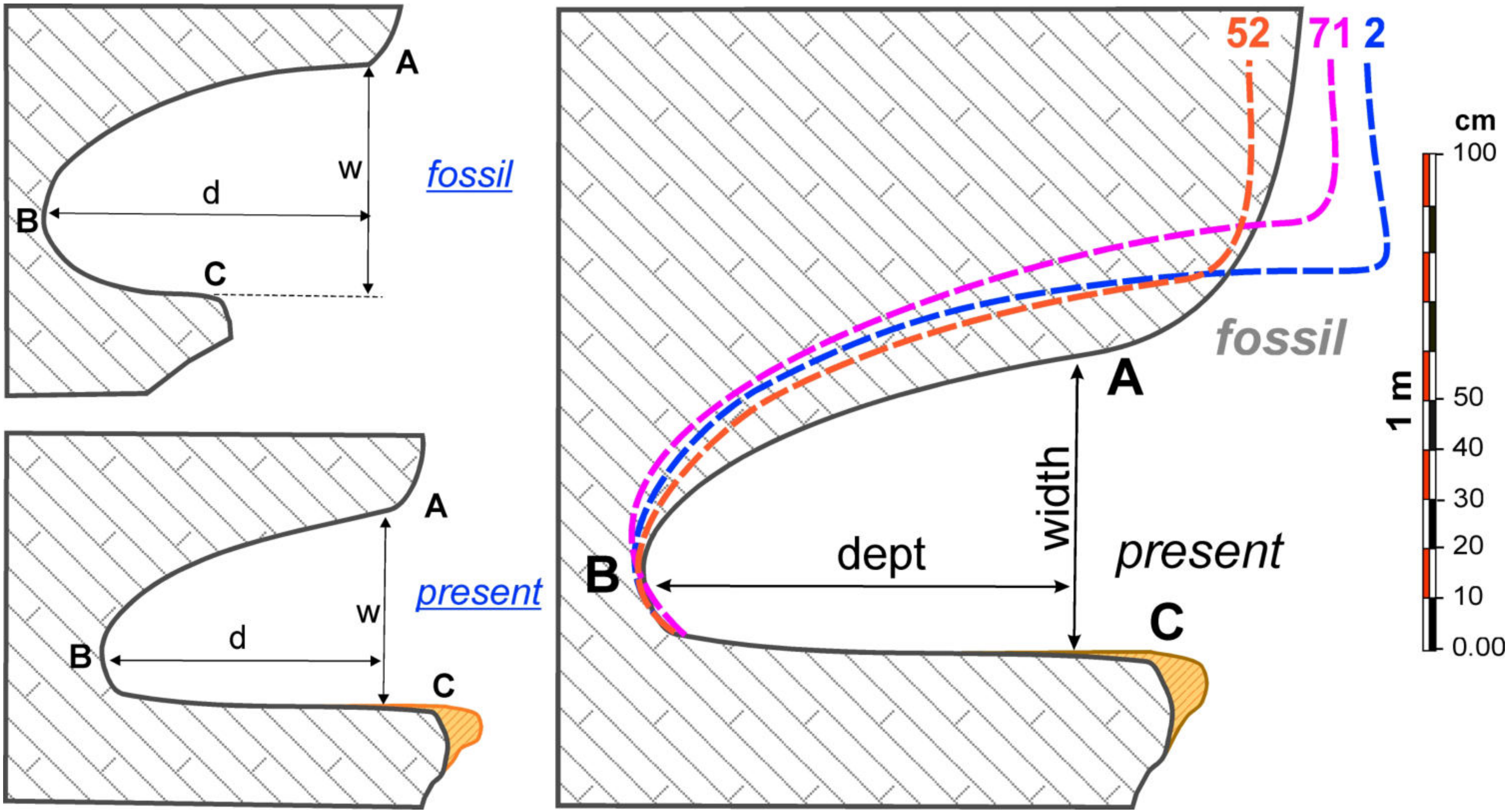
A
w
fossil
d
B
C
A
w
present
d
B
C
52
71
2
cm
100
fossil
A
1 m
50
40
width
30
20
present
dept
B
10
C
0.00

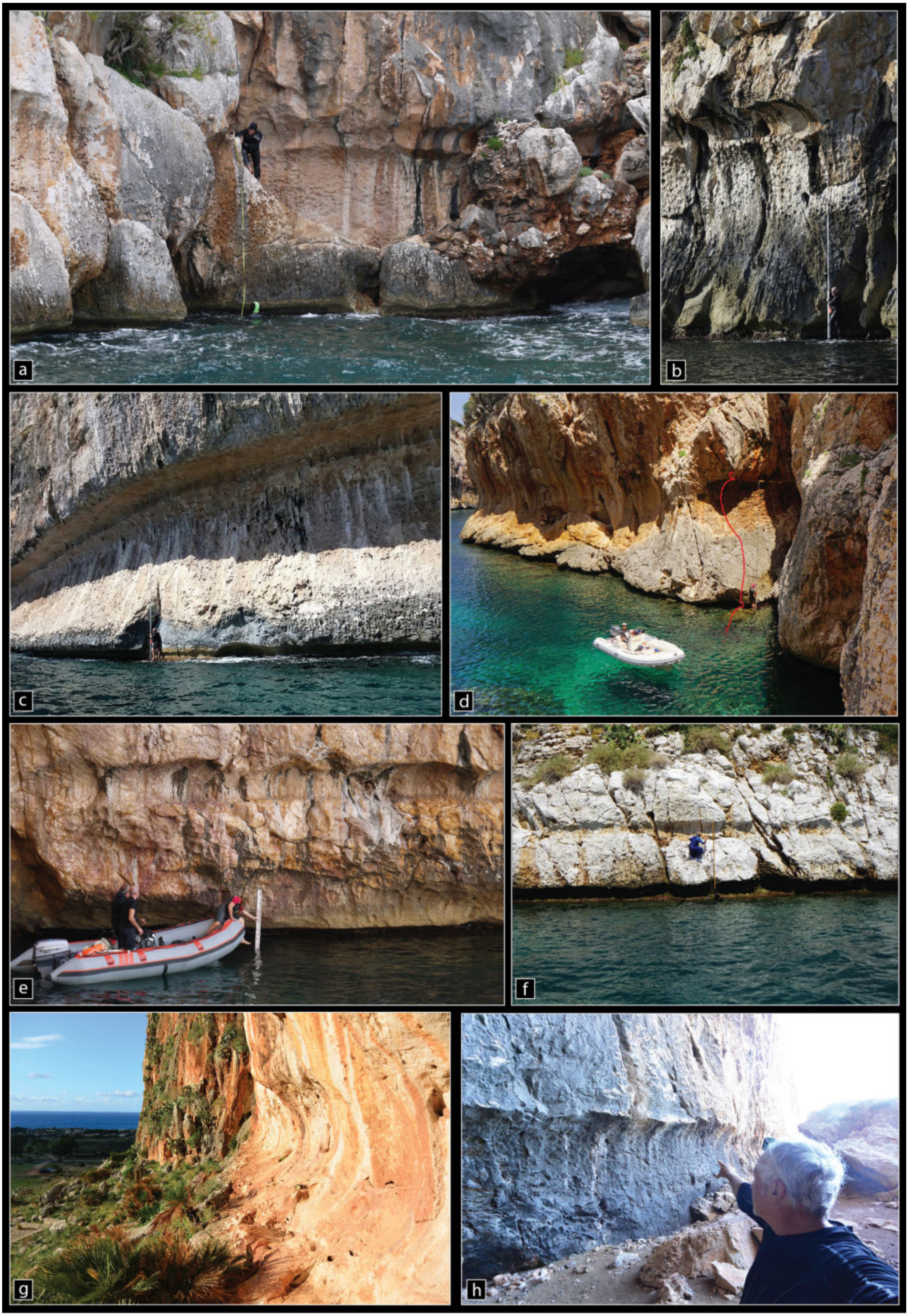
a
b
c
d
e
f
g
h

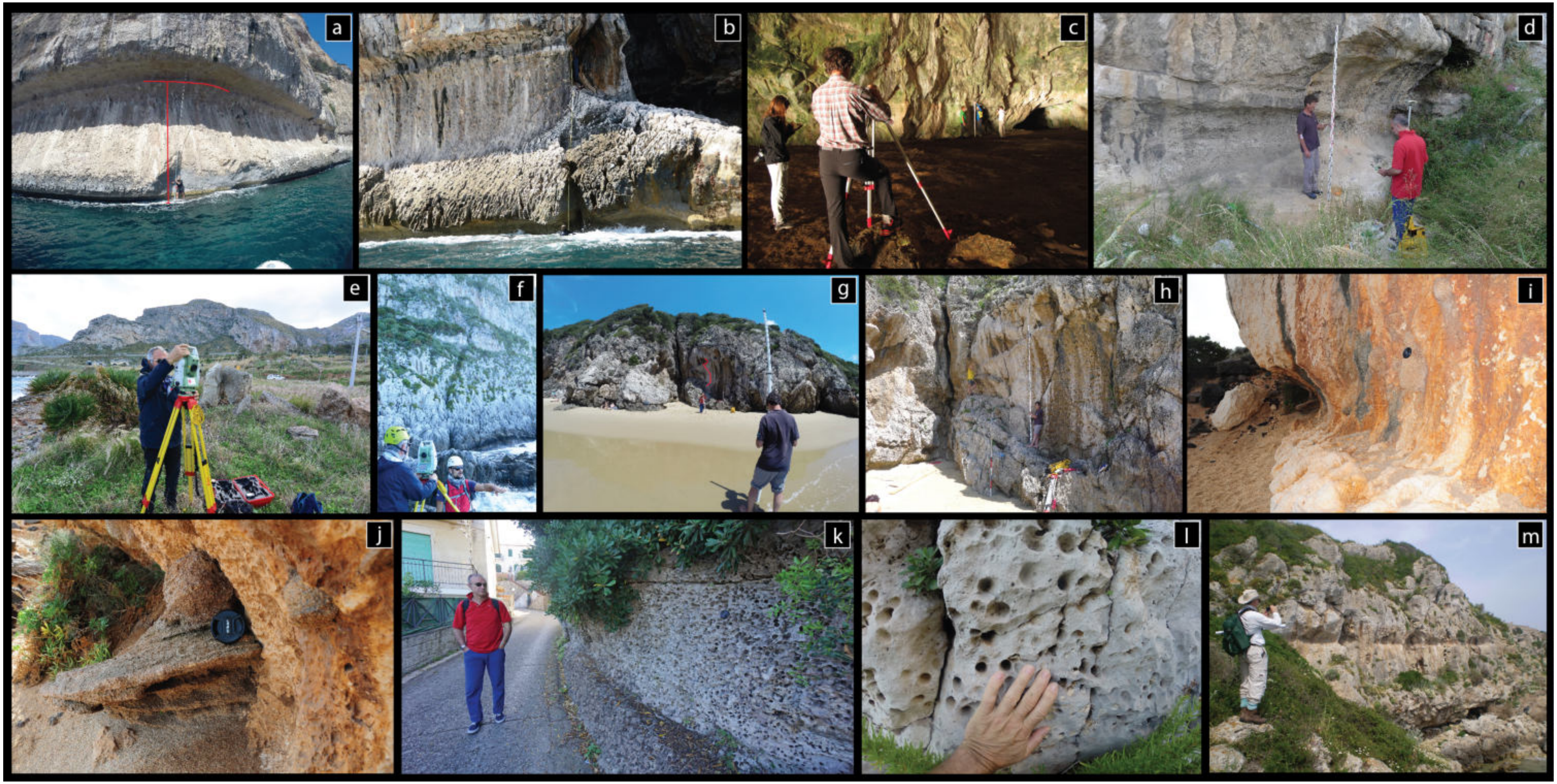

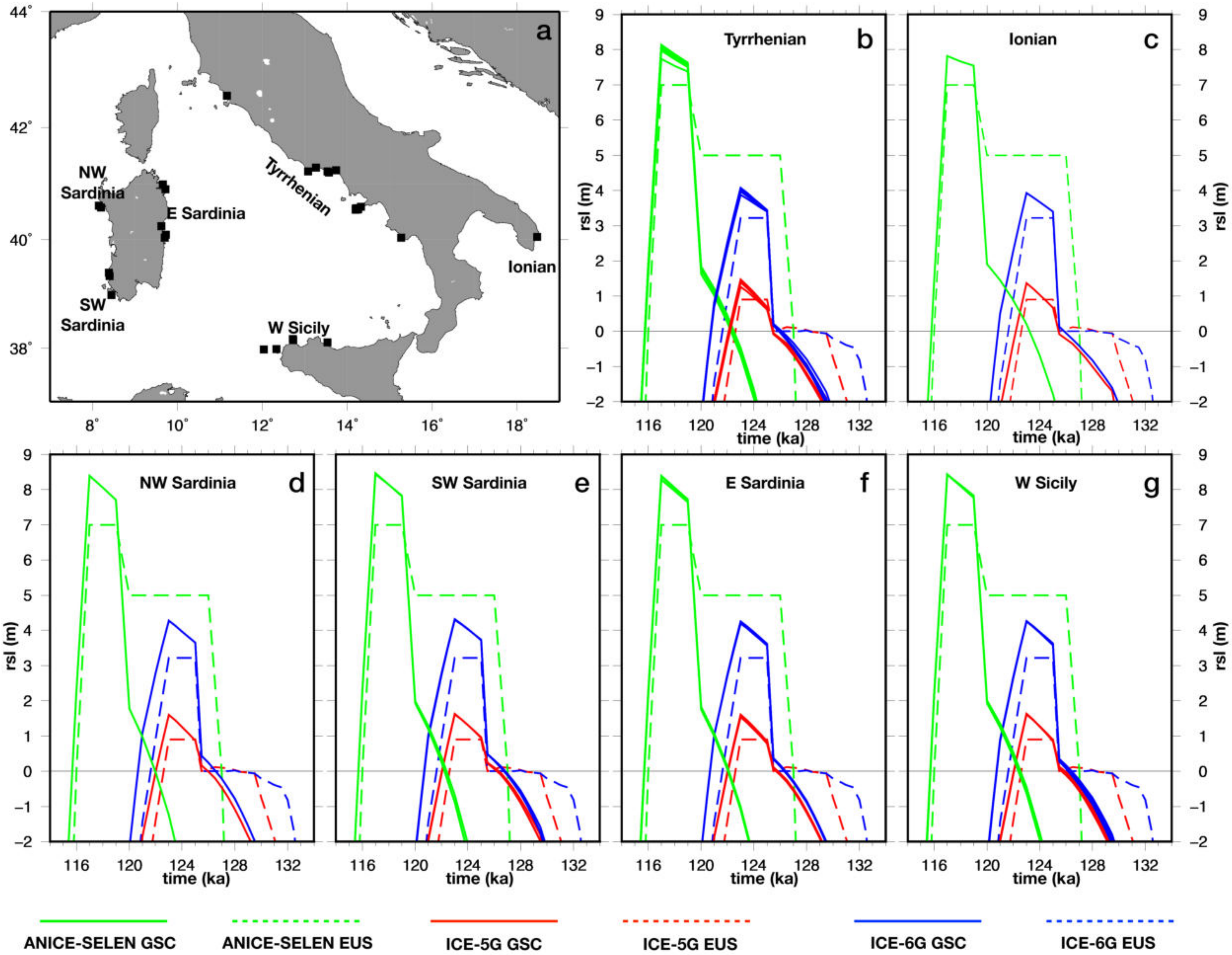

a
NW Sardinia
E Sardinia
SW Sardinia
Tyrrhenian
W Sicily
Ionian
44°
42°
40°
38°
8°
10°
12°
14°
16°
18°
Tyrrhenian
b
Ionian
c
NW Sardinia
d
SW Sardinia
e
E Sardinia
f
W Sicily
g
rsl (m)
time (ka)
116
120
124
128
132
ANICE-SELEN GSC
ANICE-SELEN EUS
ICE-5G GSC
ICE-5G EUS
ICE-6G GSC
ICE-6G EUS

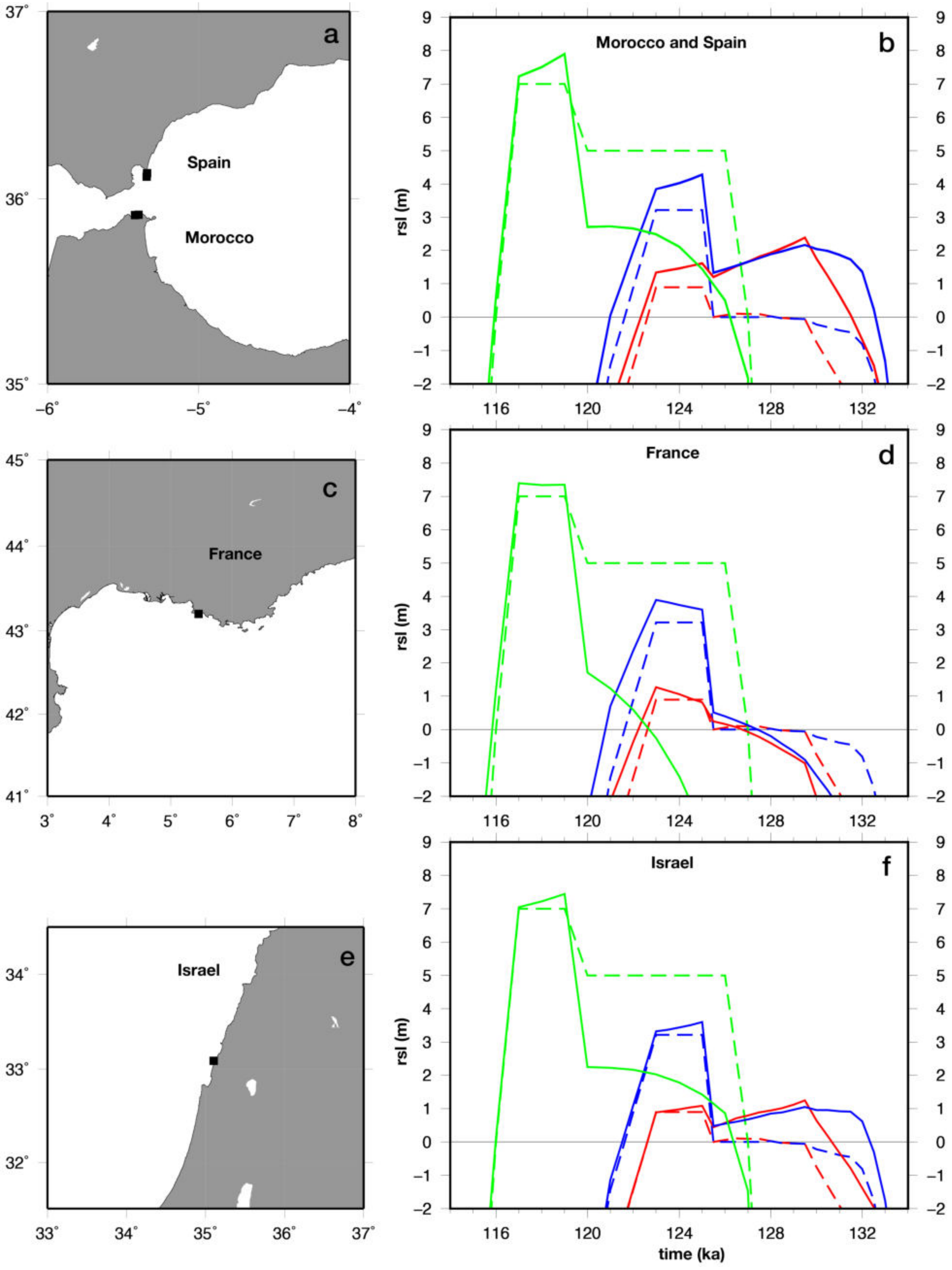
a
Spain
Morocco
b
Morocco and Spain
rsl (m)
c
France
d
France
e
Israel
f
Israel
time (ka)

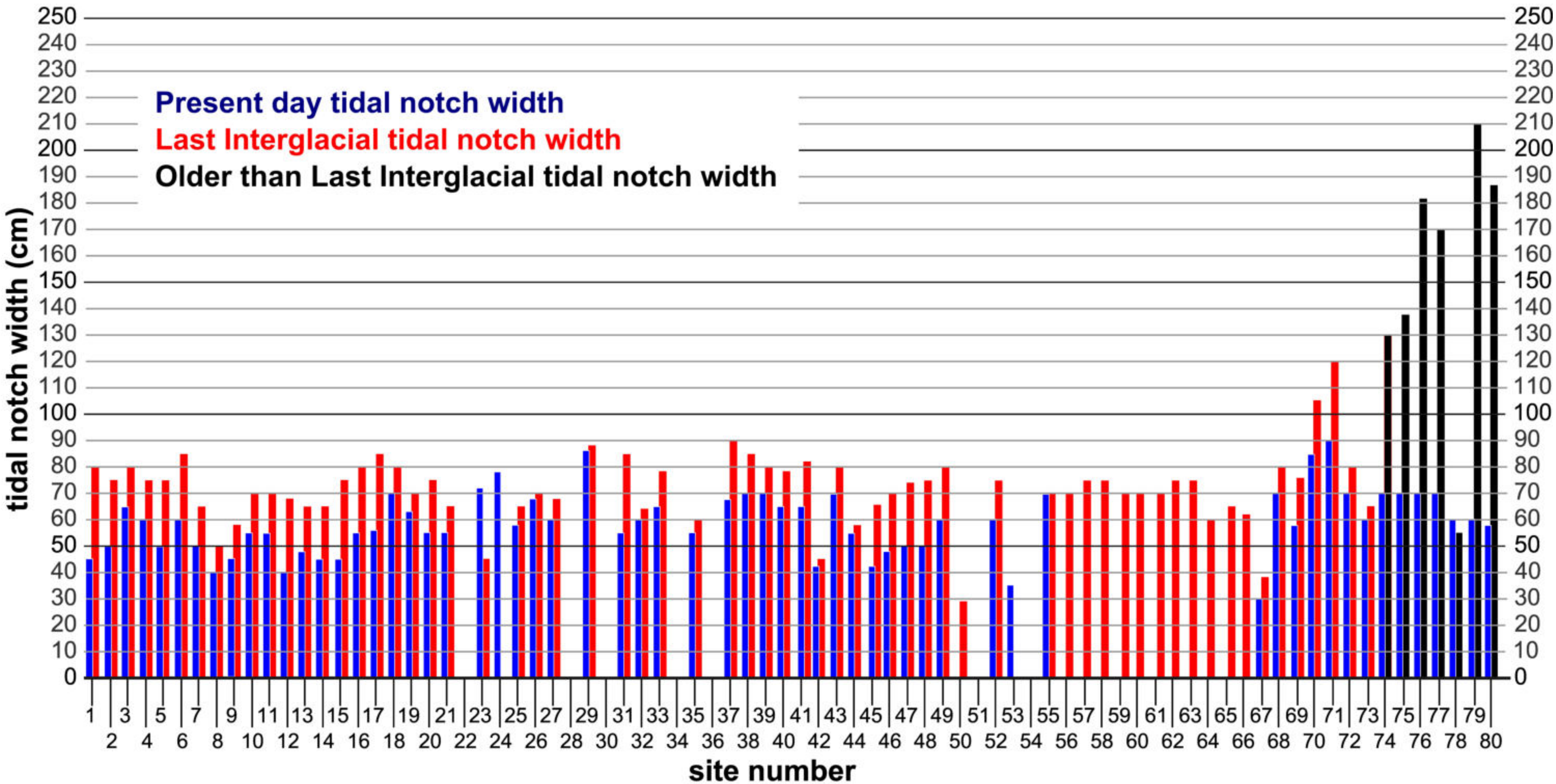
Present day tidal notch width
Last Interglacial tidal notch width
Older than Last Interglacial tidal notch width
tidal notch width (cm)
site number

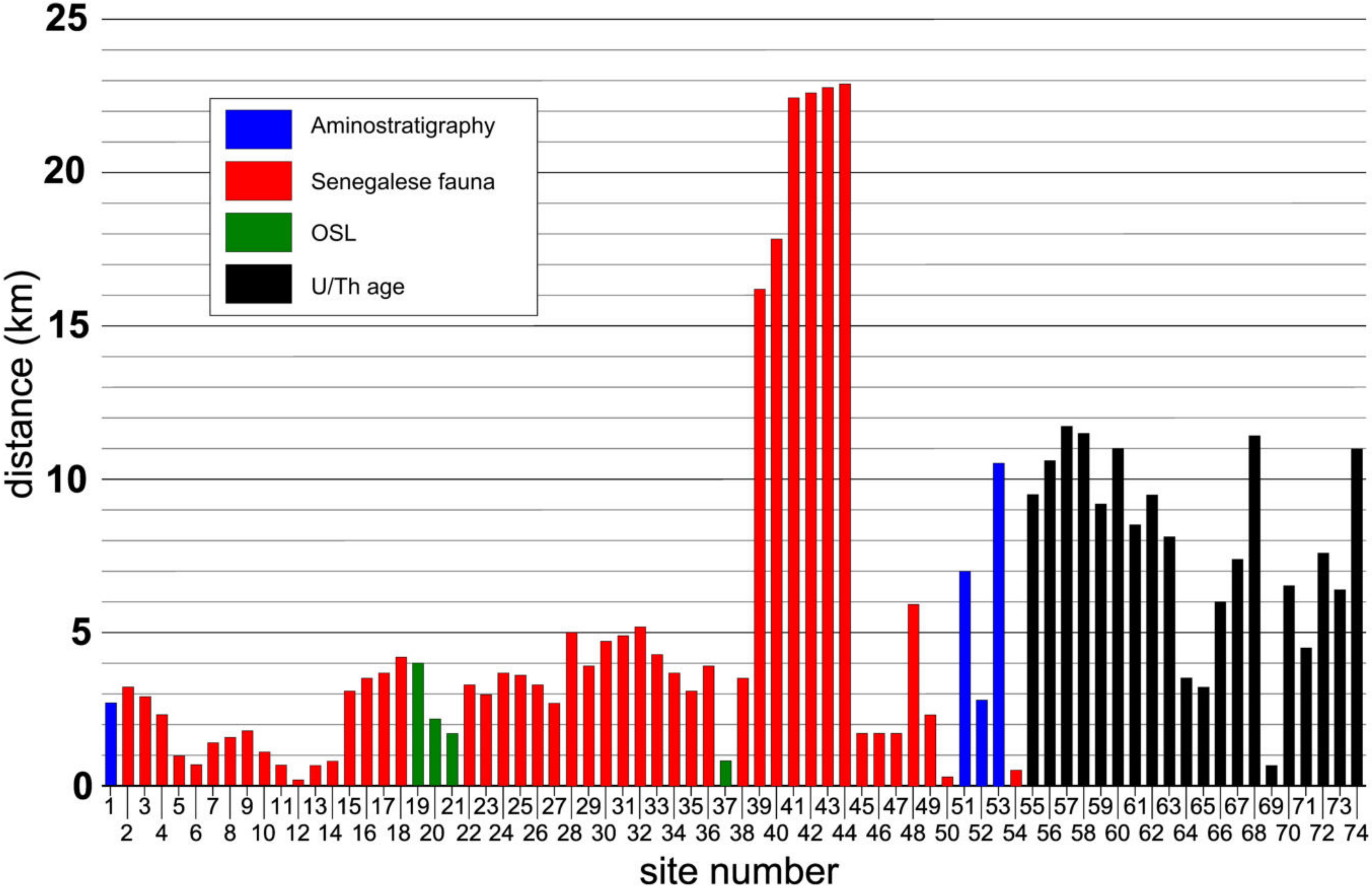

Aminostratigraphy
Senegalese fauna
OSL
U/Th age
distance (km)
site number
0
5
10
15
20
25

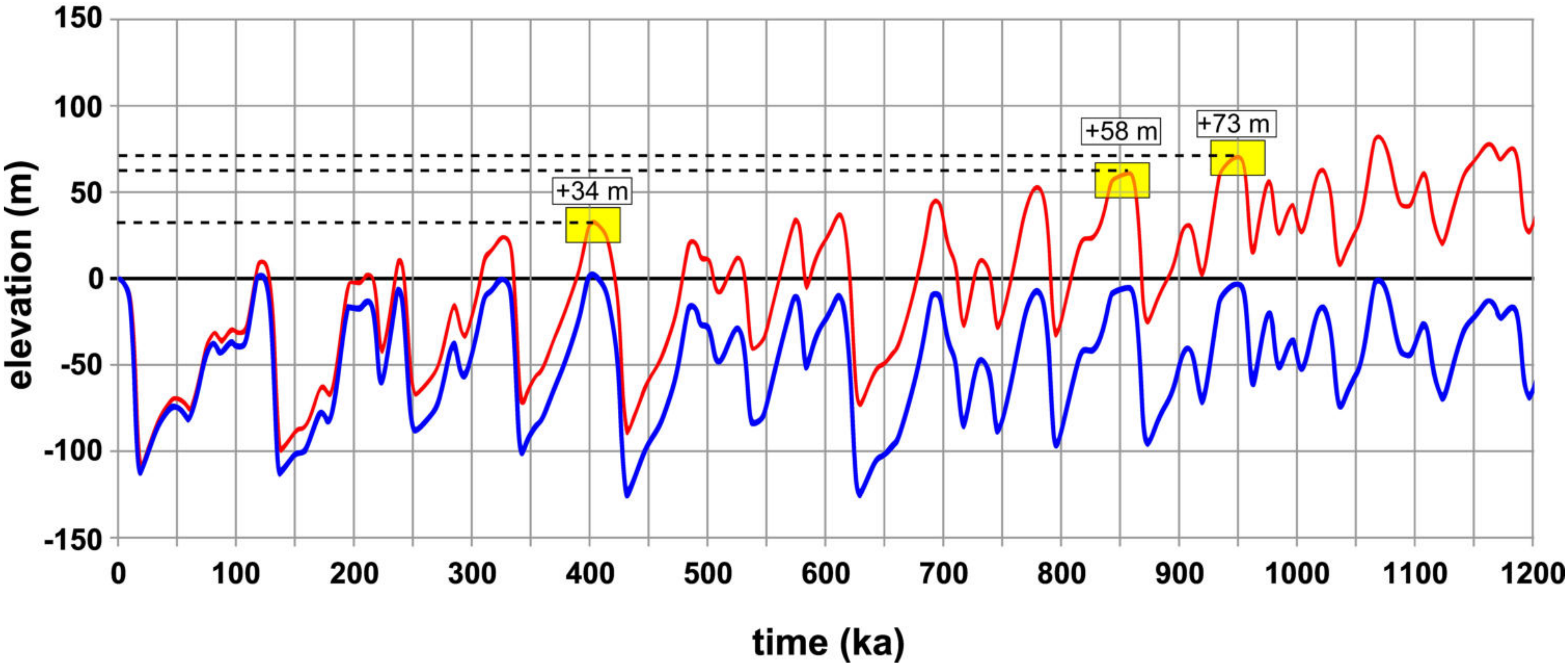

150
100
50
0
-50
-100
-150
elevation (m)
+34 m
+58 m
+73 m
0
100
200
300
400
500
600
700
800
900
1000
1100
1200
time (ka)

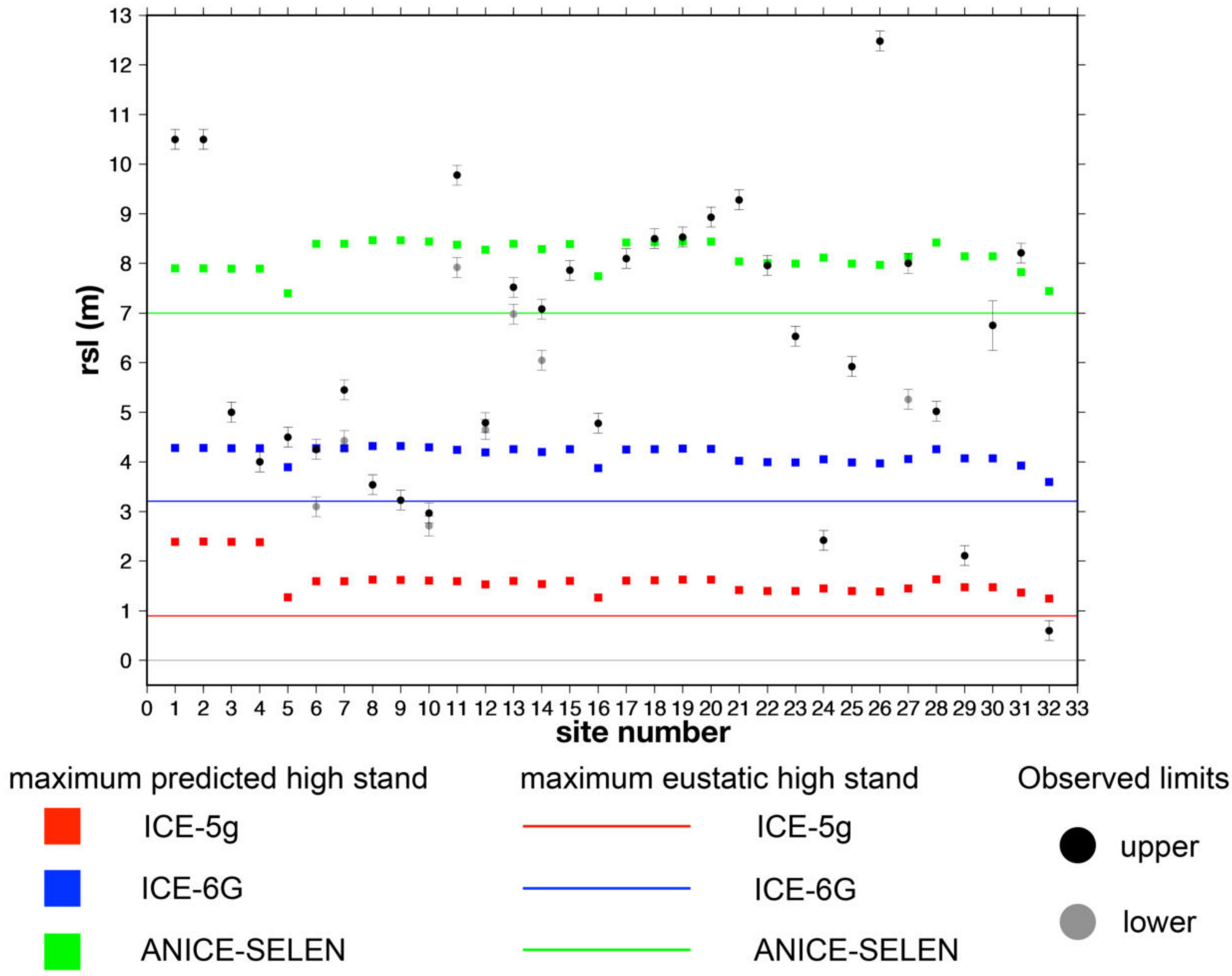

rsl (m)
site number
0
1
2
3
4
5
6
7
8
9
10
11
12
13
0
1
2
3
4
5
6
7
8
9
10
11
12
13
14
15
16
17
18
19
20
21
22
23
24
25
26
27
28
29
30
31
32
33
maximum predicted high stand
ICE-5g
ICE-6G
ANICE-SELEN
maximum eustatic high stand
ICE-5g
ICE-6G
ANICE-SELEN
Observed limits
upper
lower

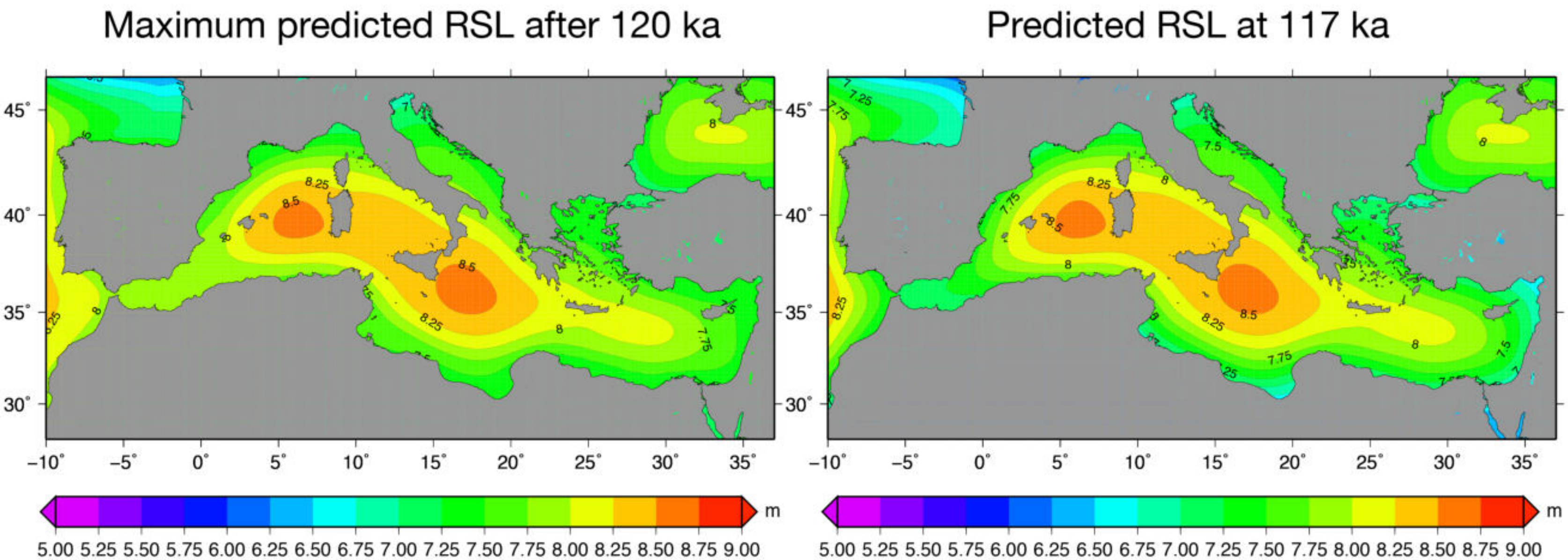
Maximum predicted RSL after 120 ka
Predicted RSL at 117 ka
45°
40°
35°
30°
−10° −5° 0° 5° 10° 15° 20° 25° 30° 35°
m
5.00 5.25 5.50 5.75 6.00 6.25 6.50 6.75 7.00 7.25 7.50 7.75 8.00 8.25 8.50 8.75 9.00


9
Sea
Capri
Marettimo
Striare
Terracina
Talamone
Capri
Tavolara
7
Pedralonga
(corrected)
Marina di Camerota
Sperlonga
Talamone

Table 1: MIS 5.5 and Present tidal notches data in the Mediterranean Sea

1) Site number; 2) Locality and site name; 3) Elevation, uncertain are explained in chapter 3.1 ; 4) Notch Morphometry; 5) Type of Notch: MTN= MIS 5.5 Tidal Notch; *PTN*= Present Tidal Notch; NM= Not Measured; NC= Not Carved; C= Consumed); 6) Distance (km) and *reference site name for the age of deposit: [1] Abate et al., 1996; [2] Antonioli, 1991; [3] Antonioli et al., 1994a; [4] Antonioli et al., 1994b; [5] Antonioli et al., 1999; [6] Antonioli et al., 2002; [7] Blanc and Segre, 1953; [8] Bosellini et al., 1999; [9] Brancaccio et al., 1986, 1990; [10] Cesaraccio and Puxeddu, 1986; [11] Delicato et al., 1999; [12] Durante, 1975; [13] Esposito et al., 2003; [14] Ferranti and Antonioli, 2007; [15] Hearty P.J., 1986, 1987; [16] Malatesta, 1954a, 1954b, 1970; [17] Mastronuzzi et al., 2007; [18] Orrù and Ulzega, 1986; [19] Orrù and Pasquini, 1992; [20] Orrù et al., 2011; [21] Palmerini and Ulzega, 1969; [22] Pascucci et al., 2014; [23] Porqueddu et al., 2011; [24] Sanna et al., 2010; [25] Segre, 1951; [26] Segre, 1957; [27] Ulzega and Ozer, 1980;

1 Site N	2 Locality (site name)	3 Elevation with uncertainty (m)	4 Average notch morphometry (m)			5 Type of Notch	6 Distance (km) and *reference site name from the site that allowed the age of deposit
			MIS 5.5 (FTN) *Present (PTN)*				
			width	depth	base		
1	Talamone	4.78 ± 0.275	0.80 *0.45*	0.60 *0.60*	0.45 *0.15*	MTN *PTN*	[15] (2,7) Campo Regio
2	Capo Caccia	3.80 ± 0.035	0.75 *0.50*	0.20 *0.12*	0.20 *0.80*	MTN *PTN*	[16] (3,2) Dragonara
3		3.70 ± 0.035	0.80 *0.65*	0.60 *0.12*	0.60 *0.80*	MTN *PTN*	[16] (2,9)
4		3.75 ± 0.035	0.75 *0.60*	0.55 *0.60*	0.55 *0.80*	MTN *PTN*	[16] (2,3)
5		3.50 ± 0.035	0.75 *0.50*	0.25 *0.10*	0.25 *0.80*	MTN *PTN*	[16] (1,0)
6		3.10 ± 0.035	0.85 *0.60*	0.60 *0.11*	0.60 *0.80*	MTN *PTN*	[16] (0,7)
7		3.65 ± 0.035	0.65 *0.50*	0.30 *0.30*	0.30 *0.80*	MTN *PTN*	[16] (1,4)
8		3.95 ± 0.035	0.50 *0.40*	0.25 *0.30*	0.25 *0.70*	MTN *PTN*	[16] (1,6)
9		3.50 ± 0.035	0.58 *0.45*	0.40 *0.40*	0.40 *0.80*	MTN *PTN*	[16] (1,8)
10		3.85 ± 0.035	0.70 *0.55*	0.20 *0.20*	0.35 *0.80*	MTN *PTN*	[16] (1,1)
11		3.85 ± 0.035	0.70 *0.55*	0.20 *0.20*	0.30 *0.80*	MTN *PTN*	[16] (0,7)
12		3.86 ± 0.035	0.68 *0.40*	0.20 *0.20*	0.30 *0.90*	MTN *PTN*	[16] (0,2)
13		4.05 ± 0.035	0.65 *0.48*	0.38 *0.40*	0.40 *0.80*	MTN *PTN*	[16] (0,7)
14		4.25± 0.035	0.65 *0.45*	0.40 *0.40*	0.40 *0.90*	MTN *PTN*	[16] (0,8)
15	Punta Giglio	4.65± 0.035	0.75 *0.45*	0.60 *0.43*	0.60 *0.60*	MTN *PTN*	[16] (3,1)
16		4.43± 0.035	0.80 *0.55*	0.60 *0.65*	0.60 *0.10*	MTN *PTN*	[16] (3,5)
17		4.45± 0.035	0.85 *0.56*	0.60 *0.60*	0.60 *0.12*	MTN *PTN*	[16] (3,7)
18		5.05± 0.035	0.80 *0.70*	0.65 *0.60*	0.65 *0.15*	MTN *PTN*	[22] (4,1)
19		5.25± 0.035	0.70 *0.63*	0.60 *0.60*	0.60 *0.90*	MTN *PTN*	[22] (4,0)
20		5.45± 0.035	0.75 *0.55*	0.65 *0.60*	0.70 *0.12*	MTN *PTN*	[22] (2,2)

21		5.35± 0.035	0.65 *0.55*	0.65 *0.60*	0.60 *0.80*	MTN *PTN*	[22] (1,7)
22	Capo Figari	4.77± 0.135	- -	- -	- -	NM NM	[25] (3,3) Golfo Aranci
23		4.79± 0.135	0.45 *0.72*	0.50 *0.80*	0.25 *0.30*	MTN *PTN*	[25] (3,0) Golfo Aranci
24		4.72± 0.135	- *0.78*	- *0.60*	- *0.58*	NM *PTN*	[25] (3,7) Golfo Aranci
25		4.79± 0.035	0.65 *0.58*	0.50 *0.63*	0.95 *0.48*	MTN *PTN*	[25] (3,6) Golfo Aranci
26		4.65± 0.035	0.70 *0.68*	0.40 *0.58*	- *0.12*	MTN *PTN*	[25] (3,3) Golfo Aranci
27	Tavolara	6,93± 0.035	0.68 *0.60*	0.50 *0.82*	0.95 -	MTN *PTN*	[19, 23] (2,7) Spalmatore di Terra
28		7,08± 0.135	- -	- -	- -	NM NM	[19, 23] (5) Spalmatore di Terra
29		6,97± 0.135	0.88 *0.86*	0.55 *0.102*	- *0.47*	MTN *PTN*	[19, 23] (3,9) Spalmatore di Terra,
30		6,93± 0.135	- -	- -	- -	NM NM	[19, 23] (4,7) Spalmatore di Terra
31		6.89± 0.135	0.85 *0.55*	0.60 *0.145*	- *0.30*	MTN *PTN*	[19, 23] (4,9) Spalmatore di Terra
32		6,13± 0.135	0.64 *0.60*	0.56 *0.60*	0.60 *0.35*	MTN *PTN*	[19, 23] (5,2) Spalmatore di Terra
33		6,81± 0.135	0.78 *0.65*	0.30 *0.35*	- *0.35*	MTN *PTN*	[19, 23] (4,3) Spalmatore di Terra
34		6,43± 0.135	- -	- -	- -	NM NM	[19, 23] (3,7) Spalmatore di Terra
35		6,05± 0.135	0.60 *0.55*	0.55 *0.50*	0.60 -	MTN *PTN*	[19, 23] (3,1) Spalmatore di Terra
36		6,43± 0.135	- -	- -	- -	NM NM	[19, 23] (3,9) Spalmatore di terra
37	Golfo Orosei (North-East Sardinia)	9.78 ± 0.035	0.90 *0.68*	0.35 *0.70*	0.60 *0.12*	MTN *PTN*	[24] (0,8) Bue marino
38		9,19 ± 0.035	0.85 *0.70*	0.40 *0.80*	0.12 *0.11*	MTN *PTN*	[27] (3,5) Cala Luna
39		7.92 ± 0.035	0.80 *0.70*	0.25 *0.80*	0.40 -	MTN *PTN*	[27] (16,2) Cala Luna
40	Capo Monte Santu	7.86 ± 0.035	0.78 *0.65*	0.60 *0.80*	0.65 *0.95*	MTN *PTN*	[27] (17,8) Cala Luna
41	Pedralonga	7,51 ± 0.135	0.82 *0.65*	0.90 *0.90*	0.135 *0.10*	MTN *PTN*	[27] (22,4) Cala Luna
42		7,52 ± 0.135	0.45 *0.42*	0.80 *0.90*	0.18 *0.135*	MTN *PTN*	[27] (22,6) Cala Luna
43		7,42 ± 0.135	0.87 *0.70*	0.50 *0.50*	0.14 *0.90*	MTN *PTN*	[27] (22,75) Cala Luna
44		6,98 ± 0.135	0.58 *0.55*	0.40 *0.46*	0.90 *0.12*	MTN *PTN*	[27] (22,9) Cala Luna
45	Sant'Antioco	2,97± 0.175	0.66 *0.42*	0.30 *0.30*	0.68 *0.80*	MTN *PTN*	[27] (1,7) Maladroxia
46		2,93± 0.275	0.70 *0.48*	0.90 *0.30*	0.11 *0.80* -	MTN *PTN* *RN*	[27] (1,7) Maladroxia
47		2,71± 0.275	0.74 *0.50*	0.48 *0.43*	0.105 *0.84*	MTN *PTN*	[20, 27] (1,7) Maladroxia

48	Masua	3.23± 0.175	0.75 *0.50*	0.50 *0.50*	0.60 *0.70*	MTN *PTN*	[18] (5,9) Fontanamare
49	Buggerru	3.54± 0.175	0.80 *0.60*	0.60 *0.80*	0.70 *0.70*	MTN *PTN*	[10, 21] (2,3) Buggerru – Rio Mannu
50	Circeo (Grotta delle Capre)	9.28± 0.175	0.29 -	0.08 -	0.08 -	MTN NC	[7, 12] (0.3) Grotta del Fossellone
51	Terracina (Pisco Montano)	7,96± 0.175	- -	- -	- -	C NC	[2] (7,0)
52	Sperlonga (Sant'Agostino)	6,53± 0.175	0.75 *0.60*	0.60 *0.70*	0.45 *0.45*	MTN *PTN*	[2] (2,8)
53	Gaeta (Grotta del Turco)	5.92± 0.275	- *0.35*	- *0.40*	- *0.35*	C *PTN*	[2] (10,5)
54	Minturno (Monte d'Argento)	12,48± 0.175	- -	- -	- -	C NM	[11, 26] (0,5) West side Monte.D'Argento
55	Capri (est)	7,40± 0.275	0.70 -	0.50 -	0.50 -	MTN *RN*	[9, 14] (9,5)
56	Capri (Tragara)	8.0± 0.275	0.70 -	0.45 -	0.45 -	MTN *RN*	[9, 14] (10,6)
57	Capri (Grotta Fontelina)	7.10± 0.275	0.75 -	0.60 -	0.60 -	MTN *RN*	[9, 14] (11,7)
58	Capri (Grotta Verde)	6,97± 0.275	0.75 -	0.65 -	0.80 -	MTN *RN*	[9, 14] (11,5)
59	Capri (Cala Articola)	6,32± 0.275	0.70 -	0.60 -	0.70 -	MTN *RN*	[9, 14] (9,2)
60	Capri (Punta del Pino)	7,07± 0.275	0.70 -	0.75 -	0.80 -	MTN *RN*	[9, 14] (11)
61	Capri (Grotta Jannarella)	6,97± 0.275	0.70 -	0.45 -	0.80 -	MTN *RN*	[9, 14] (8,5)
62	Capri (Grotta Binocolo)	5,26± 0.275	0.75 -	0.60 -	0.60 -	MTN *RN*	[9, 14] (9,5)
63	Capri (Scoglio Ricotta)	7,00± 0.275	0.75 -	0.45 -	0.80 -	MTN *RN*	[9, 14] (8,1)
64	Mitigliano	5,02± 0.275	0.60 -	0.70 -	0.40 -	MTN *RN*	[9] (3,5)
65	Palinuro	2,11± 0.275	0.65 -	0.60 -	0.60 -	MTN *RN*	[3, 13] (3,2)
66		2,16± 0.275	0.62 -	0.40 -	0.40 -	MTN *RN*	[3, 13] (6,0)
67		2,09± 0.275	0.38 *0.30*	0.20 *0.25*	0.48 *0.55*	MTN *PTN*	[3, 13] (7,4)
68	Marina di Camerota	6,75 ± 0.275	0.80	-	-	MTN	[3, 13] (11.4)
69	Capo Zafferano	2.42± 0,075	0.76 *0.58*	0.52 *0.37*	0.55 *0.45*	MTN *PTN*	[4] (0,7)
70	Marettimo	8.10± 0,175	1.05 *0.85*	0.60 *0.30*	0.70 *0.60*	MTN *PTN*	[1, 5, 16] (6,5)
71	Levanzo	8,50± 0.275	1.2 *0.90*	0.80 *0.80*	0.11 *0.90*	MTN *PTN*	[this paper] (4,5)
72	San Vito Lo Capo (Cala Mancina)	8,53± 0.275	0.80 *0.70*	0.85 *0.85*	0.70 *0.60*	MTN *PTN*	[5, 6] (7,6)
73	San Vito Lo Capo (Macari)	8,93± 0.275	0.65 *0.60*	0.60 *0.80*	0.15 *0.68*	MTN *PTN*	[5, 6] (6,4)
74	Santa Cesarea Terme (Grotta delle Striare)	8,21± 0.275	1.3 *0.70*	-	-	MTN *PTN*	[8, 17] (22)

1 Site N	2 Locality (site name)	3 Coordinates	4 Measures Date and Time (UTC +2)	5 Elevation (m)	6 Average notch measures (m) MIS 5.5 *Present* width	 depth	 base	7 Notch Morphometry MIS 5.5/present notch average concavity ratio (mean width)	8 Kind of measurement	9 MIS 5.5 Elevation (m)	10 Reference (s) for age	11 Age MIS ka
75	Castro (Grotta Romanelli)	40°00' 58.2900" N" 18°26' 00.0300"E"	24.02.2017 11.45 2001	9.25 ±0.135	1.38 *0.70*	0.88 0.75	- -	2,11	DGPS	-	Mastronuzzi et al., 2007	400-600 MIS11-13
76	Custonaci	38° 05' 37.2000" N" 12°40' 12.9600"E"	11.11.2016 15.00	73 ±0.50	1.82 *0.70*	0.68 -	0.11	2,6	DT	12	Stocchi et al., 2017;	950 MIS 25
77	San Vito Lo Capo (Grotta Racchio)	38°08' 44.5800" N" 12°44' 17.8200"E"	11.2016 16.15	58 ±0.50	1.70 0.70	0.90 -	-	2,43	DT	8	Stocchi et al., 2017;	783 MIS 21
78	San Vito Lo Capo (Grotta dei Cavalli)	38° 10' 04.5600" N" 12° 43' 12.5400"E"	11.11.2016 10.55	34 ±0.50	0.55 *0.60*	0.20 -	0.20	0,92	DT	8	Antonioli et al., 1997;	400 MIS 11
79	Sferracavallo	38°11' 58.7400" N" 13°15' 43.3200"E"	29.10.2016 11.08	40.72 ±0.135	2.10 *0.60*	0.13 -	-	3,5	DGPS	3.0	Hearty, 1986; Antonioli et al.,1997;	611 ? MIS ?
80	Capo Zafferano (Arco di Zafferano)	38°06' 43.5000" N" 13°32' 05.9400"E"	29.10.2016 17.45	23.02 ±0.135	1.87 *0.58*	0.80 -	-	3,22	DGPS	2.42	Antonioli et al., 1994b;	323 ? MIS ?

Table 2
FTN older than MIS 5.5 uplifted
1) Site number; 2) Locality and site name; 3) Coordinates; 4) Measures; 5) Elevation (m), uncertain are explained in the chapter 3.1; e; 6) Average notch measures (m); 7) Notch Morphometry; 8) Kind of measurement (DGPS= Differential Global Positioning System; DT= Digital Altimeter) 9) MIS 5.5 elevation; 10) Reference for age; 11) Age MIS ka.

Table 3

Published FTN altitude in Mediterranean Sea

1) Site number; 2) Locality and site name; 3) Coordinates; 4) Elevation 5) Notch morphometry; 6) Reference

1 Site N	2 Locality (site name)	3 Coordinates	4 Base of the notch elevation (m)	5 Average notch measures (m)		6 Reference(s)
				width	depth	
81	Cape Leona cliffs (Morocco)	35°55'16.84" N 5°24'05.75" W	10-11	2.1	0.25	Abad et al., 2013;
82	Perejil Island (Morocco)	35°54'46.17" N 5°25'00.64" W	10-11	2.1	0.25	Abad et al., 2013;
83	Gorham's Cave (Spain)	36°07'10.51" N 5°20'32.48" W	5	-	-	Rodriguez-Vidal et al.,2015;
84	Caleta Hotel (Spain)	36°8'13.03"N 5°20'25.76" W	5	1.7	1.4	Rodriguez-Vidal et al., 2007;
85	Calanques (France)	43°12'07.99" N 5°27'14.24" W	4-5	-	-	Photo by K. Lambeck;
86	Rosh Hanikra (Israel)	33°05'08.18" N 35°06'13.13" W	0.50 -0.75	0.9 – 1.8	-	Sisma Ventura et al., 2016;

A	B	C	D	E	F	G	H
Location	**Lithology**	**Method**	**Intertidal erosion rates (mm/yr)**	**Supratidal/Inner karst rates (mm/yr)**	**Reference**	**Total estimated erosion in 125 Ka (m)**	**Notes**
Gulf of Piran (Slovenia)	Intertidal Mesozoic limestones	TMEM	0.07-1.114	/	Torunski 1979	/	
NE Adriatic (Italy, Croatia)	Intertidal Mesozoic limestones	MEM, TMEM	0.01-0.34	0,001-0,04	Cucchi et al. 2006	0.125-5	
NE Adriatic (Italy, Croatia)	Intertidal Mesozoic limestones	MEM, TMEM	0.01-2.966	0,011-0,04	Furlani et al. 2009	1.375-5	
NE Adriatic (Italy, Croatia)	Intertidal Mesozoic limestones	MEM, TMEM	0.01-0.970	0,001-0,02	Furlani et al. 2011a	0.125-2.5	
NE Adriatic (Italy, Croatia)	Intertidal Mesozoic limestones	MEM, TMEM	0,001-0,3	/	Furlani and Cucchi, 2013	/	Measures collected on a vertical limestone slab in the tidal zone
Mallorca (Balearic Is.)	Supratidal Cretaceous Limestone	MEM, LS, Biological survey	/	0.007-0.482	Swantesson et al. 2006	0.875-60.25	
Mallorca (Balearic Islands)	Supratidal Upper Miocene Reef Limestone	MEM, LS, Biological survey	/	0.003-0.814	Swantesson et al. 2006	0.375-101.75	

Mallorca (Balearic Is.)	Supratidal Upper Miocene calcarenite	MEM, LS, Biological survey	/	0.003-2.095	Swantesson et al. 2006	0.375-261.875	
Mallorca (Balearic Is.)	Supratidal Upper Miocene calcarenite	MEM, LS, Biological survey	/	0.004-0.369	Swantesson et al. 2006	0.5-46.125	
Mallorca (Balearic Is.)	Supratidal Jurassic Dolomite breccias	MEM, LS, Biological survey	/	0.011-0.997	Swantesson et al. 2006	1.375-124.625	
Mallorca (Balearic Islands)	Intertidal Upper Miocene Calcarenite	TMEM	0.80-1.18	/	Gómez-Pujol, 2006	/	
Circeo (Central Italy)	Mesozoic limestone	MEM	/	0.01-0.03	this paper	1.25-3.75	Inside MIS5.5 notch

table 4

NAME	Number in Fig	Site number in Table 1	ICE-5G	ICE-6G	ANICE-SELEN
Perejil_island_(Morocco)	1	82	2.39	4.28	7.90
Cape_Leona_cliffs_(Morocco)	2	81	2.39	4.27	7.90
Gorham’s_Cave_(Spain)	3	83	2.39	4.27	7.89
Caleta_Hotel(Spain)	4	84	2.38	4.27	7.89
Calanques_(France)	5	85	1.27	3.89	7.40
Capo_Caccia	6	14	1.59	4.27	8.40
Punta_Giglio	7	20	1.59	4.27	8.40
Buggerru	8	49	1.62	4.32	8.47
Masua	9	48	1.62	4.32	8.47
Sant’Antioco	10	45	1.61	4.30	8.44
Golfo_Orosei_(Nord)	11	37	1.93	4.24	8.38
Capo_Figari	12	23	1.53	4.19	8.28
Pedralonga	13	42	1.60	4.26	8.40
Tavolara	14	28	1.54	4.20	8.29
Capo_Monte_Santu	15	40	1.60	4.25	8.39
Talamone	16	1	1.26	3.87	7.74
Marettimo	17	70	1.60	4.25	8.42
Levanzo	18	71	1.62	4.25	8.43
San_Vito_Lo_Capo_(Ca. Mancina)	19	72	1.62	4.27	8.44
San_Vito_Lo_Capo_(Macari)	20	73	1.62	4.26	8.44
Circeo_(Grotta_delle_Capre)	21	50	1.42	4.02	8.04
Terracina_(Pisco_Montano)	22	51	1.40	3.40	8.01
Sperlonga_(Sant'Agostino)	23	52	1.38	3.99	7.99
Capo_Zafferano	24	69	1.44	4.05	8.11
Gaeta_(Grotta_del_Turco)	25	53	1.40	3.99	7.99
Minturno_(Monte_d’Argento)	26	54	1.38	3.97	7.97
Capri_(Punta_del_Pino)	27	57	1.45	4.06	8.13
Mitigliano	28	64	1.63	4.26	8.42
Palinuro	29	65	1.47	4.07	8.14
Marina di Camerota	30	68	1.47	4.07	8.14
Santa_Cesarea_Term	31	74	1.36	3.93	7.82

Akko_(Israel)	32	86	1.25	3.60	7.44

Domain	Coastal sector	Locality	Site number	Coordinate	Elevation (m a.s.l)	Land motion process	Predicted effect on FTN	Selection criteria
E Balearic	W Sardinia	Punta Giglio + Capo Caccia	20	40° 34' 16.0069" N" 8° 14' 10.3907"E"	5,5	Continental margin faulting	subsidence	Highest FTN elevation
		Buggerru	49	39° 23' 40.7856" N" 8° 23' 10.2609"E"	3,5	Continental margin faulting	subsidence	Highest FTN elevation
W Tyrrhenian	E Sardinia	Pedralonga	44	40° 01' 45.3626" N" 9° 42' 21.1162"E"	7,0	Volcanic intrusion	uplift	Lowest FTN elevation
		Capo Figari	26	40° 59' 38.3400" N" 9° 39' 46.9800"E"	4,7	Continental margin faulting	uplift	Lowest FTN elevation
		Tavolara	28	40° 54' 10.0597" N" 9° 42' 57.2631"E"	7,1	Continental margin faulting	uplift	Highest FTN elevation
E Tyrrhenian	Tuscany	Talamone	1	42°33' 03.2309" N" 11°09' 55.0274"E	4,8	N/A	N/A	FTN elevation
	Latium	Terracina	51	41° 17' 17.6752" N" 13° 15' 36.1267"E"	8,0 (6,6)*	Continental margin faulting	uplift	Highest FTN elevation*
		Sperlonga	52	41° 13' 06.4207" N" 13° 31' 57.3519"E"	6,5	N/A	N/A	FTN elevation
		Gaeta	53	41° 12' 16.5378" N" 13° 34' 17.8325"E"	5,9	N/A	N/A	FTN elevation
	Campania	Capri	57	40° 32' 38.1002" N" 14° 14' 59.6253"E"	7,0	Continental margin tilting	levering	FTN at tilt axis
		Marina Camerota	68	39°59'42.09'' N 15°24'46.71 E''	6,7	Continental margin faulting	uplift	Highest FTN elevation
W Adriatic	Apulia	Striare	74	40° 02' 47.1900" N" 18° 28' 34.0700"E"	8,2	Subduction-related doming	uplift	Lowest FTN elevation
S Tyrrhenian	Sicily	Marettimo	70	37° 58' 46.7663" N" 12° 02' 21.0449"E"	8,11	Collisional folding	uplift	Lowest FTN elevation
* corrected to 6.6 m								

Table 6

Table S1

1. Tidal notch: indentation or undercutting at sea level, mainly cut in steep carbonate cliffs;
2. GIA: Glacial- and Hydro-Isostatic Adjustment is the process that drives solid Earth and mean sea surface (geoid) variations as a consequence of continental ice-sheets fluctuations.
3. MIS: Marine Isotopic Stage;
4. FTN: fossil tidal notch;
5. PTN: present tidal notch;
6. Base: the lower part of the notch,
7. Top: the higher part of the notch;
8. Width: difference in elevation between base and top of the notch;
9. Depth: Distance between the profile of the cliff and the most internal part of the notch;
10. Elevation: distance between the bases of FTN and PTN;
11. Senegalese fauna: originally defined in the Italian Mediterranean by Gignoux (1913) and Issel (1914). This fauna is mainly characterized by the gastropod Persististrombus latus Gmelin, 1791 (syn: Strombus bubonius Lamarck,1822) and others mollusca that colonized the Mediterranean Sea during a time span which these authors called the Tyrrhenian (i.e. MIS 5.5, approx 132-116 ka);
12. Roof notch: a tidal notch lacking the floor (base);
13. Abrasional notch: a notch developed near the sea floor, where sand and pebbles mechanically hit the rock;
14. GPS/RTK surveys: Global Positioning System measurements (GPS) in the Real Time Kinematic technique (RTK), which is an enhancement of GPS that improves location accuracy in real time and with 3D centimetric accuracy.
15. OSL: optically stimulated luminescence, is a late Quaternary dating technique used to date the last time quartz sediment was exposed to light;
16. Aminostatigraphy: the measurement of the extent of amino acid racemization in biological deposits in order to estimate their age.

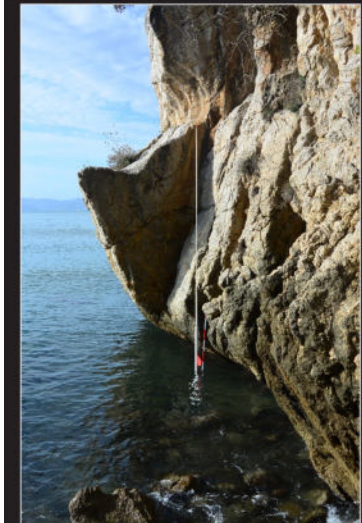
1 Talamone


2 Capo Caccia


18 Punta Giglio


26 Capo Figari


38 Golfo Orosei Nord


40 Capo Monte Santu


42 Pedralonga

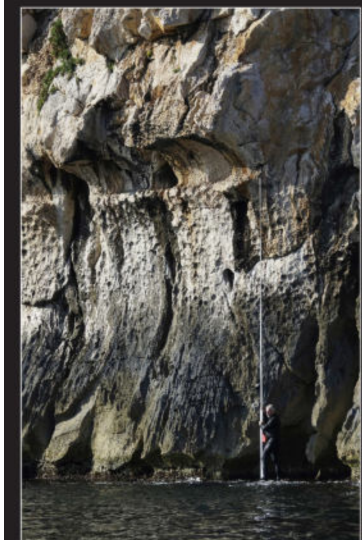
32 Tavolara

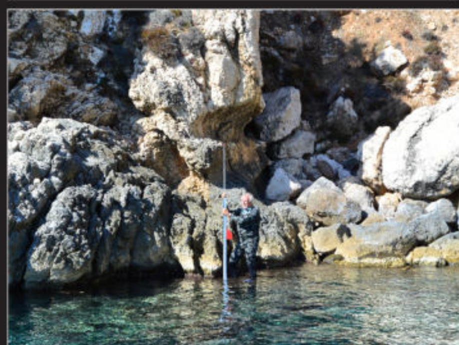
45 Sant'Antioco


48 Masua

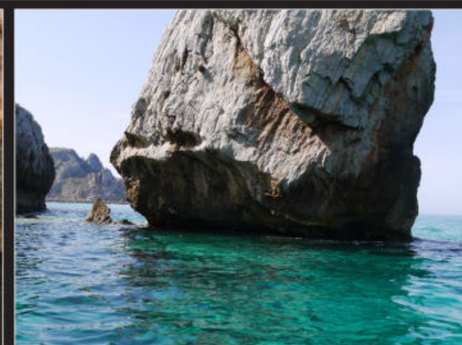
49 Buggerru

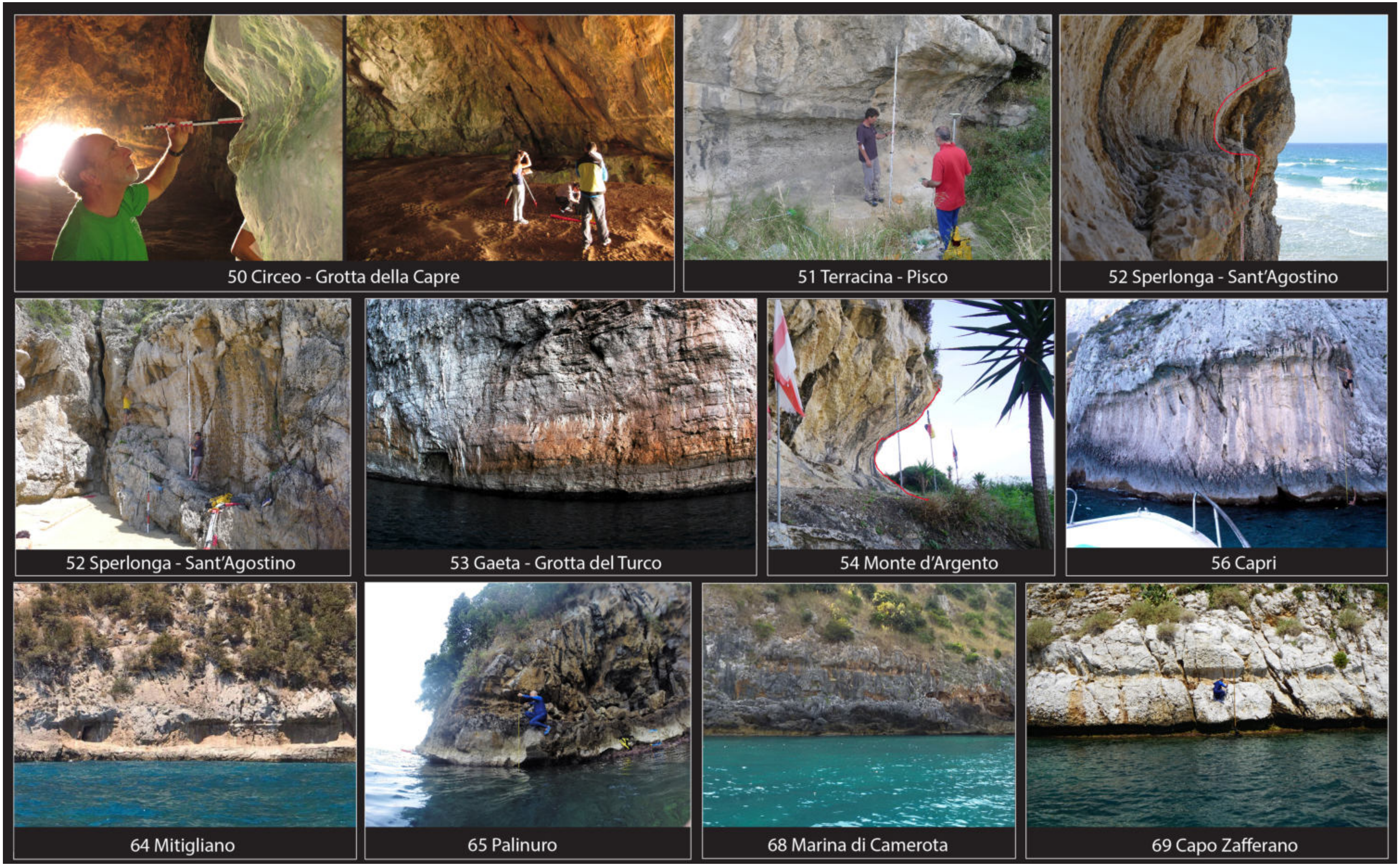

50 Circeo - Grotta della Capre

51 Terracina - Pisco

52 Sperlonga - Sant'Agostino

52 Sperlonga - Sant'Agostino

53 Gaeta - Grotta del Turco

54 Monte d'Argento

56 Capri

64 Mitigliano

65 Palinuro

68 Marina di Camerota

69 Capo Zafferano

70 Marettimo

71 Levanzo

72 San Vito - Cala Mancina

73 San Vito - Macari

74 Grotta della Striare

75 Grotta Romanelli

76 Custonaci

77 Grotta Racchio

78 Grotta dei Cavalli

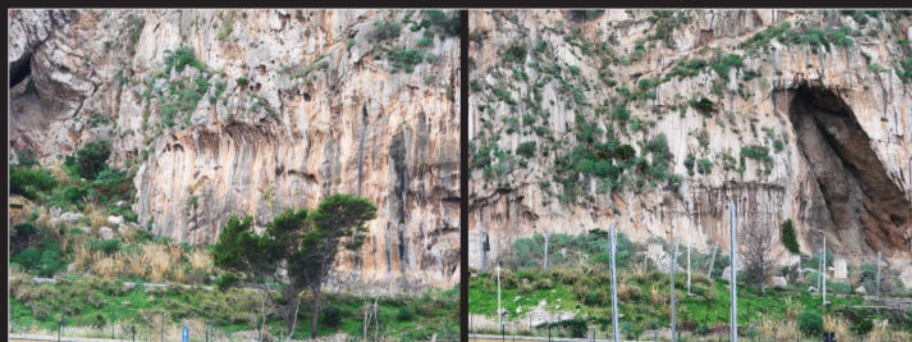

79 Sferracavallo

80 Arco di Zafferano

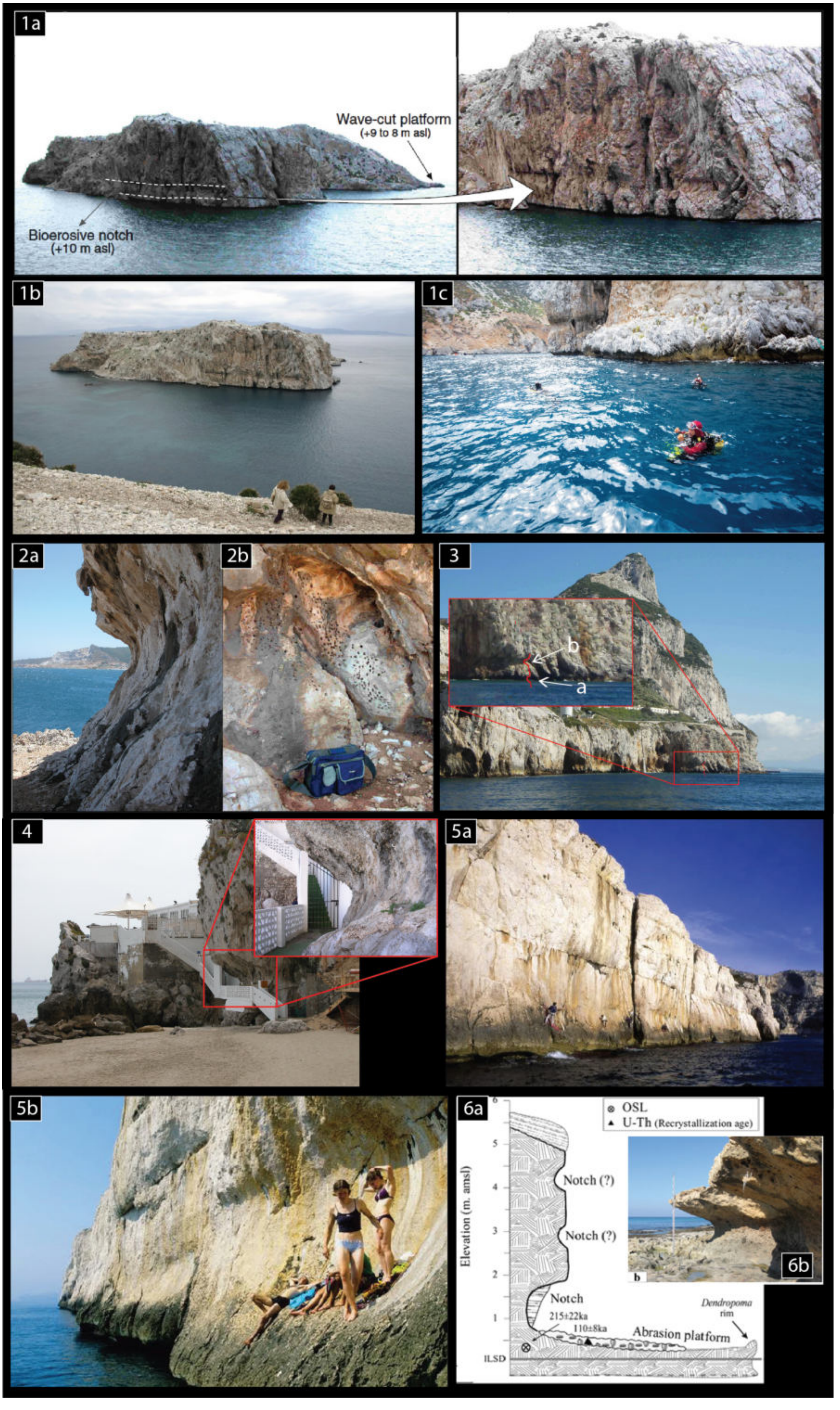
1a
Wave-cut platform
(+9 to 8 m asl)
Bioerosive notch
(+10 m asl)
1b
1c
2a
2b
3
b
a
4
5a
5b
6a
OSL
U-Th (Recrystallization age)
Elevation (m. amsl)
Notch (?)
Notch (?)
Notch
215±22ka
110±8ka
Abrasion platform
Dendropoma
rim
ILSD
6b
b

Table 7: MIS 5.5 and Present tidal notches data in the Mediterranean Sea

1) Site number; 2) Locality and site name; 3) Coordinates; 4) Measures date; 5) Elevation with uncertain, m; 6) Type of Notch: MTN= MIS 5.5 Tidal Notch; PTN= Present Tidal Notch; NM= Not Measured; NC= Not Carved; C= Consumed; 8) Notch morphometry; 9) Kind of measurement: T: Telefix; M: Tape meter; DGPS: DGPS; 10) Faunal assemblage of the nearest aged fossil deposit; Distance (km) and reference site name for the age of deposit:

1) Site number; 2) Locality and site name; 3) Coordinates; 4) Notch Morphometry; 5) Elevation with uncertain, m; 6) Average notch measures, m; 7) Type of Notch: MTN= MIS 5.5 Tidal Notch; *PTN*= Present Tidal Notch; NM= Not Measured; NC= Not Carved; C= Consumed); 8) Notch morphometry; 9 Kind of measurement; 10) Faunal assemblages in aged fossil deposit; 11) Thechnique of chronological attribuition; 12 Distance (km) from the site used for give the age of deposit. References: [1] Abate et al., 1996; [2] Antonioli, 1991; [3] Antonioli et al., 1994a; [4] Antonioli et al., 1994b; [5] Antonioli et al., 1999; [6] Antonioli et al., 2002; [7] Blanc and Segre, 1953; [8] Bosellini et al., 1999; [9] Brancaccio et al., 1986, 1990; [10] Cesaraccio and Puxeddu, 1986; [11] Delicato et al., 1999; [12] Durante, 1975; [13] Esposito et al., 2003; [14] Ferranti and Antonioli, 2007; [15] Hearty P.J., 1986, 1987; [16] Malatesta, 1954a, 1954b, 1970; [17] Mastronuzzi et al., 2007; [18] Orrù and Ulzega, 1986; [19] Orrù and Pasquini, 1992; [20] Orrù et al., 2011; [21] Palmerini and Ulzega, 1969; [22] Pascucci et al., 2014; [23] Porqueddu et al., 2011; [24] Sanna et al., 2010; [25] Segre, 1951; [26] Segre, 1957; [27] Ulzega and Ozer, 1980.

1 Site N	2 Locality (site name)	3 Coordinates	4 Measures Date and Time (UTC +2)	5 Elevation with uncertainty (m)	6 Average notch measures (m) MIS 5.5 *Present*			7 Type of Notch	8 Notch Morphometry MIS 5.5/present notch average concavity ratio for each locality and (value) for each *site*		9 Kind of measure ment	10 Faunal assemblage	11 Technique of chronologic al attribution	12 Distance (km) and reference site name for the age of deposit	13 References
					widt h	depth	base		width ratio	deep ratio					
1	Talamone	42°33' 03.2309" N" 11°09' 55.0274"E	21.10.2016 9.53	4.78 ± 0.275	0.80 *0.45*	0.60 *0.60*	0.45 *0.15*	MTN *PTN*	1,77	1,00	T	*Cerastoderma Glicimeris*	Amino-stratigraphy Senegalese fauna	[16,17] (2,7) Campo Regio [16,17] (25,4) Selva Nera	[16] Hearty PJ, Dai Pra G., 1986; [17] Hearty PJ, Dai Pra G., 1987;
2	Capo Caccia	40° 36' 23.3858" N" 8° 08' 53.2929"E"	06.07.2015 10.10	3.80 ± 0.035	0.75 *0.50*	0.20 *0.12*	0.20 *0.80*	MTN *PTN*	1,36 (1,50)	0,71 (0,16)	M	*Glycymeris g.* *Strombus b., Conusus t., Patella f.* *Patella f. Brachydontes senegalensis*	OSL Senegalese fauna	[25] (9,5) Bombarde [30] (15,8) Cala Bona [18] (3,2) Dragonara	[25] Pascucci et al., 2014; [30] Ulzega and Ozer, 1980; [18] Malatesta, 1954,1970;
3		40° 36' 07.6595" N" 8° 08' 46.1842"E"	06.07.2015 10.30	3.70 ± 0.035	0.80 *0.65*	0.60 *0.12*	0.60 *0.80*	MTN *PTN*	(1,23)	(0,50)	M	*Glycymeris g.* *Strombus b., Conusus t., Patella f.* *Patella f. Brachydontes senegalensis*	OSL Senegalese fauna	[25] (9,2) [30] (15,7) [18] (2,9)	[25] Pascucci et al., 2014; [30] Ulzega and Ozer, 1980; [18] Malatesta, 1954,1970;
4		40° 35' 50.2719" N" 8° 08' 50.7426"E"	06.07.2015 10.45	3.75 ± 0.035	0.75 *0.60*	0.55 *0.60*	0.55 *0.80*	MTN *PTN*	(1,25)	(0,91)	M	*Glycymeris g.* *Strombus b., Conusus t., Patella f.* *Patella f. Brachydontes senegalensis*	OSL Senegalese fauna	[25] (9,2) [30] (15,5) [18] (2,3)	[25] Pascucci et al., 2014; [30] Ulzega and Ozer, 1980; [18] Malatesta, 1954,1970;

5		40° 34' 44.8391" N" 8° 09' 01.6537"E"	06.07.2015 10.50	3.50 ± 0.035	0.75 *0.50*	0.25 *0.10*	0.25 *0.80*	MTN *PTN*	(1,50)	(0,25)	M	*Glycymeris g.* *Strombus b., Conusus t., Patella f.* *Patella f. Brachydontes senegalensis*	OSL Senegalese fauna	[25] (8,8) [30] (14,7) [18] (1,0)	[25] Pascucci et al., 2014; [30] Ulzega and Ozer, 1980; [18] Malatesta, 1954,1970;
6		40° 34' 37.0535" N" 8° 09' 20.1122"E"	06.07.2015 11.10	3.10 ± 0.035	0.85 *0.60*	0.60 *0.11*	0.60 *0.80*	MTN *PTN*	(1,42)	(0,54)	M	*Glycymeris g.* *Strombus b., Conusus t., Patella f.* *Patella f. Brachydontes senegalensis*	OSL Senegalese fauna	[25] (8,5) [30] (14,1) [18] (0,7)	[25] Pascucci et al., 2014; [30] Ulzega and Ozer, 1980; [18] Malatesta, 1954,1970;
7		40° 34' 09.9358" N" 8° 09' 07.6213"E"	06.07.2015 11.30	3.65 ± 0.035	0.65 *0.50*	0.30 *0.30*	0.30 *0.80*	MTN *PTN*	(1,30)	(1,00)	M	*Glycymeris g.* *Strombus b., Conusus t., Patella f.* *Patella f. Brachydontes senegalensis*	OSL Senegalese fauna	[25] (8,9) [30] (14,4) [18] (1,4)	[25] Pascucci et al., 2014; [30] Ulzega and Ozer, 1980; [18] Malatesta, 1954,1970;
8		40° 33' 47.4484" N" 8° 09' 50.9292"E"	06.07.2015 11.50	3.95 ± 0.035	0.50 *0.40*	0.25 *0.30*	0.25 *0.70*	MTN *PTN*	(1,25)	(0,83)	M	*Glycymeris g.* *Strombus b., Conusus t., Patella f.* *Patella f. Brachydontes senegalensis*	OSL Senegalese fauna	[25] (9,9) [30] (13,2) [18] (1,6)	[25] Pascucci et al., 2014; [30] Ulzega and Ozer, 1980; [18] Malatesta, 1954,1970;
9		40° 33' 53.0497" N" 8° 09' 54.4411"E"	06.07.2015 12.30	3.50 ± 0.035	0.58 *0.45*	0.40 *0.40*	0.40 *0.80*	MTN *PTN*	(1,29)	(1,00)	M	*Glycymeris g.* *Strombus b., Conusus t., Patella f.* *Patella f. Brachydontes senegalensis*	OSL Senegalese fauna	[25] (8,7) [30] (13,2) [18] (1,8)	[25] Pascucci et al., 2014; [30] Ulzega and Ozer, 1980; [18] Malatesta, 1954,1970;
10		40° 34' 13.8461" N" 8° 09' 51.9464"E"	06.07.2015 12.45	3.85 ± 0.035	0.70 *0.55*	0.20 *0.20*	0.35 *0.80*	MTN *PTN*	(1,27)	(1,00)	M	*Glycymeris g.* *Strombus b., Conusus t., Patella f.* *Patella f. Brachydontes senegalensis*	OSL Senegalese fauna	[25] (7,8) [30] (13,3) [18] (1,1)	[25] Pascucci et al., 2014; [30] Ulzega and Ozer, 1980; [18] Malatesta, 1954,1970;
11		40° 34' 23.8252" N" 8° 09' 52.2129"E"	06.07.2015 13.00	3.85 ± 0.035	0.70 *0.55*	0.20 *0.20*	0.30 *0.80*	MTN *PTN*	(1,27)	(1,00)	M	*Glycymeris g.* *Strombus b., Conusus t., Patella f.* *Patella f. Brachydontes senegalensis*	OSL Senegalese fauna	[25] (7,7) [30] (13,4) [18] (0,7)	[25] Pascucci et al., 2014; [30] Ulzega and Ozer, 1980; [18] Malatesta, 1954,1970;

12		40° 34' 46.6377" N" 8° 09' 45.7522"E"	06.07.2015 13.10	3.86 ± 0.035	0.68 *0.40*	0.20 *0.20*	0.30 *0.90*	MTN *PTN*	(1,70)	(1,00)	M	*Glycymeris g.* *Strombus b., Conusus t., Patella f.* *Patella f. Brachydontes senegalensis*	OSL Senegalese fauna	[25] (7,8) [30] (13,7) [18] (0,2)	[25] Pascucci et al., 2014; [30] Ulzega and Ozer, 1980; [18] Malatesta, 1954,1970;
13		40° 34' 49.2217" N" 8° 10' 16.3651"E"	06.07.2015 13.15	4.05 ± 0.035	0.65 *0.48*	0.38 *0.40*	0.40 *0.80*	MTN *PTN*	(1,35)	(0,95)	M	*Glycymeris g.* *Strombus b., Conusus t., Patella f.* *Patella f. Brachydontes senegalensis*	OSL Senegalese fauna	[25] (7,11) [30] (13,5) [18] (0,7)	[25] Pascucci et al., 2014; [30] Ulzega and Ozer, 1980; [18] Malatesta, 1954,1970;
14		40° 34' 52.5000" N" 8° 10' 17.9283"E"	06.07.2015 13.30	4.25± 0.035	0.65 *0.45*	0.40 *0.40*	0.40 *0.90*	MTN *PTN*	(1,44)	(1,00)	M	*Glycymeris g.* *Strombus b., Conusus t., Patella f.* *Patella f. Brachydontes senegalensis*	OSL Senegalese fauna	[25] (7,7) [30] (13,1) [18] (0,8)	[25] Pascucci et al., 2014; [30] Ulzega and Ozer, 1980; [18] Malatesta, 1954,1970;
15	Punta Giglio	40° 34' 22.0138" N" 8° 11' 54.1236"E"	07.07.2015 09.30	4.65± 0.035	0.75 *0.45*	0.60 *0.43*	0.60 *0.60*	MTN *PTN*	1,34 (1,66)	1,07 (1,39)	M	*Glycymeris g.* *Strombus b., Conusus t., Patella f.* *Patella f. Brachydontes senegalensis*	OSL Senegalese fauna	[25] (5,3) [30] (10,6) [18] (3,1)	[25] Pascucci et al., 2014; [30] Ulzega and Ozer, 1980; [18] Malatesta, 1954,1970;
16		40° 34' 13.5433" N" 8° 12' 05.3012"E"	07.07.2015 10.10	4.43± 0.035	0.80 *0.55*	0.60 *0.65*	0.60 *0.10*	MTN *PTN*	(1,45)	(0,92)	M	*Glycymeris g.* *Strombus b., Conusus t., Patella f.* *Patella f. Brachydontes senegalensis*	OSL Senegalese fauna	[25] (4,8) [30] (9,8) [18] (3,5)	[25] Pascucci et al., 2014; [30] Ulzega and Ozer, 1980; [18] Malatesta, 1954,1970;
17		40° 34' 11.9178" N" 8° 12' 24.3416"E"	07.07.2015 10.30	4.45± 0.035	0.85 *0.56*	0.60 *0.60*	0.60 *0.12*	MTN *PTN*	(1,52)	(1,00)	M	*Glycymeris g.* *Strombus b., Conusus t., Patella f.* *Patella f. Brachydontes senegalensis*	OSL Senegalese fauna	[25] (4,4) [30] (9,6) [18] (3,7)	[25] Pascucci et al., 2014; [30] Ulzega and Ozer, 1980; [18] Malatesta, 1954,1970;
18		40° 34' 18.0312" N" 8° 12' 34.2002"E"	07.07.2015 10.40	5.05± 0.035	0.80 *0.70*	0.65 *0.60*	0.65 *0.15*	MTN *PTN*	(1,14)	(1,08)	M	*Glycymeris g.* *Strombus b., Conusus t., Patella f.* *Patella f. Brachydontes senegalensis*	OSL Senegalese fauna	[25] (4,1) [30] (9,5) [18] (4,2)	[25] Pascucci et al., 2014; [30] Ulzega and Ozer, 1980; [18] Malatesta, 1954,1970;

19		40° 34' 16.4426" N" 8° 12' 40.4623"E"	07.07.2015 10.45	5.25± 0.035	0.70 *0.63*	0.60 *0.60*	0.60 *0.90*	MTN *PTN*	(1,11)	(1,00)	M	*Glycymeris g.* *Strombus b., Conusus t., Patella f.* *Patella f. Brachydontes senegalensis*	OSL Senegalese fauna	[25] (4,0) [30] (9,5) [18] (4,2)	[25] Pascucci et al., 2014; [30] Ulzega and Ozer, 1980; [18] Malatesta, 1954,1970;
20		40° 34' 16.0069" N" 8° 14' 10.3907"E"	07.07.2015 11.30	5.45± 0.035	0.75 *0.55*	0.65 *0.60*	0.70 *0.12*	MTN *PTN*	(1,35)	(1,08)	M	*Glycymeris g.* *Strombus b., Conusus t., Patella f.* *Patella f. Brachydontes senegalensis*	OSL Senegalese fauna	[25] (2,2) [30] (7,5) [18] (6,3)	[25] Pascucci et al., 2014; [30] Ulzega and Ozer, 1980; [18] Malatesta, 1954,1970;
21		40° 34' 16.7601" N" 8° 14' 36.4720"E"	07.07.2015 11.40	5.35± 0.035	0.65 *0.55*	0.65 *0.60*	0.60 *0.80*	MTN *PTN*	(1,18)	(1,08)	M	*Glycymeris g.* *Strombus b., Conusus t., Patella f.* *Patella f. Brachydontes senegalensis*	OSL Senegalese fauna	[25] (1,7) [30] (6,9) [18] (6,8)	[25] Pascucci et al., 2014; [30] Ulzega and Ozer, 1980; [18] Malatesta, 1954,1970;
22	Capo Figari	40° 59' 16.7530" N" 9° 39' 16.2538"E"	15.06.2008 13.15	4.77± 0.135	- -	- -	- -	NM NM	0,92	0,70	M	*Conus t.* *Strombus b*	Senegalese fauna	[28] (3,3) Golfo Aranci	[28] Segre, 1952;
23		40° 59' 24.1901" N" 9° 39' 25.9513"E"	15.06.2008 13.15	4.79± 0.135	0.45 *0.72*	0.50 *0.80*	0.25 *0.30*	MTN *PTN*	(0,62)	(0,62)	M	*Conus t.* *Strombus b*	Senegalese fauna	[28] (3,0) Golfo Aranci	[28] Segre, 1952;
24		40° 59' 36.7594" N" 9° 39' 42.8390"E"	15.06.2008 13.30	4.72± 0.135	- *0.78*	- *0.60*	- *0.58*	NM *PTN*	-	-	M	*Conus t.* *Strombus b*	Senegalese fauna	[28] (3,7) Golfo Aranci	[28] Segre, 1952;
25		40° 59' 46.6335" N" 9° 39' 51.7674"E"	16.03.2017 11.30	4.79± 0.035	0.65 *0.58*	0.50 *0.63*	0.95 *0.48*	MTN *PTN*	(1,12)	(0,79)	T	*Conus t.* *Strombus b*	Senegalese fauna	[28] (3,6) Golfo Aranci	[28] Segre, 1952;
26		40° 59' 38.3400" N" 9° 39' 46.9800"E"	16.03.2017 12.30	4.65± 0.035	0.70 *0.68*	0.40 *0.58*	- *0.12*	MTN *PTN*	(1,03)	(0,69)	T	*Conus t.* *Strombus b*	Senegalese fauna	[28] (3,3) Golfo Aranci	[28] Segre, 1952;
27	Tavolara	40° 54' 09.4066" N" 9° 42' 54.7413"E"	31.05.2005 11.30	6,93± 0.035	0.68 *0.60*	0.50 *0.82*	0.95 -	MTN *PTN*	1,17 (1,13)	0,74 (0,61)	T	*Conus t + Patella f.*	Senegalese fauna at +5 m	[26, 21] (2,7) Spalmatore di Terra	[26] Porqueddu et al., 2011; [21] Orrù and Pasquini, 1992;
28		40° 54' 10.0597" N" 9° 42' 57.2631"E"	31.05.2005 12.10	7,08± 0.135	- -	- -	- -	NM NM	-	-	M	*Conus t + Patella f.*	Senegalese fauna at +5 m	[26, 21] (5) Spalmatore di Terra	[26] Porqueddu et al., 2011; [21] Orrù and Pasquini, 1992;
29		40° 54' 28.8401" N" 9° 43' 42.5178"E"	16.02.2017 15.30	6,97± 0.135	0.88 *0.86*	0.55 *0.102*	- *0.47*	MTN *PTN*	(1,02)	(0,54)	T	*Conus t + Patella f.*	Senegalese fauna at +5 m	[26, 21] (3,9) Spalmatore di Terra,	[26] Porqueddu et al., 2011; [21] Orrù and Pasquini, 1992;
30		40° 54' 33.6501" N" 9° 43' 54.1298"E"	31.05.2005 12.30	6,93± 0.135	- -	- -	- -	NM NM	-	-	M	*Conus t + Patella f.*	Senegalese fauna at +5 m	[26, 21] (4,7) Spalmatore di Terra	[26] Porqueddu et al., 2011; [21] Orrù and Pasquini, 1992;
31		40° 54' 36.0387" N" 9° 44' 14.9503"E"	16.02.2017 15.45	6.89± 0.135	0.85 *0.55*	0.60 *0.145*	- *0.30*	MTN *PTN*	(1,54)	(0,41)	T	*Conus t + Patella f.*	Senegalese fauna at +5 m	[26, 21] (4,9) Spalmatore di Terra	[26] Porqueddu et al., 2011; [21] Orrù and Pasquini, 1992;
32		40° 54' 47.0000" N" 9° 44' 29.0000"E"	31.05.2005 13.05	6,13± 0.135	0.64 *0.60*	0.56 *0.60*	0.60 *0.35*	MTN *PTN*	(1,06)	(0,93)	M	*Conus t + Patella f.*	Senegalese fauna at +5 m	[26, 21] (5,2) Spalmatore di Terra	[26] Porqueddu et al., 2011; [21] Orrù and Pasquini, 1992;
33		40° 55' 02.4486" N" 9° 43' 28.8485"E"	31.05.2005 13.30	6,81± 0.135	0.78 *0.65*	0.30 *0.35*	- *0.35*	MTN *PTN*	(1,20)	(0,86)	T	*Conus t + Patella f.*	Senegalese fauna at +5 m	[26, 21] (4,3) Spalmatore di Terra	[26] Porqueddu et al., 2011; [21] Orrù and Pasquini, 1992;
34		40° 54' 52.8101" N" 9° 43' 04.0781"E"	31.05.2005 13.40	6,43± 0.135	- -	- -	- -	NM NM	-	-	M	*Conus t + Patella f.*	Senegalese fauna at +5 m	[26, 21] (3,7) Spalmatore di Terra	[26] Porqueddu et al., 2011; [21] Orrù and Pasquini, 1992;

35		40° 54' 41.1907" N" 9° 42' 44.5510"E"	16.02.2017 13.45	6,05± 0.135	0.60 *0.55*	0.55 *0.50*	0.60 -	MTN *PTN*	(1,09)	(1,10)	T	*Conus t + Patella f.*	Senegalese fauna at +5 m	[26, 21] (3,1) Spalmatore di Terra	[26] Porqueddu et al., 2011; [21] Orrù and Pasquini, 1992;
36		40° 54' 41.0000" N" 9° 42' 46.0000"E"	31.05.2005 14.00	6,43± 0.135	- -	- -	- -	NM NM	-	-	M	*Conus t + Patella f.*	Senegalese fauna at +5 m	[26, 21] (3,9) Spalmatore di terra	[26] Porqueddu et al., 2011; [21] Orrù and Pasquini, 1992;
37	Golfo Orosei (Nord)	40° 14' 30.1709" N" 9° 37' 24.7770"E"	12.07.2016 16.05	9.78 ± 0.035	0.90 *0.68*	0.35 *0.70*	0.60 *0.12*	MTN *PTN*	1,22 (1,32)	0,44 (0,50)	T	*Stalagmite* *Patella ferruginea*	OSL Senegalese fauna	[27] (0,8) Bue marino [30] (1,9) Cala Luna	[27] Sanna et al., 2010; [30] Ulzega and Ozer, 1980;
38		40° 11' 35.5522" N" 9° 37' 43.0153"E"	12.07.2016 10.45	9,19 ± 0.035	0.85 *0.70*	0.40 *0.80*	0.12 *0.11*	MTN *PTN*	(1,21)	(0,50)	T	*Stalagmite* *Patella ferruginea*	OSL Senegalese fauna	[27] (6,1) Bue marino [30] (3,5) Cala Luna	[27] Sanna et al., 2010; [30] Ulzega and Ozer, 1980;
39		40° 05' 43.5676" N" 9° 42' 59.8173"E"	12.07.2016 12.45	7.92 ± 0.035	0.80 *0.70*	0.25 *0.80*	0.40 -	MTN *PTN*	(1,14)	(0,31)	T	*Stalagmite* *Patella ferruginea*	OSL Senegalese fauna	[27] (18,8) Bue marino [30] (16,2) Cala Luna	[27] Sanna et al., 2010; [30] Ulzega and Ozer, 1980;
40	Capo Monte Santu	40° 05' 08.3000" N" 9° 43' 56.4700"E"	12.07.2016 13.30	7.86 ± 0.035	0.78 *0.65*	0.60 *0.80*	0.65 *0.95*	MTN *PTN*	1,20	0,75	T	*Stalagmite* *Patella ferruginea*	OSL Senegalese fauna	[27] (20,3) Bue marino [30] (17,8) Cala Luna	[27] Sanna et al., 2010; [30] Ulzega and Ozer, 1980;
41	Pedralonga	40° 01' 54.7435" N" 9° 42' 20.2327"E"	23.09.2016 12.00	7,51 ± 0.135	0.82 *0.65*	0.90 *0.90*	0.135 *0.10*	MTN *PTN*	1,22 (1,26)	0,92 (1,00)	T	*Stalagmite* *Patella ferruginea*	OSL Senegalese fauna	[27] (25,0) Bue marino [30] (22,4) Cala Luna	[27] Sanna et al., 2010; [30] Ulzega and Ozer, 1980;
42		40° 01' 54.1288" N" 9° 42' 20.2844"E"	23.09.2016 12.15	7,52 ± 0.135	0.45 *0.42*	0.80 *0.90*	0.18 *0.135*	MTN *PTN*	(1,07)	(0,89)	T	*Stalagmite* *Patella ferruginea*	OSL Senegalese fauna	[27] (25,4) Bue marino [30] (22,6) Cala Luna	[27] Sanna et al., 2010; [30] Ulzega and Ozer, 1980;
43		40° 01' 49.0524" N" 9° 42' 19.3672"E"	23.09.2016 12.30	7,42 ± 0.135	0.87 *0.70*	0.50 *0.50*	0.14 *0.90*	MTN *PTN*	(1,23)	(1,00)	T	*Stalagmite* *Patella ferruginea*	OSL Senegalese fauna	[27] (25,6) Bue marino [30] (22,75) Cala Luna	[27] Sanna et al., 2010; [30] Ulzega and Ozer, 1980;
44		40° 01' 45.3626" N" 9° 42' 21.1162"E"	23.09.2016 12.45	6,98 ± 0.135	0.58 *0.55*	0.40 *0.46*	0.90 *0.12*	MTN *PTN*	(1,24)	(0,87)	T	*Stalagmite* *Patella ferruginea*	OSL Senegalese fauna	[27] (25,8) Bue marino [30] (22,9) Cala Luna	[27] Sanna et al., 2010; [30] Ulzega and Ozer, 1980;
45	Sant'Antioco	38° 59' 09.8613" N" 8° 26' 53.8987"E"	24.09.216 10.45	2,97± 0.175	0.66 *0.42*	0.30 *0.30*	0.68 *0.80*	MTN *PTN*	1,71 (1,57)	1,71 (1,00)	T	*Conus t. Strombus b.* *Conus+ Patella f.*	Senegalese fauna	[30] (1,7) Maladroxia [30] (11) Cala Su Turcu [22] (6,0) Cala Sapone	[30] Ulzega and Ozer, 1980; [22] Orrù et al., 2011;
46		38° 59' 07.9080" N" 8° 26' 55.1040"E"	24.09.216 11.15	2,93± 0.275	0.70 *0.48*	0.90 *0.30* *0.05*	0.11 *0.80* -	MTN *PTN* *RN*	(2,08)	(3,00)	T	*Conus t. Strombus b.* *Conus+ Patella f.*	Senegalese fauna	[30] (1,7) Maladroxia [30] (11) Cala Su Turcu [22] (6,0) Cala Sapone	[30] Ulzega and Ozer, 1980; [22] Orrù et al., 2011;
47		38° 59' 06.1726" N" 8° 26' 53.1652"E"	24.09.216 12.30	2,71± 0.275	0.74 *0.50*	0.48 *0.43*	0.105 *0.84*	MTN *PTN*	(1,48)	(1,12)	T	*Conus t. Strombus b.* *Conus+ Patella f.*	Senegalese fauna	[30] (1,7) Maladroxia [30] (11) Cala Su Turcu [22] (6,0) Cala Sapone	[30] Ulzega and Ozer, 1980; [22] Orrù et al., 2011;
48	Masua	39° 20' 10.5619" N" 8° 24' 27.6915"E"	28.09.2014 9.30	3.23± 0.175	0.75 *0.50*	0.50 *0.50*	0.60 *0.70*	MTN *PTN*	1,5	1,00	M	*Conus t. + Patella f.*	Senegalese fauna	[20] (5,9) Fontanamare	[20] Orrù and Ulzega, 1986;
49	Buggerru	39° 23' 40.7856" N" 8° 23' 10.2609"E"	28.09.2014 11.30	3.54± 0.175	0.80 *0.60*	0.60 *0.80*	0.70 *0.70*	MTN *PTN*	1,33	0,75	M	*Conus t. + Patella f.* *Conus t + Glycymeris*	Senegalese fauna	[11] (2,3) Buggerru – Rio Mannu [23] (11) Acqua Durci [23] (15) Rio Piscinas	[11] Cesaraccio and Puxeddu, 1986; [23] Palmerini and Ulzega, 1969;
50	Circeo (Grotta delle Capre)	41° 13' 26.0440" N" 13° 04' 57.3301"E"	11.2014 11.30	9.28± 0.175	0.29 -	0.08 -	0.08 -	MTN NC	-	-	DGPS	*Persistrombus* and other Senegalese fauna	Senegalese fauna	[7,13] (0.3) Grotta del Fossellone	[7] Blanc and Segre, 1953; [13] Durante, 1975;

51	Terracina (Pisco Montano)	41° 17' 17.6752" N" 13° 15' 36.1267"E"	13.06.2016 15.00	7,96± 0.175	- -	- -	- -	C NC	-	-	DGPS	*Cerastoderma sp*	Amino-stratigraphy aminozone E	[2] (7,0)	[2] Antonioli et al., 1986;
52	Sperlonga (Sant'Agostino)	41° 13' 06.4207" N" 13° 31' 57.3519"E"	13.06.2016 12.10	6,53± 0.175	0.75 *0.60*	0.60 *0.70*	0.45 *0.45*	MTN *PTN*	1,25	0,86	DGPS	*Glycimeris V.*	Amino-stratigraphy aminozone E E	[3] (2,8)	[3] Antonioli et al., 1991;
53	Gaeta (Grotta del Turco)	41° 12' 16.5378" N" 13° 34' 17.8325"E"	15.11.2014 11.40	5.92± 0.275	- *0.35*	- *0.40*	- *0.35*	C *PTN*	-	-	M	*Glycimeris V,*	Amino-stratigraphy aminozone E	[3] (10,5)	[3] Antonioli et al., 1991;
54	Minturno (Monte d'Argento)	41° 14' 23.0097" N" 13° 44' 12.5566"E"	13.06.2016 9.40	12,48± 0.175	- -	- -	- -	C NM	-	-	DGPS	*Senegalese fauna Conus textudinarius*	Senegalese fauna	[29,12] (0,5) West side Monte.D'Argento	[29] Segre, 1957; [12] Delicato et al., 1999;
55	Capri (est)	40° 32' 59.3015" N" 14° 15' 28.3630"E"	05.2015	7,40± 0.275	0.70 -	0.50 -	0.50 -	MTN *RN*	-	-	M	*Persistrombus*	U\Th age, Senegalese fauna	[9,10,15] (9,5)	[9] Brancaccio et al., 1978; [10] Brancaccio et al., 1990; [15] Ferranti and Antonioli 2007;
56	Capri (Tragara)	40° 32' 39.5257" N" 14° 15' 11.2623"E"	23.05.2004 10.30	8.0± 0.275	0.70 -	0.45 -	0.45 -	MTN *RN*	-	-	M	*Persistrombus*	U\Th age, Senegalese fauna	[9,10] (10,6)	[9] Brancaccio et al., 1978; [10] Brancaccio et al., 1990;
57	Capri (Grotta Fontelina)	40° 32' 38.1002" N" 14° 14' 59.6253"E"	23.05.2004 10.30	7.10± 0.275	0.75 -	0.60 -	0.60 -	MTN *RN*	-	-	M	*Persistrombus*	U\Th age, Senegalese fauna	[9,10,15] (11,7)	[9] Brancaccio et al., 1978; [10] Brancaccio et al., 1990; [15] Ferranti and Antonioli 2007;
58	Capri (Grotta Verde)	40° 32' 21.4388" N" 14° 13' 15.1499"E"	23.05.2004 10.30	6,97± 0.275	0.75 -	0.65 -	0.80 -	MTN *RN*	-	-	M	*Persistrombus*	U\Th age, Senegalese fauna	[9,10,15] (11,5)	[9] Brancaccio et al., 1978; [10] Brancaccio et al., 1990; [15] Ferranti and Antonioli 2007;
59	Capri (Cala Articola)	40° 32' 18.5965" N" 14° 12' 15.9734"E"	23.05.2004 10.30	6,32± 0.275	0.70 -	0.60 -	0.70 -	MTN *RN*	-	-	M	*Persistrombus*	U\Th age, Senegalese fauna	[9,10,15] (9,2)	[9] Brancaccio et al., 1978; [10] Brancaccio et al., 1990; [15] Ferranti and Antonioli 2007;
60	Capri (Punta del Pino)	40° 32' 27.6567" N" 14° 11' 53.3286"E"	23.05.2004 10.30	7,07± 0.275	0.70 -	0.75 -	0.80 -	MTN *RN*	-	-	M	*Persistrombus*	U\Th age, Senegalese fauna	[9,10,15] (11)	[9] Brancaccio et al., 1978; [10] Brancaccio et al., 1990; [15] Ferranti and Antonioli 2007;
61	Capri (Grotta Jannarella)	40° 33' 13.7133" N" 14° 11' 59.6013"E"	23.05.2004 10.30	6,97± 0.275	0.70 -	0.45 -	0.80 -	MTN *RN*	-	-	M	*Persistrombus*	U\Th age, Senegalese fauna	[9,10,15] (8,5)	[9] Brancaccio et al., 1978; [10] Brancaccio et al., 1990; [15] Ferranti and Antonioli 2007;
62	Capri (Grotta Binocolo)	40° 33' 41.5848" N" 14° 12' 33.2047"E"	23.05.2004 10.30	5,26± 0.275	0.75 -	0.60 -	0.60 -	MTN *RN*	-	-	M	*Persistrombus*	U\Th age, Senegalese fauna	[9,10,15] (9,5)	[9] Brancaccio et al., 1978; [10] Brancaccio et al., 1990; [15] Ferranti and Antonioli 2007;
63	Capri (Scoglio Ricotta)	40° 33' 38.2729" N" 14° 15' 29.8759"E"	23.05.2004 10.30	7,00± 0.275	0.75 -	0.45 -	0.80 -	MTN *RN*	-	-	M	*Persistrombus*	U\Th age, Senegalese fauna	[9,10,15] (8,1)	[9] Brancaccio et al., 1978; [10] Brancaccio et al., 1990; [15] Ferranti and Antonioli 2007;
64	Mitigliano	40° 35' 11.4300" N" 14° 19' 36.8600"E"	01.08.2017 13.40	5,02± 0.275	0.60 -	0.70 -	0.40 -	MTN *RN*	-	-	M	*Persistrombus*	U\Th age, Senegalese	[9,10] (3,5)	[9] Brancaccio et al., 1978;

													fauna		[10] Brancaccio et al., 1990;
65	Palinuro	40° 01' 55.3198" N" 15° 16' 26.4856"E"	07.07 2016 13.15	2,11± 0.275	0.65 -	0.60 -	0.60 -	MTN *RN*	1,27	0,80	M	*Persistrombus*	U\Th age, Senegalese fauna	[4,14] (3,2)	[4] Antonioli et al., 1996; [14] Esposito et al., 2003;
66		40° 01' 58.4137" N" 15° 16' 56.6662"E"	07.07 2016 13.45	2,16± 0.275	0.62 -	0.40 -	0.40 -	MTN *RN*	-	-	M	*Persistrombus* and Senegalese fauna	U\Th age, Senegalese fauna	[4,14] (6,0)	[4] Antonioli et al., 1996; [14] Esposito et al., 2003;
67		40° 01' 29.4110" N" 15° 17' 32.5298"E"	08.07 2016 16.15	2,09± 0.275	0.38 *0.30*	0.20 *0.25*	0.48 *0.55*	MTN *PTN*	(1,27)	(0,80)	M	*Persistrombus* and Senegalese fauna	U\Th age, Senegalese fauna	[4,14] (7,4)	[4] Antonioli et al., 1996; [14] Esposito et al., 2003;
68	Marina di Camerota	39°59'42.09'' N 15°24'46.71 E''	30.07.2016 10.30	6,75 ± 0.275	80	-	-	MTN	-	-		*Persistrombus* and Senegalese fauna	U\Th age, Senegalese fauna	[4,14] (11.4)	[4] Antonioli et al., 1996; [14] Esposito et al., 2003;
69	Capo Zafferano	38° 06' 31.6324" N" 13° 32' 19.1686"E"	12.08.2016 11.30	2.42± 0,075	0.76 *0.58*	0.52 *0.37*	0.55 *0.45*	MTN *PTN*	1,31	1,40	DGPS	*Arca*	U\Th age, Senegalese fauna	[4] (0,7)	[4] Antonioli et al., 1996;
70	Marettimo	37° 58' 46.7663" N" 12° 02' 21.0449"E"	28.05.2014 12.10	8.10± 0,175	1.05 *0.85*	0.60 *0.30*	0.70 *0.60*	MTN *PTN*	1,23	2,00	M	*Persistrombus*	U\Th age, Senegalese fauna	[18,1,5] (6,5)	[18] Malatesta, 1957; [1] Abate et al., 1996; [5] Antonioli et al., 1999c;
71	Levanzo	37° 59' 14.0825" N" 12° 19' 47.4514"E"	06.2015 9.30	8,50± 0.275	1.2 *0.90*	0.80 *0.80*	0.11 *0.90*	MTN *PTN*	1,33	1,00	M	*Persistrombus*	U\Th age, Senegalese fauna	(4,5)	This paper
72	San Vito Lo Capo (Cala Mancina)	38° 10' 32.4000" N" 12° 43' 01.3800"E"	13.11 2016 11.35	8,53± 0.275	0.80 *0.70*	0.85 *0.85*	0.70 *0.60*	MTN *PTN*	1,14	1,00	M	*Persistrombus*	U\Th age, Senegalese fauna	[5,6] (7,6)	[5] Antonioli et al., 1999c; [6] Antonioli et al., 2002;
73	San Vito Lo Capo (Macari)	38° 09' 18.7200" N" 12° 43' 47.7000"E"	13.11.2016 10.00	8,93± 0.275	0.65 *0.60*	0.60 *0.80*	0.15 *0.68*	MTN *PTN*	1,08	0,75	M	*Persistrombus*	U\Th age, Senegalese fauna	[5,6] (6,4)	[5] Antonioli et al., 1999c; [6] Antonioli et al., 2002;
74	Santa Cesarea Terme (Grotta delle Striare)	40° 02' 47.1900" N" 18° 28' 34.0700"E"	25.11.2016 14.20	8,21± 0.275	1.3 *0.70*	-	-		-	-	DGPS	-	U\Th age on speleothems	(11)	[8] Bosellini et al., 1999; [24] Parente 1999; [31] Mastronuzzi et al., 2007